ENVIRONMENTAL ASSESSMENT AND MICROBIAL FUEL CELL BASED REMEDIATION FOR HEAVY METALS CONTAMINATION IN BAGMATI RIVER WITH SIMULTANEOUS BIO-ELECTRICITY GENERATION

M.Sc. Thesis

(2023)

For partial fulfillment of the requirement for the Master of Science in Biotechnology

Submitted to

Central Department of Biotechnology

Tribhuvan University

Kirtipur, Kathmandu, Nepal

Submitted by

Sujeeta Maharjan

TU Reg. No. : 5-2-469- 133-2014

Roll no: BT619/075

Supervisor

Asst. Prof. Jarina Joshi, PhD

Central Department of Biotechnology (CDBT)

ENVIRONMENTAL ASSESSMENT AND MICROBIAL FUEL CELL BASED REMEDIATION FOR HEAVY METALS CONTAMINATION IN BAGMATI RIVER WITH SIMULTANEOUS BIO-ELECTRICITY GENERATION

M.Sc. Thesis

(2023)

For partial fulfillment of the requirement for the Master of Science in Biotechnology

Submitted to

Central Department of Biotechnology

Tribhuvan University

Kirtipur, Kathmandu, Nepal

Submitted by

Sujeeta Maharjan

TU Reg. No. : 5-2-469- 133-2014

Roll No: BT619/075

Supervisor

Asst. Prof. Jarina Joshi, PhD

Central Department of Biotechnology (CDBT)

Tribhuvan University
CENTRAL DEPARTMENT OF BIOTECHNOLOGY
Kirtipur, Kathmandu, Nepal

Central Department of Biotechnology
T. U.
Kirtipur-2064

Date: August 16, 2023

RECOMMENDATION

This is to certify that the research work entitled **"ENVIRONMENTAL ASSESSMENT AND MICROBIAL FUEL CELL BASED REMEDIATION FOR HEAVY METALS CONTAMINATION IN BAGMATI RIVER WITH SIMULTANEOUS BIO-ELECTRICITY GENERATION"** has been carried out by **Ms. Sujeeta Maharjan** under my supervision. This thesis work was performed for the partial fulfillment of the Master of Science in Biotechnology under the course code BT 621. The result presented here is her original findings. I, hereby, recommend this thesis for final evaluation.

.....

Asst. Prof. Jarina Joshi (PhD)
(Supervisor)
Central Department of Biotechnology
Tribhuvan University, Kirtipur

Tribhuvan University

CENTRAL DEPARTMENT OF BIOTECHNOLOGY

Kirtipur, Kathmandu, Nepal

Central Department of Biotechnology T. U. Kirtipur-2064

Date: August 16, 2023

CERTIFICATE OF EVALUATION

This is to certify that this thesis entitled **"ENVIRONMENTAL ASSESSMENT AND MICROBIAL FUEL CELL BASED REMEDIATION FOR HEAVY METALS CONTAMINATION IN BAGMATI RIVER WITH SIMULTANEOUS BIO-ELECTRICITY GENERATION"** presented to the evaluation committee by **Ms. Sujeeta Maharjan** is found satisfactory for the partial fulfillment of Master of Science in Biotechnology.

.....

Prof. Dr. Krishna Das Manandhar
(Head of Department)
Central Department of Biotechnology
Tribhuvan University, Kirtipur

.....

Assoc. Prof. Smriti Gurung (PhD)
(External Examiner)
Environmental Science and Engineering
Kathmandu University, Dhulikhel, Kavre

.....

Prof. Dr. Rajani Malla
(Internal Examiner)
Central Department of Biotechnology
Tribhuvan University, Kirtipur

.....

Asst. Prof. Jarina Joshi (PhD)
(Supervisor)
Central Department of Biotechnology
Tribhuvan University, Kirtipur

ACKNOWLEDGEMENT

I would like to express my heartfelt gratitude to all those who have contributed to the successful completion of this research project.

First and foremost, I would like to extend my deepest appreciation to my research supervisor, **Dr. Jarina Joshi**, Asst. Prof., Central Department of Biotechnology, Kirtipur, Kathmandu for her invaluable guidance, support, and mentorship. Her expertise, insightful feedback, and encouragement have been instrumental in shaping this research and pushing me toward excellence. I also extend my appreciation to **Prof. Dr. Krishna Das Manandhar**, Head of the Department of Central Department of Biotechnology, Kirtipur, Kathmandu for granting access to the laboratory facilities required for my research.

I would also like to acknowledge the **University Grants Commission (UGC)**, Sano-Thimi, Bhaktapur for their financial support, which made this research possible. Their generous funding allowed me to carry out the necessary experiments, collect data, and analyze the results.

I am thankful to **ENPHO (Environment and Public Health Organization)** laboratory, Thapagaun, Baneshwor for the AAS (Atomic Absorption Spectrometry) analysis of the samples for quantification of heavy metals concentration and to **CMDN (Center for Molecular Dynamics Nepal)**, Thapathali, Kathmandu for the Metagenomic analysis of the samples.

Furthermore, I extend my gratitude to my senior, colleagues, juniors for their co-operation, fruitful discussions, and valuable input throughout the research process. Their collective efforts and intellectual contributions have significantly contributed to the overall quality of this work. I am indebted to every individual who willingly devoted their time and efforts to this research. Their cooperation and willingness to share their experiences and insights have greatly enriched the findings of this study.

I would also like to acknowledge the assistance provided by the staff and resources at **Prof. Dr. Amar Kumar Yadav**, Central Department of Chemistry, Kirtipur, Kathmandu, whose support was essential in carrying out the necessary experiments and accessing relevant literature. I also extend my thanks to the academic staff who provided the necessary information and support.

Last but not least, I am immensely grateful to my family and loved ones for their unwavering support, understanding, and encouragement. Their belief in me and their constant motivation has been a source of strength throughout this research journey.

In conclusion, I am deeply appreciative of all the individuals and organizations mentioned above for their significant contributions and support. Without their help, this research would not have been possible.

LIST OF TABLES

LIST OF FIGURES

TABLE OF CONTENTS

Contents

ABSTRACT

This research focused on the use of a dual-chambered Microbial Fuel Cell (MFC) for the simultaneous remediation of heavy metals and bio-electricity generation from Bagmati River water. The MFC operates by releasing electrons through microbial oxidation in the anodic chamber, which are transferred to the cathode chamber via an external circuit. This electron flow results in the generation of electricity and the reduction of heavy metals to less toxic forms. Proton exchange membranes separate the chambers, allowing the passage of protons during oxidation. Water samples from the Bagmati River in Kathmandu were collected at three locations (Kupondol, Balkhu, and Chovar). Two rounds of sample collection took place during winter (January-February, 2022) and summer (June-July, 2022). Different physical, chemical, and biological parameters of the samples were assessed. Spectrophotometric and Atomic Absorption Spectroscopy (AAS) were used for the determination of chemical parameters. Upon the Metagenomic analysis, the alpha and beta diversity of the bacteria were studied. Electrogenic bacteria such as the genus *Pseudomonas, Rhodobacter, Rhodoferax*, and *Shewanella* were present in the water samples, with *Pseudomonas, Rhodobacter, Rhodoferax*, and other bacterial species from BMII-CV3 used as the MFC inoculum (bacterial consortium). Arsenic and Mercury concentrations were below the Maximum Contaminant Level (MCL) of 0.005 mg/L, while lead concentration was significantly high in BMII-CV3. Heavy metal-resistant bacteria of the genus *Citrobacter* were also isolated from BMII-CV3. Synthetic water was used to optimize the MFC configuration and the optimal configuration included an anolyte of COD 3500mg/L, an anodic chamber with 1% bacterial consortium, a graphite rod electrode, and a platinum electrode in the cathodic chamber, operating at a pH of 7.0 ± 0.02 and 28°C for an average of 8 days. Under an external resistance of 1.1 KΩ, the MFC operated with Bagmati water enriched of 1% bacterial consortium achieved a maximum voltage of 0.08 ± 0.001 V, current density of 0.8 ± 0.01 A/m^2, and power density of 0.070 ± 0.002 W/m^2. This was followed by Bagmati water without bacterial enrichment, generating a voltage of 0.07 V, a current density of 0.6364 ± 0.06 A/m^2, and a power density of 0.0448 ± 0.009 W/m^2. The MFC operated with synthetic water obtained the lowest voltage of 0.005 V, along with a current density of 0.05 ± 0.006 A/m^2 and power density of 0.0002 W/m^2. Heavy metal determination was performed using Differential Pulse Anodic Stripping Voltammetry, with arsenic showing the highest removal efficiency at approximately 100%, followed by lead at around 99%. Chromium exhibited the least effective removal. While no significant differences were observed among the three MFC operations, the MFC using Bagmati water enriched with 1% bacterial consortium demonstrated higher efficiency in heavy metal removal compared to the others. MFC thus had the potential in removing heavy metals as well as bio-electricity generation.

Keywords: Bagmati River**,** Heavy Metal Pollution, Metagenomic sequencing, Microbial Fuel Cell, Bio-electricity, Heavy metal remediation

CHAPTER I

INTRODUCTION

1.1. Background

The Bagmati River originates in Baghdwar, flows southwest from Shivapurilekh in the north of the Kathmandu basin at an altitude of 2650m, and eventually merges with the Ganges in India. Within the Kathmandu valley, it runs south, then west along the border of Kathmandu and Lalitpur districts, before turning south again after receiving the Vishnumati River (Dahal et al., 2011) .This river is vital to urban areas in Nepal, particularly in the Kathmandu valley. The Bagmati River holds great significance for drinking water, irrigation, small-scale hydroelectricity, industry, recreation, livestock usage, domestic needs, culture, and religion, representing the essence of Nepalese civilization as a sacred waterway (Pal et al., 2021)

Another notable feature of the Bagmati River is its proximity to the renowned Pashupatinath Temple, which holds immense religious significance for Hindus and is recognized as a World Heritage Site. The river flows alongside the temple, attracting numerous Hindu pilgrims who engage in bathing rituals as part of their religious practices. (Pantha et al., 2021). The river's role in sustaining the livelihoods and daily activities of the local population cannot be overstated. Overall, the Bagmati River holds immense cultural, religious, and practical significance for the people of Nepal, contributing to the rich heritage and development of the region.

Wastewater entering Bagmati River comes primarily from domestic, storm-water, and industrial sources(Pal et al., 2021) thus, despite its huge significance, it has been heavily polluted as a result of rapid urbanization, population growth, and inadequate management of sewage connections. Domestic, industrial, and agricultural effluents contribute to pollution, along with improper disposal of solid waste along the river banks. The interconnected nature of the river and the groundwater system means that the pollution directly affects the shallow wells located in the vicinity of the river. This further compounds the water quality issues, as the contaminated river water can infiltrate into the groundwater, making it unsafe for consumption and other uses (Pantha et al., 2021). The high levels of microbial and chemical contaminants pose a significant threat to public health and the ecosystem, of the different types of pollutants and contaminants, metal toxicity from pollutants such as heavy metals further compounds the issues faced by the river (Giri et al., 2022).

Various technologies are available for minimizing toxic metal ions in water, including coagulation/flocculation, ion exchange, chemical precipitation, membrane filtration, adsorption, reverse osmosis, electrochemical precipitation, and electro-dialysis. However, these methods have disadvantages such as high sludge generation, chemical requirements, bio-chemical fouling, resin contamination, expensive recovery, and limited

applicability for low metal concentrations, membrane fouling, periodic replacement, high energy input, and pretreatment requirements. As a result, there is a need for an alternative, eco-friendly technique with reduced energy requirements (Bagchi & Behera, 2020). Bio-electrochemical systems (BES) have emerged as a promising approach, combining energy generation with wastewater treatment. BES utilizes microorganisms to generate electricity while simultaneously treating wastewater and removing/recovering heavy metals. This approach offers the advantages of clean fuel production and the production of high-value chemicals, with minimal external energy input. Microbial Fuel Cells (MFC) is a recent and innovative application of BES, enabling the treatment of organic-rich wastewater, removal/recovery of heavy metals, and simultaneous electricity generation (Kaushik & Singh, 2020). This approach holds promise as a sustainable and efficient method for addressing heavy metal pollution in water.

1.1.1. Water Pollution and Heavy metal Contamination

Water is crucial for sustaining life, but ensuring its availability and quality poses a challenge. Despite being classified as a renewable resource, an unbalanced water cycle can lead to water crises. It is especially concerning because human needs primarily rely on freshwater, which constitutes only 3% of the total water on Earth. Moreover, 85% of freshwater exists in the form of glaciers, making it inaccessible for direct human use. Two types of freshwater that can be utilized by humans are groundwater and surface water. Groundwater generally has better quality as it is not directly exposed to pollutants. However, it is not sustainable in the long term and can harm the environment, leading to issues like land subsidence. On the other hand, surface water is more susceptible to pollution as it is directly affected by human activities (Amira et al., 2019). Industrialization and waste mismanagement have polluted water bodies with hazardous chemicals like heavy metals, pesticides, disinfectants, and pharmaceutical residues. This contamination harms water ecosystems and poses risks to human health (R. Kumar et al., 2020). Various factors, including high residential density, commercial activities, industrial demand, improper irrigation, agricultural waste, global warming, and medical waste, have contaminated natural water sources. As a result, freshwater scarcity has emerged, compromising the health of living organisms and the overall environment (Yaqoob et al., 2021). Industrial waste, which contains hazardous chemicals such as dyes, pesticides, oils, aromatic hydrocarbons, and heavy metals, is a major contributor to water pollution. Heavy metals, in particular, are of global concern due to their persistence, bioaccumulation, ability to magnify the food chain, and toxic effects. Consequently, heavy metals are receiving increased attention as hazardous materials in the context of water pollution (Hazrat et al., 2019).

Heavy metals are naturally occurring metals with atomic numbers greater than 20 and high elemental densities (> 5gm/cm^3). They are extensively studied as environmental pollutants due to their potential toxicity to organisms, which depends on the dose and duration of exposure. In the environmental context, certain heavy metals and metalloids are particularly relevant. The environmentally significant and highly toxic heavy metals and metalloids include Chromium (Cr), Nickel (Ni), Copper (Cu), Zinc (Zn), Cadmium (Cd),

Lead (Pb), Mercury (Hg), and Arsenic (As). These pollutants are commonly found in the environment, with Chromium, Manganese, Nickel, Copper, Zinc, Cadmium, and Lead being the most prevalent. Among heavy metals, Arsenic, Lead, Mercury, Nickel, Chromium, and Cadmium are especially hazardous due to their high density (> 4000 kg/m^3) and toxicity. These metals can pose risks to organisms even at very low concentrations ((nanograms (ng) or microgram (µg)). Their widespread presence and potential adverse effects make them a significant concern in environmental and public health contexts (R. Kumar et al., 2020). Heavy metals can originate from natural sources such as weathering of rocks and volcanic activity, as well as from human activities like mining, industrial processes, agriculture, and the use of chemical fertilizers and fossil fuels. These sources collectively impact the presence and distribution of heavy metals in the environment (Hazrat et al., 2019).

Some of the heavy metals, their sources, properties and impacts on environment and human health are as follows:

Arsenic, a highly significant heavy metal, poses concerns from both ecological and individual health perspectives. It is a toxic and carcinogenic semimetal, commonly found as oxides, sulfides, or salts of iron, sodium, calcium, copper, etc. (Jaishankar et al., 2014). Arsenic can take four different forms depending on its oxidation state: Arsenite (As^{+3}) arsenate (As^{+5}), arsenic (As^{0}), and arsine (As^{-3}). Inorganic Arsenite and arsenate are the most abundant forms of these four arsenic compounds that are commonly found in water. Arsenite is comparatively highly toxic to the environment and living organisms than arsenate (Nicomel et al., 2015). Human exposure to arsenic can occur naturally, through industrial sources, or unintentionally. Contamination of drinking water can arise from arsenical pesticides, natural mineral deposits, or improper disposal of arsenical chemicals. The widespread presence and potential adverse effects of arsenic make it a significant concern for both environmental and public health considerations (Jaishankar et al., 2014).Lead is considered the second most toxic metal after arsenic (As). It exists in both organic and inorganic forms. Inorganic lead is commonly found in dust, soil, old paint, and various consumer products, while organic lead (specifically Tetra-ethyl Pb) is predominantly found in leaded gasoline. Both forms of lead are toxic, but organic lead complexes are particularly harmful to biological systems compared to inorganic lead (A. Kumar et al., 2020). Lead exposure primarily occurs through inhaling lead-contaminated dust and aerosols, as well as consuming lead-contaminated food, water, and paints. Lead absorption is highest in the kidneys, followed by the liver, heart, and brain, with the skeleton containing a significant portion. The nervous system is particularly susceptible to lead poisoning, leading to early symptoms like headaches, poor attention span, irritability, memory loss, and dulled cognitive functions. Lead is a potent systemic toxin affecting multiple organs including the kidneys, liver, central nervous, hematopoietic, endocrine, and reproductive systems (Tchounwou et al., 2012).

Mercury is one of the most toxic metals, characterized by its high mobility and persistence in the environment. Mercury exists naturally in three forms (elemental, organic, and inorganic), each with its own toxicity profile (Tchounwou et al., 2012). Its inorganic forms, such as $HgCl_2$, Hg_2Cl_2, are highly mobile due to their water solubility. Mercury (Hg) exists in three oxidation states: 0, +1, and +2 and its emissions primarily come from thermal power plants, fossil fuel combustion, mining, hospital waste, thermometers, and industries such as chloralkali and barometer production. (R. Kumar et al., 2020). Humans encounter all mercury forms via accidents, pollution, contaminated food, dental care, medical and industrial processes, agriculture, and occupation (Tchounwou et al., 2012). The most absorbed mercury forms are elemental (Hg^0) and methyl mercury (MeHg). Methyl mercury, from fish consumption, is absorbed through gastrointestinal tract and readily crosses placental and blood-brain barriers due to lipid solubility and accumulates in the kidneys, nervous system, and liver with low excretion rates leading to their malfunction (Tchounwou et al., 2012).Chromium in the natural environment exists in two valence states: Cr (VI) and Cr (III). Cr (III) is non-toxic and commonly found in insoluble minerals. It can serve as an essential microelement for organisms at low concentrations. On the other hand, Cr (VI) is highly soluble, mobile, and toxic. Chromium, mainly from industries like metal processing and tanneries, enters air, water, and soil, causing increased environmental concentrations, especially in the hexavalent form [Cr (VI)]. It acts as a mutagen, carcinogen, and teratogen, posing a risk to human health. Cr (VI) can enter the food chain through contaminated drinking water. Exposure to Cr(VI) compounds leads to multi-organ toxicity in humans, including kidney damage, allergies, asthma, and respiratory tract cancer (Tchounwou et al., 2012). The presence of Cr(VI) in wastewater and drinking water represents a significant threat to both humans and ecosystems (Li et al., 2018).

1.1.2. Approach to removing heavy metals

Wastewater treatment methods for heavy metals can be categorized into physical, chemical, and biological methods. Physical and chemical methods are highly effective but require significant investment and can potentially cause secondary pollution. On the other hand, biological methods are advantageous due to their low cost and the absence of secondary pollution (Chen et al., 2018). Therefore search for an alternate energy source as well as an eco-friendly technique is required. Biological removal of heavy metals is preferable to conventional methods due to its cost-effectiveness, eco-friendliness, and efficiency in eliminating low concentrations of heavy metal ions from wastewater. Various bioremediation methods have been proposed for the removal of heavy metals, including bio-sorption (using dead biomass), phytoremediation (plant-mediated removal), bio-reduction (converting oxidation states of metal ions), and bioaccumulation (uptake into intracellular space). These methods involve both metabolically independent (dead materials) and metabolically dependent (live cells of bacteria, fungi, and algae) agents (Singh et al., 2023).

Bio-electrochemical systems (BES) offer a promising solution as an alternative energy source and an eco-friendly technique for wastewater treatment. BES allows for the simultaneous generation of electricity and the remediation of wastewater (Bagchi & Behera, 2020). It harnesses the power of microorganisms to efficiently convert organic compounds into electrical energy or produce valuable fuels such as hydrogen (H_2) and methane (CH_4). BES operates with minimal external energy requirements, making it a sustainable and cost-effective option for energy generation and wastewater treatment (Chakraborty et al., 2020) and one of its example is Microbial Fuel Cell (MFC).

1.1.3. Microbial Fuel Cell

Microbial Fuel Cell (MFC) is a bio-electrochemical system that converts chemical energy into electrical energy through microbial oxidation and the production of ATP. This process involves the release and transfer of electrons to a terminal electron acceptor, resulting in electricity generation (Chaturvedi & Verma, 2016). Microbial Fuel Cells (MFCs) consist of anodic and cathodic chambers made of materials like glass, polycarbonate, or Plexiglas. Each chamber contains an electrode, such as carbon paper, carbon cloth, graphite, or Pt (Platinum), and is separated by a Proton Exchange Membrane (PEM). In the anodic compartment, microbes metabolize organic compounds (electron donors), producing protons and electrons. Protons migrate to the cathode through the cationic membrane, while electrons travel through the external electrical circuit from the anode to the cathode (Kaushik & Singh, 2020). The cathodic chamber contains an electron acceptor, such as oxygen, ferricyanide, or heavy metals, where reduction reactions occur (Muthukalum et al., 2020). Thermodynamically, the cathode compartment should have a higher potential than the anode compartment, enabling spontaneous electron transfer without external power. Microorganisms form a biofilm on the anode's surface, acting as a biocatalyst for electrochemical redox reactions. The type of redox reactions in MFCs depends on the organic matter and electron acceptor used (Muthukalum et al., 2020)MFCs offer a novel approach where organically rich wastewater can be treated, while simultaneously removing and recovering heavy metals, along with electricity generation (Kaushik & Singh, 2020). The redox potential of heavy metals in the cathode chamber is crucial in determining their removal and reduction to a lower oxidation state (Kaushik & Singh, 2020).

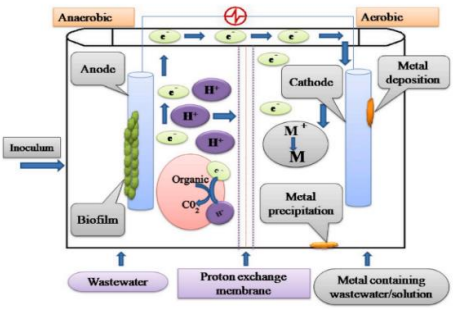

(Kaushik & Singh, 2020)

Figure 1 Schematics of metal removal and power generation by dual chamber MFC with abiotic Cathode

In the MFC, the anode facilitates the anaerobic oxidation of a substrate. A common substrate used, such as glucose, undergoes the following reaction:

Anode: $C_6H_{12}O_6 + 6H_2O \rightarrow 6CO_2 + 24H^+ + 24e^-$ ($E^\circ = 0.014$ V)

The protons and electrons generated from this reaction migrate to the cathode to complete the overall reaction:

Cathode: $6O_2 + 24H^+ + 24e^- \rightarrow 12H_2O$ ($E^\circ = 1.23$ V) (Bagchi & Behera, 2020)

1.2. Current Studies

MFC technology is emerging with potential applications in various areas, including the recovery of pure materials, treatment of specific pollutants, bioremediation, heavy metal recovery, dye decolorization, biosensor applications, denitrification (Kaushik & Singh, 2020). Some of the recent use of MFCs have been described as follows:

The removal efficiency of gold from a solution of pure tetrachloroaurate ions was studied by Al-Asheh et al. (2022) using Microbial Fuel Cell (MFC) technology. The study investigated the impact of various factors on the removal efficiency, including the type of catholyte solution, initial gold concentration, presence of copper ions, pH, and initial biomass concentration. The results demonstrated that after a contact time of 5 hours, a removal efficiency of 95% was achieved for gold ions in a wastewater sample containing an initial concentration of 250 ppm(parts per million), at ambient temperature, using a yeast concentration of 80 g/L. Furthermore, after 48 hours of operating the cell under the same conditions, the removal efficiency reached 98.86% for $AuCl_4$ (tetrachloroaurate) – ions in the solution. When the waste solution had an initial gold concentration of 250 ppm, a pH value of 2, and an initial yeast concentration of 80 g/L, the study achieved a 100% removal efficiency for gold. In contrast, the most favorable condition for copper removal was observed at a pH of 5.2, resulting in removal efficiency of 53% from the waste solution. Overall, these findings highlight the effectiveness of using microbial fuel cell technology for gold removal from solutions containing tetrachloroaurate ions and provide insights into the influence of various factors on removal efficiency. In study, Li et al. (2018) investigated the bio-electrochemical reduction of Cr (VI) to Cr (III) using dual-chamber microbial fuel cells (MFCs) with different types of cathodes. The MFC with a carbon cloth cathode demonstrated complete removal of 80 mg/L Cr (VI), exhibiting higher power density compared to MFCs with carbon brush and carbon felt cathodes. The electrochemical performance of the carbon cloth cathode, as determined by Linear Sweep Voltammetry (LSV), showed an increase with higher initial concentrations of Cr (VI). The MFC achieved a maximum power density of 1221.94 mW/m² when the catholyte contained 120 mg/L Cr (VI), significantly surpassing the power density achieved with catholyte containing 50 mg/L or 80 mg/L Cr (VI). The electrochemical reduction of $Cr_2O_7^{2-}$ (dichromate ions) to (Chromium tri-hydroxide) $Cr(OH)_3$ on the surface of the carbon cloth cathode led to the complete removal of 100% Cr (VI). These findings highlight the potential of MFC technology for the high output power and effective removal of Cr (VI).

The study suggests that scaling up MFCs could offer significant potential for the treatment of heavy metals. Kumar et al., (2020) investigated the bio-anode-assisted removal of mercury (Hg^{2+}) using microbial fuel cells (MFCs). A bio-anode consisting of an acetate-grown microbial electroactive biofilm was utilized to facilitate the reduction of Hg^{2+} ions at the cathode in two-chambered MFCs. The MFCs, with Hg^{2+} as the sole electron acceptor, exhibited an open-circuit voltage of 778±18.4 mV and a power density of 32.6±0.5 mW/m². Through 24-hour tests, the MFCs achieved an impressive Hg^{2+} removal efficiency of up to 98% at a rate of 0.4 mg/L/h, reducing the initial concentration of 10 mg/L to a final concentration of 0.2 mg/L in the catholyte. Analysis using inductively-coupled plasma mass spectrometry confirmed the deposition of up to 8.84 mg/L of Hg on the cathode surface. Remarkably, even a low concentration of Hg^{2+} at 0.270 mg/L was efficiently removed at a rate of 0.19 mg/L/h by the MFCs. Furthermore, the cathode potential varied in response to the concentration or availability of Hg^{2+} in the catholyte. These findings demonstrate the successful utilization of bio-anodes in MFCs for the removal of Hg^{2+}, achieving high removal efficiencies and deposition of Hg on the cathode surface.

1.3. Hypothesis

Null Hypothesis (H_0): There is no significant variation in Heavy metal removal from wastewater

Alternate Hypothesis (H_1): MFC treatment shows significant variation in Heavy metal removal from wastewater

1.4. Objectives

1.4.1. General objectives

The general objectives of the research were to assess the potentiality of the MFCs to remove Heavy Metals from the wastewater of urban Bagmati with concomitant production of electricity.

1.4.2. Specific Objectives

1. Assessment of selected physico-chemical parameters
2. Assessment of selected Heavy Metals
3. To establish lab scale MFC set up/operation
4. Optimization of the MFC
5. Wastewater treatment of Heavy Metals by lab scale MFC set up/operation
6. Estimate and compare % removal of Heavy Metals after MFC treatment

1.5. Rationale

The presence of contaminants like As, Pb, Hg, and Cr in the Bagmati River water poses a significant environmental concern that requires attention and remedial actions. These factors have collectively led to the deterioration of water quality and the ecosystem of the river and have had significant consequences beyond its aesthetic impact (Giri et al.,

2022). The polluted water not only affects the surface water quality but also impacts the subsurface and groundwater quality. Traditional methods of heavy metal removal from water, such as chemical precipitation or adsorption, may have limitations in terms of efficiency, cost-effectiveness, and potential secondary pollution. In this context, exploring innovative approaches like microbial fuel cells (MFCs) that can simultaneously generate bio-electricity and remediate heavy metals can offer a promising and sustainable solution to tackle the pollution in the Bagmati River, but significant challenges persist in reversing the damage and restoring the river's health. Measures such as the establishment of wastewater treatment plants, public awareness campaigns, and stricter waste management regulations are being implemented to mitigate pollution. However, addressing the pollution of the Bagmati River remains a complex task. The visible impact of these efforts is still awaited, indicating the long-term nature of the restoration process. It is crucial to recognize that restoring the ecological balance of the river is not only vital for the well-being of the river itself but also for protecting public health and preserving clean water resources in the region [Pantha et al. (2021)]. By conducting an environmental assessment and remediation study using MFC technology in the Bagmati River, this research aims to contribute to the understanding and development of effective strategies for mitigating heavy metal pollution, ensuring the sustainable management of water resources, and promoting the overall well-being of the ecosystem and surrounding communities.

1.6. Research Scope

Bioremediation with BES, like MFCs, shows promise for heavy metal removal due to its unique ability to create both oxidative and reductive environments within a single cell. (Bagchi & Behera, 2020). The robust microbial consortia in the anodic chamber can handle organic load fluctuations, and highly reactive species, like OOH and OH radicals, are generated in the cathodic chamber via a two-electron pathway. This positions BES as a potential treatment option for emerging contaminants such as heavy metals (Chakraborty et al., 2020). Studies reveal heavy pollution in the urban areas of Bagmati River due to untreated municipal wastewaters, raising significant concerns for sustainable development (Kaushik & Singh, 2020). Pollution in this holy river holds religious significance and heavy metal remediation is essential due to their persistence, bioaccumulation, and toxicity, affecting the food chain. While Microbial Fuel Cells (MFCs) have shown promise in metal recovery and voltage generation, cost-effective modifications are being explored (Chaturvedi & Verma, 2016) to enable MFC commercialization, potentially providing year-round, low-cost electricity from waste resources through decentralized production. Research are conducted to reduce costs and enhance energy sustainability, showing potential for MFC upscaling (Kaushik & Singh, 2020). Studies focus on developing cost-effective, highly porous, conductive electrode materials to enhance microbial biofilm formation and modification techniques, crucial for MFC application advancement (Kaushik & Singh, 2020).

CHAPTER II

LITERATURE REVIEW

With changing human lifestyles and population growth, a wide range of non-biodegradable contaminants are being introduced into water sources like pharmaceuticals, pesticides, detergents, surfactants, food additives, dyes, disinfectants, antibiotics, and heavy metals. These non-biodegradable contaminants pose a significant challenge to water quality management and require appropriate mitigation strategies (Chakraborty et al., 2020).

2.1. Heavy metal Pollution in water bodies

The river and aquatic ecosystem are heavily affected by the direct discharge of industrial effluents and sewage degrading the water quality. As a result of these pollutants, the water quality has deteriorated to the point where it is no longer suitable for activities such as taking holy baths and other purposes, as it was in the past (Pantha et al., 2021). The pollution of water bodies with heavy metals is a global issue due to their persistence in the environment, bioaccumulation in organisms, their ability to magnify in the food chain, and their toxic effects, thus heavy metals are receiving increased attention as hazardous materials (Hazrat et al., 2019).Arsenic, cadmium, chromium, copper, lead, nickel, and zinc are commonly found heavy metals in wastewater, posing risks to human health and the environment (Jaishankar et al., 2014). Heavy metals enter the environment through natural processes and human activities, including soil erosion, weathering of the earth's crust, mining, industrial discharges, urban runoff, sewage, agricultural pesticide use, and more (Jaishankar et al., 2014).

2.2. Contaminants of Concern

Heavy metals such as arsenic, lead, mercury, nickel, chromium, and cadmium are extremely hazardous contaminants. Their high density (> 4000 kg/m^3) and toxic effects, even at low concentrations in the range of nanograms (ng) or micrograms (µg), make them particularly concerning (Bagchi & Behera, 2020). Some of the heavy metals, their properties, sources and mechanism of toxicity are described as follows:

2.2.1. Arsenic

Arsenic, a naturally occurring metalloid, is highly mobile in the environment, and is present in both inorganic and organic forms in natural waterways, with inorganic arsenic being more toxic than organic arsenic. Groundwater can contain both forms of arsenic due to variations in redox conditions (Badr & Al Qahtani, 2013). Under reducing conditions (subsurface water), Arsenite predominates, while arsenate is prevalent in oxidizing environments (Surface water). The pH also plays a significant role at acidic pH > 3, the ionic pentavalent [As^{+5}] forms dominate, while As^{+3} is dominant at alkaline pH 9, and ionic

at highly alkaline pH > 9 (Thakur et al., 2010).Arsenic accumulation in humans occurs through various pathways such as drinking water, crops, and vegetables. Prolonged ingestion of inorganic arsenic, especially when it exceeds 50 µg/L in drinking water, can lead to the development of different types of skin lesions (hyperpigmentation, hyperkeratosis) and malignancies (skin, lung, kidney, and bladder) collectively known as Arsenicosis (Nicomel et al., 2015). Arsenic and its derivatives are mutagenic, teratogenic, and carcinogenic. In Nepal, arsenic contamination in groundwater-based drinking water systems has become a significant environmental health concern, particularly in densely populated areas like the Terai provinces. Cases of dermatosis, melanosis, and keratosis, which are the milder stages of Arsenicosis, have been reported in regions like Bara, Parsa, and Nawalparasi. Additionally, complaints of bronchitis, gastroenteritis, peripheral neuropathy, gangrene of limbs, precancerous skin lesions, and cancer have also been documented (Thakur et al., 2010).

Figure 2 Keratosis; symptom of Arsenicosis reported in Nawalparasi, Nepal, Channel News Asia (CNA), 2022

During arsenic biotransformation, bacteria, algae, fungi, and humans can methylate harmful inorganic arsenic compounds. This process leads to the formation of monomethyl arsenic acid (MMA) and dimethylarsinic acid (DMA). In this biotransformation, inorganic arsenic species (iAs) are enzymatically converted to methylated arsenicals, which serve as end metabolites and biomarkers of chronic arsenic exposure.

The transformation pathway is as follows:

iAs(V) → iAs(III) → MMA(V) → MMA(III) → DMA(V)

Bio-methylation acts as a detoxification process, and the end products, methylated inorganic arsenic such as MMA (V) and DMA (V), are excreted in the urine, indicating chronic arsenic exposure. However, MMA (III), an intermediate product, is not excreted and remains within cells. It's important to note that monomethyl arsenic acid (MMA III), as an intermediate product, is highly toxic compared to other arsenicals. It is believed to

play a significant role in arsenic-induced carcinogenesis, contributing to the development of cancer associated with arsenic exposure (Jaishankar et al., 2014). It's important to note that the toxicity and behavior of arsenic are influenced by its speciation and environmental conditions. Monitoring and understanding these factors is crucial for assessing and managing arsenic contamination in water sources.

2.2.2. Lead

Lead is a highly toxic heavy metal that accumulates in the food chain, affecting various organisms, including humans (Singh et al., 2012). Mining, smelting, industrial effluents, fertilizers, pesticides, and sewage sludge are the main sources of lead pollution. Lead disrupts metabolic activities in plants, leading to reduced seed germination, growth, root and shoot biomass, mineral disruption, inhibited cell division, and photosynthesis. It induces the production of Reactive Oxygen Species (ROS) and enhances antioxidant enzyme activity, causing harmful effects like inhibition of photosynthesis, ATP production, lipid peroxidation, and DNA damage. While plants have mechanisms to adapt to heavy metal concentrations, excessive accumulation beyond their detoxification capacity can be toxic (Malar et al., 2014).In humans, lead is absorbed into the bloodstream and stored in soft tissues, bones, and teeth, with a majority (95%) accumulating in bones and teeth (Sanders. T et al., 2009). Lead poisoning stems primarily from oral ingestion and gut absorption, with the absorbed lead traveling to organs like the liver, kidneys, and bones, accumulating over time; its distribution to various tissues hinges on red blood cells binding lead to hemoglobin, while its detrimental impact on the central nervous system, especially in children, links high lead intake, especially during anemia, to lowered intelligence and impaired motor function(A. Kumar et al., 2020).

Gautam et al. (2020) conducted a study on 50 rag pickers in Kathmandu, finding that the mean Blood Lead Level (BLL) among the participants was 11.6 ± 7.23 µg/dL (microgram/deciliter). Although 54% of the cases had a high eosinophil count, it was not significantly associated with BLL. In another study focused on workers involved in electronic waste recycling, the mean BLL was higher at 12.89 µg/dL. Four cases with beta-Thalassemia trait had high BLL levels. However, no significant association was found between BLL and the number of years worked as a rag picker, and no significant associations were observed between BLL and hematological and biochemical parameters. In a study by Dhimal et al. (2016), 64.4% of the 312 children aged 6-36 months had BLLs exceeding the CDC cut-off point (≥ 5µg/dL). The presence of enamel paints on various parts of the house was significantly associated with BLLs. Children who played with dirt and dust had BLLs 4.5 times higher. Ethnic groups such as Dalits, disadvantaged Janajatis, non-Dalit Terai caste groups, religious minorities, and relatively advantaged Janajatis had significantly higher BLLs compared to the upper caste group. The study emphasizes the need to address lead exposure, particularly by reducing the lead burden in paints and raising awareness about the risks of lead poisoning in childhood.

2.2.3. Mercury

Mercury is a toxic heavy metal known for causing public health disasters in Minamata Bay, Japan, and Iraq. It exists in different forms: inorganic mercury, which includes metallic mercury (Hg^0), mercury vapor, and mercurous or mercuric salts (Hg^{2++} or Hg^{++}), and organic mercury, which involves mercury bonded to carbon-containing structures (methyl, ethyl, phenyl groups). The behavior, pharmacokinetics, and clinical impact of mercury vary depending on its chemical structure. There is some conversion between the different forms of mercury within the body. Anthropogenic activities like agriculture, municipal wastewater discharges, mining, incineration, and industrial wastewater discharges are major sources of mercury pollution. Outgassing of mercury from dental amalgam, ingestion of contaminated fish, and occupational exposure are identified by the World Health Organization as the primary routes of human exposure to mercury (Bernhoft, 2012). Inhaled elemental mercury vapor is easily absorbed through mucus membranes and the lungs, oxidizing to other forms. However, a considerable amount of elemental mercury can deposit in the brain. Methyl mercury, on the other hand, is readily absorbed through the gut, accumulates in various tissues, and undergoes demethylation upon entering the brain, converting to elemental mercury. The various forms of mercury have distinct biological behaviors and implications, and their interconversion within the body contributes to their toxicity (Bernhoft, 2012). Human exposure to methylmercury primarily occurs through the consumption of contaminated aquatic animals. In the study of Thapa et al (2014), the risk of mercury exposure through fish consumption from Lake Phewa in Nepal was investigated. Fish consumption from Lake Phewa varied significantly among different groups, with hotel owners and fishermen having the highest consumption. This puts hotel owners at a higher risk of mercury (MeHg) intake compared to others since it exceeded the Provisional Tolerable Weekly Intake (PTWI) of 1.6 µg per kg body weight of MeHg as recommended by FAO/WHO (2003). Among commercially important fish species from higher trophic positions, *Tilapia* is considered safer for consumption due to lower mercury levels. However, based on research, a 60 kg person can safely consume up to 2 kg of fish per week without exceeding the Provisional Tolerable Weekly Intake (PTWI) for mercury, thus avoiding health risks associated with mercury poisoning at current contamination levels.

Mercury primarily affects the brain but can impair various organs, including nerves, kidneys, and muscles. It disrupts membrane potential and intracellular calcium homeostasis. Mercury damages protein structures, including tertiary and quaternary structures, and alters cellular function by binding to selenohydryl and sulfhydryl groups. This interaction with methyl mercury hampers cellular structure (Jaishankar et al., 2014).

2.2.4. Chromium

Chromium exists in different oxidation states, with the most common forms being trivalent (Cr^{+3}) and hexavalent (Cr^{+6}).Cr^{+3} is immobile and insoluble in water, while Cr^{+6} is highly soluble and mobile. Speciation analysis is important for understanding the activities of these metal ions in the environment. Hexavalent chromium (Cr^{+6}), in its oxidized state,

is toxic to humans and is a concern in groundwater contamination. Industries such as metallurgy, electroplating, paint production, tanning, wood preservation, chemical production, and pulp and paper production contribute significantly to chromium pollution. The pollution caused by chromium has adverse effects on biological and ecological species, with hexavalent chromium being of particular concern. Excessive levels of chromium beyond permissible limits are destructive to plants and disrupt biological processes. It enters the food chain through the consumption of plant materials. Phyto-toxicity caused by chromium includes reduced root growth, leaf chlorosis, inhibition of seed germination, and decreased biomass. Various plants, including maize, wheat, barley, cauliflower, Citrullus, and vegetables, are affected by chromium toxicity, resulting in chlorosis and necrosis (Jaishankar et al., 2014).

In the environment, trivalent chromium (Cr^{+3}) has weak membrane permeability and is generally considered harmless. However, hexavalent chromium (Cr^{+6}) is more active in penetrating cell membranes, particularly through channels for anions such as sulfate (SO_4^{2-}) and hydrogen phosphate (HPO_4^{2-}), as well as through phagocytosis.Cr^{+6} is a strong oxidizing agent and can be reduced to pentavalent and tetravalent chromium species, which are different from Cr^{+3}. Glutathione plays a role in stabilizing the pentavalent form, and intracellular reduction of Cr^{+6} away from the target region is considered a detoxification mechanism. However, if intracellular reduction occurs near the target site, it may activate chromium. Interactions between Cr^{+6} and biological reductants like thiols and ascorbate lead to the generation of reactive oxygen species, including superoxide ion, hydrogen peroxide, and hydroxyl radical. This oxidative stress in the cell can cause damage to DNA and proteins. (Jaishankar et al., 2014)

Table 1 Permissible limits for various heavy metals in wastewater treatment effluents

Heavy metals	WHO Permissible Limits(mg/L)	USEPA Permissible Limits(mg/L)	Health Hazards
Arsenic(As)	0.5	-	Carcinogenic, producing liver tumors, skin, and gastrointestinal effects
Lead(Pb)	0.01	0.006	Suspected carcinogen, loss of appetite, anemia, muscle, and joint pains, diminishing IQ, cause sterility, kidney problem, and high blood pressure
Mercury(Hg)	0.001	0.00003	Corrosive to skin, eyes, and muscle membrane, dermatitis, anorexia, kidney damage, and severe muscle pain
Chromium(Cr)	0.05	0.05	Suspected human carcinogen, producing lung tumors, allergic dermatitis

WHO, 4th ed. (2017); USEPA (2018)

2.3. Microbial Fuel Cell Technology

In 1791, Luigi Galvani observed the bio-electric phenomenon (Galvani, 1791), while in 1893, Friedrich Wilhelm Ostwald established connections between fuel cell components and

chemical reactions. In 1910, Michael Cresse Potter demonstrated organisms generating current and voltage during his organic compound degradation research (Potter M. C, 1908). He later utilized *Saccharomyces* and *Escherichia coli* cultures with platinum electrodes for energy generation, creating a rudimentary microbial fuel cell (MFC) in 1911(Potter M.C, 1911). The MFC gained traction in 1960 when space agencies aimed to convert waste into electricity for long space flights. Early biological fuel cells employed bacteria and algae, with the Rohrback group crafting a prototype using *Clostridium butyricum* for hydrogen production from glucose fermentation (Rohrback G. H, 1962). The incorporation of ceramics in MFCs for simultaneous power generation and wastewater treatment was pioneered by Jeong et al. in 2008. Although successful pilot studies (You et al., 2021) have occurred and ongoing research seeks MFC optimization, challenges like scalability technology and cost hinder widespread commercial adoption (James, 2022).

2.3.1. Types of MFCs

Based on the design, there are mainly two types of MFC, Single-chambered and Double-chambered MFC.

2.3.1.1. Single Chambered MFCs

In a single-chambered Microbial Fuel Cell (MFC), the anode and cathode are located in the same compartment, sharing the same electrolyte. The cathode is exposed to air and is porous, allowing the diffusion of protons and their reduction on the side exposed to oxygen. Cathodes can be made of porous carbon electrodes or Proton Exchange Membrane (PEM) bonded with flexible carbon cloth electrodes. To prevent drying, cathodes are coated with graphite, and electrolytes are added steadily, acting as catholyte. Proper water or fluid management is crucial to prevent cathode drying and maintain efficiency. However, single-chamber MFCs have disadvantages such as liquid leakage, water evaporation, and oxygen diffusion into the anodic chamber. These issues can be addressed by using Polytetrafluoroethylene (PTFE) as an additional diffusion layer on the cathode. The use of PTFE has been found to improve columbic efficiency and maximum power density. This approach is a common and effective method for electricity generation during wastewater treatment in the sewage industry on a large scale. (Muthukalum et al., 2020).

2.3.1.2. Double-Chambered MFCs

Double-chambered Microbial Fuel Cells (MFCs) consist of two separate compartments, one for the anode and the other for the cathode. These compartments are connected through a Proton Exchange Membrane (PEM) or a salt bridge, allowing the transfer of protons and completion of the circuit. The PEM or salt bridge acts as a barrier to prevent oxygen diffusion into the anodic chamber and minimize solution crossover, resulting in higher Columbic efficiency compared to single-chambered MFCs. However, scaling up double-chambered MFCs can be challenging, leading to more focus on single-chambered MFCs in research and utilization. Double-chambered MFCs operate in batch mode and require a suitable growth medium for microbial culture. They can generate power in diverse conditions and offer flexibility in compartment design. The cathodic compartment

does not necessarily require a catholyte and can utilize air supply alone. This configuration is also effective in the removal of heavy metals with positive redox potentials such as silver, gold, and chromium. (Muthukalum et al., 2020)

2.3.2. Components of MFC

2.3.2.1. Anode

Anodes in Microbial Fuel Cells (MFCs) play a crucial role as biofilm substrates and current collectors. Carbon is the preferred material for anodes due to its versatility, non-reactivity, high electrical conductivity, and biocompatibility. Carbon cloth and carbon felt, being more porous than graphite sheets or carbon paper, provide larger surface areas for microbial colonization. The introduction of graphite brush anodes has further enhanced the electrode surface area within a given reactor volume. Nanomaterials with high conductivity and surface area have also been utilized in the anode chamber of MFCs. (Vishwanathan A. S. 2021).

2.3.2.2. Cathode

Cathodes in Microbial Fuel Cells (MFCs) serve as the interface for electron transfer, combining electrons, protons, and the terminal electron acceptor. They play a critical role in determining the efficiency of MFCs. Cathodes can be classified as chemical or biological, depending on the type of electron acceptor used. Oxygen is commonly used as a terminal electron acceptor but requires expensive platinum catalysts due to the poor kinetics of the oxygen reduction reaction. To reduce operating costs, carbon-based materials and nanocomposites without precious metals have been developed as economical alternatives for cathodes, improving the efficiency of the oxygen reduction reaction. (Vishwanathan A. S. 2021).

2.3.2.3. Proton Exchange Membrane

Proton exchange membranes, like Nafion®, were initially used in MFCs to selectively allow protons into the cathode chamber, but they were costly. Expensive membranes have been replaced with alternative options such as Zirfon® (Pasupuleti et al, 2010), ion exchange membranes (Leong et al, 2013), ceramic filtration membranes (Yang et al, 2016), polymeric membrane separators (Bakonyi et al, 2018), and/activated carbon separators (Gao et al, 2018), silk fibroin membranes (Pasternak et al, 2019), and polystyrene (Mathuriya and Pant, 2019). These materials offer general transport properties and are more cost-effective for MFC applications (Vishwanathan A. S. 2021).

2.3.2.4. Microbes

Mixed consortia of electrogenic and electro-trophic microbes are more effective in generating current in MFCs compared to pure cultures of bacteria. Synergistic interactions between different microbial species within these consortia allow for efficient utilization of available substrates, leading to the formation of electrochemically active biofilms. The growth and performance of these biofilms can be enhanced through selective control of growth conditions, synthetic biology techniques, and engineering approaches. (Vishwanathan A. S. 2021).

Numerous factors affect MFC performance, including substrate, electron transfer mechanism, temperature, pH, terminal electron acceptors, configuration, PEM type, and electrode material (Aghababaie et al., 2015). Electrode material is crucial for MFC performance as it directly influences the kinetics of the system (Mustakeem, 2015).Some of the factors are described as follows:

A. Temperature

The performance of MFCs is significantly influenced by temperature, with optimal power generation and COD removal observed at temperatures between 30°C and 40°C (Heidrich et al., 2018). Extremely high (>45°C) or low (<15°C) temperatures hinder power generation, while the best COD removal occurs within the range of 25-35°C. MFCs show tolerance to temperature changes in real-world wastewater treatment applications, with power generation changes typically less than 10% between 20-35°C (Heidrich et al., 2018). Notably, the optimal temperatures for power generation may differ from those for COD removal, as distinct microbial species are involved in biodegradation and electrochemical activity (Li & Chen, 2018).

B. pH

The anode pH significantly impacts MFC performance. Optimal pH between 6.5 and 7.5 results in higher power densities, up to over 1200 mW/m^2, and nearly three times higher COD removal compared to extreme pH ranges. Slower microbial activities occur at sub-optimal pH levels. Low power generation at high pH (>10) may be due to poor proton transfer across the PEM, known as a rate-limiting factor (Strik, D. P, 2013). Below pH 3, reactor performance deteriorates as the acidic environment becomes unsuitable for most electrogenic microbes, though certain species can perform well even under severe low-pH conditions (Jia. Q et al, 2014).

C. External Resistance

External resistance (R_{ext}) in MFCs restricts electron flow from the anode to the cathode, influencing potential (V) and current (I) outputs according to Ohm's Law (Rismani-Yazdi et al., 2011). Increased external resistance reduces power density and treatment efficiency. Anode potential, determining electron availability, is regulated by external resistance, impacting growth competition between electrogenic and non-electrogenic microbial communities. Microbial communities are most susceptible to external resistance changes when anode potential is low. Power generation in MFCs weakened at extremely low (e.g., 10 Ω) or high (e.g., 10 kΩ) external resistances. Low resistance hindered the microbial acceptance of the anode as an electron acceptor due to its low redox potential, while high resistance resembled an open circuit, impeding electron transfer by the microbes (S. Li & Chen, 2018).

D. Substrate type

Wastewater suitability depends on substrate biodegradability, pH, ionic strength, and toxicity (Heidrich et al., 2018). Higher ionic strength reduces the internal resistance, leading to increased cathode potential and overall circuit voltage. Swine wastewater and

landfill leachate are rich in biodegradable organics and high ionic strengths but may contain toxic compounds like ammonium and heavy metals, negatively impacting microbial growth and fuel cell performance (Li, S., & Chen, G. 2018).

2.4. Redox Potential of Heavy Metals

The redox potential of metals plays a significant role in determining their removal or reduction to a lower oxidation state in the cathode chamber of an MFC. Metals that act as electron acceptors in MFCs undergo redox reactions, and their removal or reduction depends on their specific redox potentials.

2.4.1. Arsenic

The redox potential of As (III) was determined to be 0.47 V concerning a conventional three-electrode cell using a modified glassy carbon electrode (GCE) as the working electrode with a surface area of 0.07 cm^2. The reference electrode employed was Ag/AgCl (saturated KCl), and the counter electrode used was a platinum wire s

$$H_3AsO_3 + 3H^+ + 3e^- \longrightarrow As(S) + H_2O$$ (Rajkumar et al., 2011)

2.4.2. Lead

The redox potential of Pb(II) was determined to be -0.6 V using a three-electrode setup. The working electrode used was a modified glassy carbon electrode (Φ= 3 mm), the reference electrode was Ag/AgCl with KCl as the electrolyte, and the counter electrode was a platinum wire (diameter: 1mm). The electrolyte support used was an acetate buffer ssolution with a concentration of 0.1 M and a pH of 4.5 (Zinoubi et al., 2017).

$$Pb^{2+} + 2e^- \rightleftharpoons Pb(S)$$ (Zinoubi et al., 2017)

2.4.3. Mercury

The redox potential of Hg(II) was determined to be 0.3 V using a three-electrode setup. The working electrode used was a GCE (diameter= 3 mm), the reference electrode was Ag/AgCl with KCl as the electrolyte, and the counter electrode was a platinum wire (Φ= 1 mm). The electrolyte support used was an acetate buffer solution with a concentration of 0.1 M and a pH of 4.5 (Zinoubi et al., 2017).

$$Hg^{2+} + 2e^- \rightleftharpoons Hg(S)$$ (Zinoubi et al., 2017)

The high redox potential of mercury (Hg^{2+}) at +0.91 V makes it highly efficient in accepting electrons, allowing it to be effectively removed from contaminated wastewater using an MFC (Kaushik & Singh, 2020).

2.4.4. Chromium (VI)

The redox potential of Cr(VI) was determined to be 0.77 V using a three-electrode configuration. The working electrode employed was a glassy carbon electrode (GCE) with an exposed area of 0.0707 cm^2 from CH Instruments, Austin, TX, USA. The reference electrode used was Ag/AgCl with a 3 M KCl electrolyte, and the counter electrode was made of platinum (Stojanović et al., 2018).Chromium (VI) possesses a redox potential of +1.33 V in an acidic environment, surpassing the redox potential of oxygen (O_2) at 1.23 V.

Consequently, it can function as a promising terminal electron acceptor, as demonstrated by the following reaction:

$$Cr_2O_7^{2-}(aq) + 14H^+ + 6e^- \rightarrow 2Cr^{3+}(aq) + 7H_2O;\ 1.33\ V$$

$$Cr^{3+} + 3e^- \longrightarrow Cr(S)$$

$$CrO^{2-} + 2H_2O + 3e^- \longrightarrow Cr^0 + 4OH^-$$

(Kaushik & Singh, 2020)

2.5. Remediation of Heavy Metal by MFC

Microbial fuel cells are commonly used with only the anode chamber for the degradation of pollutants through bio-catalytic oxidation. The cathode chamber serves as the circuit closure or the destination for electrons and protons. Various compounds with high redox potentials, such as oxygen, ferricyanide, permanganate, H_2O_2, nitrate, trichloroethene, and perchlorate, can be utilized as effective electron acceptors in the cathode chamber (Mathuriya et al, 2014). Metal ions present as contaminants in wastewater, which do not biodegrade, can be used as electron acceptors to reduce and precipitate them. This approach enables microbial fuel cells to not only remove heavy metal ions from wastewater but also recover them. The reactions involved in microbial fuel cells for wastewater treatment and metal recovery include bio-electrochemical, electrochemical, and chemical reactions, occurring in the anode and cathode chamber. Bio-electrochemical reactions occur at the anode, where electrons are released during microbial metabolism. These electrons then travel through an external load and reach the cathode chamber, where electrochemical reactions, such as the reduction of oxygen or metal ions, take place (Liu et al, 2011). Numerous studies have explored MFCs' ability to remove heavy metals, but the mechanisms behind their removal remain inadequately understood. The commonly investigated removal mechanisms in abiotic cathodes include reduction and deposition at the cathode surface (Colantonio, 2016; Isosaari and Sillanpää, 2017). Additionally, heavy metal removal in abiotic cathodes has been demonstrated through chemical precipitation and electrochemical reduction (Colantonio, 2016).In bio-cathodes, heavy metal removal is demonstrated through various mechanisms, such as bio-reduction, bioaccumulation, bio-sorption, and bio-mineralization (Wu et al., 2017).Y. Li et al., 2016 conducted research using a single-chambered Microbial Fuel Cell (MFC) operated with synthetic water supplemented with a small volume of anaerobic sludge and an initial concentration of 0.2 mg/L of arsenic (As). The MFC utilized a carbon fiber felt electrode (1 cm x 4 cm x 4 cm) as the anode and a plain carbon paper electrode coated with 0.5 mg/cm^2 of platinum on one side, with a projected surface area of 16 cm^2, as the cathode. With the use of a 1000Ω resistor, the MFC achieved a maximum power density of 752.6 ± 17 mW/m^2 and achieved nearly 100% removal of As(III) within 7 operational days, completely oxidizing it to As(V). The MFC also exhibited a total organic carbon removal efficiency of 84%. High-throughput 16S rRNA gene pyrosequencing analysis revealed the presence of arsenic-resistant bacteria, including *Actinobacteria, Comamonas*, and *Pseudomonas,* as well as arsenic-oxidizing bacteria such as *Enterobacter*. Additionally, electrochemically

active bacteria like *Lactococcus* and *Enterobacter* were identified. These microorganisms interacted synergistically, playing key roles in As(III) oxidation and bioelectricity generation within the MFC system. In the process of Zero Valent Iron (ZVI) treatment, arsenic is typically removed through co-precipitation and adsorption by hydrous ferrous oxides (HFOs) formed via the oxy-hydrolysis of Fe^{2+} in water. The released Fe^{2+} further undergoes oxidation to Fe^{3+} by O^{2-}producing oxidants such as H_2O_2 and $OH^{\cdot}$. This oxidation process converts As(III) to As(V).In an experiment combining a Microbial Fuel Cell (MFC) with ZVI, the MFC supplies the necessary electrical energy to drive the ZVI corrosion process. A single-chamber air cathode MFC was utilized, and a beaker with two electrodes facilitated ZVI corrosion and arsenic removal. This particular study achieved the removal of As(V) from the aqueous solution. The concentration of As(III) decreased from 300 to 9.8 µg/L, with a maximum power density generated of 477 mW/m^2 (Xue et al. 2013).

In the study by Rajendran et al., 2021, a double-chamber Microbial Fuel Cell (MFC) was employed to simultaneously generate power and remove lead (Pb^{2+}) using *Shewanella putrefaciens* as the biocatalyst. Synthetic water served as the anolyte with a catholyte; lead concentration of 20 ppm at pH 3. The cathodic electrode consisted of carbon cloth coated with platinum. The anode was modified with iodine (I_2) doped polythiophene nanoparticles (PTh-NP) on carbon cloth (CC). The modified CC with I_2-doped PTh-NP exhibited enhanced electrochemical characteristics compared to pristine CC and CC with undoped PTh-NP. The electrical conductivity was further improved with the development of a biofilm on the modified CC, observed after 51 hours using cyclic voltammetry. Lead removal was evaluated for concentrations of 20 ppm, 30 ppm, and 40 ppm. The optimal concentration for lead removal was determined to be 30 ppm, resulting in a maximum power density of 0.84 W/m^2 and a current density of 1.45 A/m^2 at an optimum resistance of 250 Ω. After the process, a Total Organic Carbon (TOC) removal efficiency of 95.1% and a Pb^{2+} removal efficiency of 89.6% were achieved for the optimal lead concentration. Wang et al., 2011 successfully demonstrated the removal of Hg^{2+} as an electron acceptor in a two-chambered microbial fuel cell (MFC). The MFC utilized graphite felt (anode) and carbon paper (cathode) with dimensions of 3.5 x 3 cm and 1.12 cm, and surface areas of 35.6 cm^2 and 21 cm^2, respectively. The anolyte consisted of sludge mixed with artificial wastewater, while the catholyte was wastewater supplemented with $HgCl_2$. An anion exchange membrane (AMI-7001) with a surface area of 19.6 cm^2 (diameter=5 cm) was used. The study found that the initial pH had an impact on the efficiency of Hg^{2+} removal due to electrochemical and chemical reactions. Optimization of the pH, using an initial Hg concentration of 50 mg/L, revealed the following effluent Hg concentrations after a 5-hour reaction: 3.08 ± 0.07 mg/L (pH 2), 4.21 ± 0.34 mg/L (pH 3), 4.84 ± 0.00 mg/L (pH 4), and 5.25 ± 0.36 mg/L (pH 4.8). In a 10-hour reaction, the effluent Hg concentration ranged from 0.44 mg/L to 0.69 mg/L for different initial Hg^{2+} concentrations (25, 50, and 100 mg/L). Lower initial pH and higher Hg^{2+} concentration were found to result in a larger maximum power density. The study achieved a maximum power density of 433.1 mW/m^2 using a 100 mg/L Hg^{2+} solution at pH 2. In the study, Song et al., 2016 demonstrated a

simple method for fabricating a bio-cathode in a chromium (VI) reducing microbial fuel cell (MFC). They used a three-set of double-chambered MFCs operated at 25°C. The anode consisted of a graphite felt electrode (50 x 20 x 5 mm) and anolyte containing activated sludge with a glucose culture medium, maintained at pH 7.0. The catholyte contained a cathode medium with 40 mg/L of potassium dichromate. Three different cathodes were tested: graphite felt cathode, graphite felt bio-cathode, and graphene bio-cathode. A Nafion 117 proton exchange membrane was used, and an external resistance of 1000Ω was applied. The results showed that the MFC with the graphene bio-cathode achieved the highest voltage of 411 ± 12 mV, a power density of 163.8 ± 3.4 mW/m^2, and 100% chromium removal efficiency. The graphite-felt bio-cathode performed moderately, with a voltage of 167 ± 11 mV, a power density of 28.6 ± 0.1 mW/m^2, and 58.3 ± 0.2% chromium removal. The graphite felt cathode had the lowest performance, with a voltage of 107 ± 10 mV, a power density of 20.8 ± 0.3 mW/m^2, and 17.5 ± 2.5% chromium removal.

2.6. Determination of heavy metals concentration using Differential Pulse Anodic Stripping Voltammetry

Differential pulse voltammetry (DPV) measures the difference between the current just before the end of the pulse and just before the application of the pulse. The peak-shaped waveform occurs when the difference between these currents versus the applied potential graph is plotted (Kurbanoglu et al., 2017).In DPV, small amplitude, short pulses are superimposed on a linear ramp. Current is measured before the application of the pulse and at the end of each pulse, and the difference between the currents is calculated. This procedure effectively reduces the background current due to the DC ramp, and thus this procedure results in a Faradaic current free of most capacitive current. The major advantage of DPV is low capacitive current, which leads to high sensitivity (Venton & DiScenza, 2020). The study conducted by Devi et al. (2018) utilized the CHI 760E Electrochemical Workstation to perform Differential Pulse Voltammetry (DPV) for the detection of Hg ions. The experimental setup involved a three-electrode cell configuration, with a Glassy Carbon Electrode (GCE) of 3mm diameter as the working electrode, a platinum electrode as the counter electrode, and an Ag/AgCl 1M KCl (Silver /Silver Chloride 1M Potassium Chloride) electrode as the reference electrode. The electrolyte used was 0.1M PBS (Phosphate Buffer Solution). The GCE underwent three different modifications: Bare GCE, GCE coated with reduced graphene oxide (rGO) and thiol groups (GCE/rGO/-SH), and GCE coated with reduced graphene oxide, thiol groups, and gold nanoparticles (GCE/rGO-SH/Au-NPs).To prepare the electrodes for analysis, they were dipped in a standard solution containing 5µM Hg^+ (5ml) for 20 minutes and then dried in a hot air oven for 5 minutes. Subsequently, the electrodes were immersed in distilled water to remove any loosely bound soluble materials on the electrode surface. DPV was performed using the CHI 760E while the electrodes were placed in an electrochemical vessel containing 0.1M PBS. The scan potential ranged from 0 to 0.3 volts, and the scan rate was set to 100 mV/s. Notably, no oxidation peak was observed at the oxidation potential of +0.172V when using the bare GCE and GCE/rGO-SH electrodes.

However, a strong peak was observed at +0.172V when using the working electrode GCE/rGO-SH/Au-NPs. The optimized electrode, GCE/rGO-SH/Au-NPs, was utilized for the detection of Hg in a real tap water sample. Two separate solutions were prepared by mixing 1µM and 5µM concentrations of Hg with 1ml of the tap water sample, resulting in a final volume of 10ml. Differential Pulse Voltammetry (DPV) was performed using the optimized electrode with the prepared Hg solutions. The DPV results demonstrated a % recovery of 94% for the 5µM Hg concentration and 97.5% for the 1µM Hg concentration. This indicates that the electrode successfully detected and quantified the presence of Hg in the tap water sample, with a high level of accuracy and sensitivity. These findings highlight the potential of the GCE/rGO-SH/Au-NPs electrode as a reliable and efficient tool for the analysis of Hg in real-world water samples, such as tap water. The high percentage of recovery suggests that the electrode can be a valuable tool for environmental monitoring and quality assessment of water sources (Devi et al., 2018). Wu et al., (2016) used the Gamry Interface 1000 potentiostat to perform Differential Pulse Voltammetry (DPV) for the determination of Cr(III) using a modified Screen Printed Carbon Electrode (SPCE, DRP-110, 3.4×1.0×0.05cm). The working electrodes used were a bare SPCE, chitosan-modified SPCE (Chi-SPCE), gold-modified SPCE (Au-SPCE), and chitosan gold-modified SPCE (Chi-Au SPCE). The reference and counter electrodes used were Ag/AgCl and Platinum, respectively. In their experiment, a 10µM concentration of Cr(III) was mixed with 0.1M acetate buffer of pH 5.0 in an electrochemical vessel. The metal ion was deposited onto the working electrode by applying a deposition potential of -1.3V for 180 seconds. Differential Pulse Voltammetry was then performed using the following parameters: scan potential -1.3 to 0.8V, pulse amplitude 50mV, pulse width 0.05 seconds, sample period 0.1 seconds, and step potential 2mV.No peak was observed at bare SPCE and Au-SPCE, but a strong peak for Cr(III) was detected at +0.55V when using Chi-SPCE. The peak was further enhanced when Chi-Au-SPCE was used. Chi-Au-SPCE was selected for the detection of Cr(III) in wastewater from the plating industry in Malaysia. To prepare the wastewater sample for analysis, the pH was initially adjusted to 1.5 by adding H_2SO_4. Cr(VI) in the wastewater was then converted to Cr(III) by the addition of Na_2SO_3. The mixture was shaken in a water bath for 2 hours, and the same DPV parameters were applied for analysis. A standard calibration curve of concentration versus current was prepared using concentrations ranging from 0 to 100 µM. Based on this calibration curve, a concentration of 31.33 µM of Cr(III) was detected in the wastewater sample.

CHAPTER III

METHODOLOGY

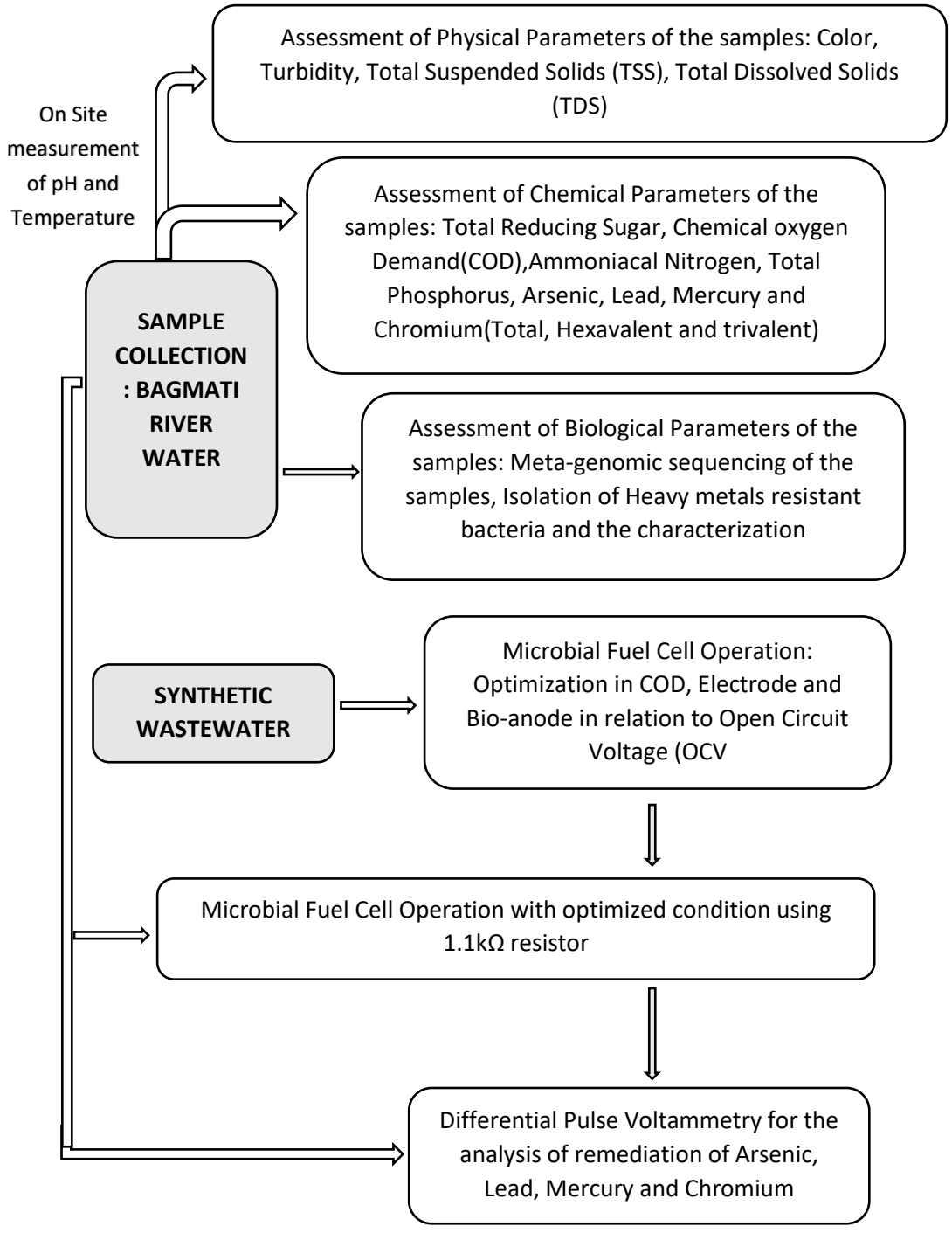

Figure 3 Research Design of the study

3.1. MATERIALS

All the instruments, media, chemicals, and various reagents used during the research had been attached in Appendix I, and II, respectively.

3.2. SAMPLING SITES

A total of six water samples were collected from the Bagmati River, encompassing three different sites: Kupondol, Balkhu, and Chovar. The samples were collected during two distinct seasons; Winter and Summer. Out of the six samples, three were collected during January/February, while the remaining three were collected during June/July.

3.3. SAMPLE COLLECTION AND ASSESSMENT

The sampling process involved several steps. Firstly, the sampling bottles were labeled with the name of the sampling site and the date of collection. On-site measurements of pH (pH meter PH5011) and temperature were taken using a pH meter and thermometer, respectively. Before sampling, the bottles (2.25L) were rinsed with water from the Bagmati River. The sampling was conducted by immersing the hands to a depth of approximately 15-20 cm (Musselman, 2012), and the bottles were capped while still submerged in the water. For the detection of Arsenic, Lead, and Mercury using Atomic Absorption Spectroscopy (AAS), small 500ml bottles provided by the ENPHO (Environment and Public Health Organization) laboratory were used. For the analysis of Mercury, the bottles contained 2.5ml of 12 N HCL, while for the analysis of Arsenic and Lead, they contained 2.5ml of 15N HNO_3 priory. The bottles were then transferred to the Biofuel Laboratory of the Central Department of Biotechnology in Kirtipur, Kathmandu (**Note:** no acid were added in the bottle), and to the ENPHO laboratory in Thapagaun, Baneshwor (**Note:** Acid added bottle with sample), for further study.

Figure 4 Sample Collection in June/July, A: Kupondol B: Balkhu C: Chovar

The collected samples were taken to the Biofuel laboratory in Central Department of Biotechnology for analysis of various physical, chemical, and biological parameters. This analysis aimed to determine the characteristics of the samples.

3.3.1. QA/QC (Quality Assurance/Quality Control)

Safety measures were followed during sampling, including the use of gloves and aprons. The sample bottles (2.25L) were pre-rinsed with river water before sample collection. After measuring pH and temperature, the measuring device was rinsed with distilled water and wiped dry. The external surfaces of the bottles were also wiped dry and securely capped before transport to the ENPHO laboratory and the Biofuel laboratory in the Central Department of Biotechnology. During the bacterial DNA extraction from water samples, duplicate extractions were performed to mitigate the risk of obtaining no bands during gel electrophoresis. Following this, during the isolation of heavy metals resistant bacteria, MFC operation, BSL-1 (Biosafety Level) cabinet was used and for MFC Operation Sterilized Synthetic water was utilized.

3.3.2. Physical Parameters of the Samples

Total Suspended Solids (TSS) and Total Dissolved Solids (TDS) were determined through gravimetric analysis. The Whatman filter paper was dried at 58°C, and the initial weights of the filter paper and the collection vessel (e.g., conical flask) were recorded. A filtration setup was prepared using pre-weighed filter paper and a conical flask. A 50ml sample was filtered, and the filtrate was collected in the conical flask. The filter paper was then dried in an oven at 58°C to determine TSS. For TDS analysis, the filtrate was boiled until a residue was left behind. TDS and TSS were calculated using the formulas.

$$\mathrm{TSS(mg/L)} = \frac{\mathrm{Final - Initial\ weight\ of\ filter\ paper\ (mg)}}{\mathrm{Volume\ of\ sample(ml)}} \times 1000$$

$$\mathrm{TDS\ (mg/L)} = \frac{\mathrm{Final - Initial\ weight\ of\ Conical\ Flask\ (mg)}}{\mathrm{Volume\ of\ sample(ml)}} \times 1000$$

(Ma et al., 2020)

3.3.3. Chemical Parameters of the Samples

3.3.3.1. Total Reducing Sugar (Smith & Cresser (Eds.), 2003)

To construct a standard calibration curve, reference solutions with concentrations ranging from 10mg/L to 200mg/L were prepared using a stock solution of 1000mg/L Glucose. Each reference solution had a final volume of 3ml. For the blank and sample, 3ml of deionized water and the sample were taken in separate test tubes. To each test tube, 1 ml of DNS (Di-Nitro Salicylic Acid) reagent was added, and the tubes were then placed in boiling water for 8 minutes. The color change from yellow to orange indicated the presence of Glucose. Absorbance measurements at 540nm were performed using a UV-Spectrophotometer (UV- 1800), and background correction was done using the absorbance reading of the blank solution.

3.3.3.2. Chemical Oxygen Demand (Smith & Cresser (Eds.), 2003)

Chemical Oxygen Demand (COD) is an analytical parameter used to assess water quality and measure the level of organic pollution in water bodies. It operates on the principle of oxidizing almost any organic species using a strong oxidizing agent under acidic conditions. To determine COD, a standard curve was constructed using a series of reference solutions with concentrations ranging from 50 mg/L to 4000mg/L. These solutions were prepared from a stock of 4000mg/L and 1000mg/L Potassium Hydrogen Phthalate, with a final volume of 2ml. For each reference solution, blank, and sample, 1.2ml of Digestion Solution was added, followed by the addition of 2.8ml of catalyst solution (preparation mentioned in Appendix II). The tubes were shaken after each chemical addition. The tubes were then placed in a digester and inside a hot air oven at 150°C for 2 hours. After digestion, the tubes were cooled, and background correction was performed by measuring the absorbance at 600nm using a UV Spectrophotometer (UV-1800). It is important to note that the degree of COD digestion is indicated by the increase in chromic ions (trivalent), resulting in a change in the color of the digestion solution to a green shade. A pale blue shade indicates less COD digestion.

3.3.3.3. Ammoniacal Nitrogen (Smith & Cresser (Eds.), 2003)

Ammoniacal Nitrogen (NH_3-N) is a parameter used to measure the amount of ammonia in water bodies, and controlling ammonia levels is crucial for the well-being of aquatic life. The Nesslerization method was employed to determine ammonia concentrations.

To construct the standard calibration curve, a series of reference solutions with concentrations ranging from 0.5mg/L to 15mg/L were prepared using a stock solution of 100mg/L Ammonia Nitrogen. The final volume of each reference solution was 5ml. For the blank, 5 ml of deionized water was taken in a test tube. For the sample, 100ml of the sample was taken in a conical flask, and 5ml of borate buffer was added to minimize the hydrolysis of cyanates and organic nitrogen compounds. Distillation of 30ml of the sample was performed into 5ml of boric acid solution in a Falcon tube, ensuring that the condenser tip was dipped below the level of the boric acid solution. The distillate was measured and diluted to 50ml with deionized water. From the diluted distillate, 5ml was taken for further analysis. To all the test tubes containing 5ml of the reference solutions, blank, and sample, 0.2ml of Nessler's reagent (Preparation mentioned in Appendix II) was added and thoroughly mixed. The solutions were allowed to sit for 20 minutes, and the development of a yellowish-brown color indicated the concentration of Ammoniacal nitrogen. Background correction was performed using the blank, and the absorbance was measured at a wavelength of 425nm using a UV Spectrophotometer (UV-1800).

3.3.3.4. Total Phosphorus (Smith & Cresser (Eds.), 2003)

Excessive phosphorus levels can lead to eutrophication in water bodies, necessitating the control of phosphorus to mitigate the potential for eutrophication. To determine total phosphorus, a standard calibration curve was constructed using a series of working solutions with concentrations ranging from 0.08 mg/L to 4mg/L. These solutions were prepared from a stock solution of 100mg/L Potassium Dihydrogen Phosphate (KH_2PO_4),

with a final volume of 5ml. For each reference solution, blank (deionized water), and sample, 0.1ml of 5.5mol/L Sulphuric acid (H_2SO_4) was added, followed by the addition of 0.4ml of Ammonium Molybdate Antimony Potassium Tartrate Solution. The solutions were thoroughly mixed. Additionally, 2 ml of ascorbic acid was added to each solution and mixed. After allowing the solutions to sit for 5 minutes, the development of a bluish color indicated the presence of phosphorus in the sample. Background correction was performed using the blank, and the absorbance was measured at a wavelength of 650nm using a UV Spectrophotometer (UV-1800).

3.3.3.5. Determination of the level of Arsenic, Lead, Mercury, and Chromium

Water samples from the Bagmati River were sent to the ENPHO laboratory in Thapagaun, Baneshwor, Kathmandu for the determination of arsenic (As), lead (Pb), and mercury (Hg) using Atomic Absorption Spectroscopy (AAS). AAS is a technique used to analyze the concentration of these elements in water samples. For the detection of chromium (Cr), a different method called spectrophotometry (Diphenyl Carbazide method) was employed. A standard calibration curve was constructed using a series of reference solutions with concentrations ranging from 0.1 mg/L to 1mg/L. These reference solutions were prepared from a stock solution of 20mg/L Potassium dichromate ($K_2Cr_2O_7$), with a final volume of 5ml. The spectrophotometric measurement allowed for the determination of chromium concentrations in the water samples.

3.3.3.6. Determination of hexavalent Chromium (Wiryawan et al., 2018)

Initially, 4 ml of reference solution was taken in a test tube. Then, 0.15ml of H_3PO_4 was added to the solution, followed by the addition of 0.15ml of 0.05% DPC (Diphenyl Carbazide). To maintain a total volume of 5 ml, the remaining 0.7 ml of deionized water was added, and the solution was thoroughly mixed. The resulting solutions were allowed to rest for 5 minutes to develop color. Background correction was performed using a blank, and the absorbance of the solutions was measured at a wavelength of 540nm using a UV Spectrophotometer (UV-1800).

3.3.3.7. Determination of Total Chromium (Wiryawan et al., 2018)

The reference solution, along with the blank and samples, was acidified with 0.075ml of 1:3 sulfuric acid, and a drop of potassium permanganate ($KMNO_4$) was added to each tube. The tubes were then placed in boiling water, and potassium permanganate was added drop by drop until a permanent red color appeared. After that, the tubes were cooled, and 0.15ml of H_3PO_4 was added, followed by the addition of 0.15ml of 0.05% DPC. The solutions were left for 5 minutes for color development. Background correction with the blank was performed, and the absorbance of the solutions was measured at a wavelength of 540nm using a UV Spectrophotometer (UV-1800). To determine the concentration of trivalent chromium, the concentration of hexavalent chromium was subtracted from the total chromium concentration.

3.3.4. Biological Parameters of the Samples

Three out of the six samples collected during Jun/Jul were sent to CMDN (Center for Molecular Dynamics Nepal), Thapathali, Kathmandu, for Meta-genomic Analysis allowing for the analysis of microbial community dynamics. The DNA extraction protocol for these samples and PCR conditions has been provided in Appendix III. Additionally, heavy metal-resistant bacteria were isolated from the water samples during the process for efficient removal of specific heavy metals. These isolated bacteria underwent characterization through biochemical tests.

3.3.4.1. Isolation and screening of heavy metals resistant bacteria

The spread plate method was utilized to isolate heavy metal-resistant bacteria. Nutrient Agar (NA) media was prepared and supplemented with specific concentrations of heavy metals (Rajbanshi, 2009): 0.003M Sodium Arsenite ($NaAsO_2$), Lead acetate (CH_3COOPb), and 20mg/L of Mercuric Chloride ($HgCl_2$), as well as 0.005M Sodium Arsenite ($NaAsO_2$), Lead acetate (CH_3COOPb), and 40mg/L of Mercuric Chloride ($HgCl_2$), for the initial isolation. Since heavy metals should not be autoclaved, the calculated amounts of these metals were added to the sterilized NA media, which was then poured into the Petri dishes. The selection of resistant bacteria was based on colonial differences, and the isolated resistant strains were cultured again in the same media mentioned earlier, but with an additional 20mg/L of $K_2Cr_2O_7$, to check for co-resistance to Chromium. The isolates that exhibited better resistance were further cultured in different NA media, which were supplemented with varying concentrations of heavy metals and Chromium: 0.005M $NaAsO_2$, CH_3COOPb, and 40mg/L $HgCl_2$, $K_2Cr_2O_7$, with 0.007M $NaAsO_2$, CH_3COOPb, and 60mg/L $HgCl_2$, $K_2Cr_2O_7$, and with 1mg/L $NaAsO_2$, 50mg/L CH_3COOPb, and 50mg/L $HgCl_2$, 50mg/L $K_2Cr_2O_7$ (Chakraborty et al., 2020; Fang & Achal, 2019) .The isolate that demonstrated the highest resistance was subcultured and streaked to obtain a pure culture for further characterization.

3.3.4.2. Characterization of the Heavy metal resistant Bacteria

The analysis of Colonial characteristics and Gram staining of the isolated bacteria were first performed followed by the biochemical tests. Based on the gram reaction and biochemical tests, the bacteria were primarily identified (Manandhar & Sharma, 2013)

3.4. MFC Construction, Operation and Optimization

A dual-chambered Microbial Fuel Cell (MFC) constructed from plexiglass was utilized in the research, with each chamber of the capacity of 350ml. The anode and cathode chambers were separated by a proton exchange membrane (PEM) called Nafion 177 (diameter =6.8cm). The anode chamber was designed to be biotic and anaerobic, while the cathode chamber was abiotic and aerobic. For the anodic electrode, a graphite rod from batteries (diameter: 0.7cm, length: 5.7cm) and a graphite felt electrode (2.8 × 11 cm) were employed. On the other hand, the cathode consisted of a platinum electrode (10 × 10 × 0.5 mm) and a graphite felt electrode. Two plexiglass plates were joined together

using a gasket and the PEM was placed in between them and secured with a knot. The MFC operated under controlled conditions, with incubation in a BOD incubator at 28°C.

Figure 5 Dual chambered MFC operated with Bagmati River water at 28°C

3.4.1. Electrode Treatment

Graphite Felt (11×2.8 cm) underwent ultra-sonication with 70% methanol for 15 minutes, followed by ultra-sonication with 70% acetone, water, and treatment under UV light for 15 minutes to remove fine and organic particles. The Graphite Rod (length: 5.7cm, diameter: 0.7cm) was initially abraded using silicon carbide paper to remove any attached carbon powder. It was then ultra-sonicated in deionized water for 10 minutes and treated with 0.6M HCl (Hydrochloric acid) for 30 minutes. Afterward, it underwent ultra-sonication in 70% acetone for 10 minutes, followed by multiple rinses with deionized water. Finally, it was subjected to heat treatment at 45°C for 2 hours (George et al., 2016).For Platinum(10×10×0.5mm), it was wiped with 70% ethanol and was then UV-treated for 15 minutes.

3.4.2. Membrane Treatment

The Nafion 177 membrane (diameter: 6.8cm), was subjected to several treatments for purification and activation. It was first treated with 3% H_2O_2 (Hydrogen peroxide) at 100°C for 2 hours, followed by treatment with deionized water. Next, it was treated with 0.5 M H_2SO_4 (Sulphuric acid) and then again with deionized water at 100°C for 2 hours. These treatments aimed to remove organic impurities and activate the membrane for better performance in the MFC (Sevda et al., 2023).

During the operation of the MFC, synthetic water with a pH of 7.0 was used. This decision was made to allow for optimization since the parameters in Bagmati Water tend to change over time. The composition of the synthetic water can be found attached in Appendix II.

3.4.3. Adjustment in COD

For the anodic compartment, 330ml of sterile synthetic water was inoculated with 1% inoculum prepared from the sample in NB (Nutrient Broth). A graphite rod was used as

the electrode for the anodic compartment, while for the cathode, Platinum was used. The cathodic solution consisted of synthetic water along with 1mg/L $NaAsO_2$, 50mg/L CH_3COOPb, $HgCl_2$, and $K_2Cr_2O_7$. The pH of both compartments was maintained at 7.0 ± 0.02. Different synthetic water samples with Chemical Oxygen Demand (COD) ranging from 800mg/L to 3500mg/L were used in the anode. The Open Circuit Voltage (OCV) was measured using a digital Multi-meter. The OCV was recorded every 2 hours for several days. Once the voltage reached its maximum and started to drop, anodic sampling was done for COD measurement to assess COD removal after MFC operation. After this, the MFC was discarded. The synthetic water sample that resulted in a good OCV and significant COD removal was selected for further optimization procedures.

3.4.4. Adjustment in electrode composition

The synthetic water with the optimized COD was used as the anodic media for the MFC. The overall construction and operation were the same as described previously. However, a variation was introduced in the anodic electrode setup.

Three different MFC configurations were tested for the anodic electrode:

1. Graphite rod anode - Platinum cathode
2. Graphite felt anode - Graphite felt cathode
3. Graphite felt anode - Platinum cathode

After evaluating the performance of each configuration in terms of OCV and COD removal, the setup with the electrode that exhibited the best OCV and COD removal was selected as the optimized configuration.

3.4.5. Adjustment in Bio-anode composition

The synthetic water with optimized COD and the selected anodic electrode configuration was used for the anodic compartment. The overall construction and operation remained the same as described previously, except for the anodic media. In this case, the synthetic water was fortified with 1mg/L $NaAsO_2$, 50mg/L CH_3COOPb, $HgCl_2$, and $K_2Cr_2O_7$, and three different bacterial cultures were introduced:

1. 1% bacterial consortium from BMII-CV3

2. 1% resistant bacteria (isolated from heavy metal resistance)

3. A mixture of 1% (bacterial consortium from BMII-CV3 and resistant bacteria)

For each operation and optimization, a Control MFC was also set up, where the anodic media lacked any bacterial culture. This control setup aimed to distinguish between voltage generated due to chemical reactions and voltage resulting from microbial reactions. The OCV for all these optimization setups was compared, and the results were represented graphically. The optimized protocol that demonstrated the best OCV was then selected for further MFC operation, using both synthetic and Bagmati water. A resistor of 1.1KΩ was used in these MFC operations. Furthermore, current, current density

and power density were calculated following R. Kumar et al (2020) for the chosen optimized protocol during the MFC operation.

$$\text{Current (I)} = \frac{\text{Voltage(V)}}{\text{Resistor(R)}}$$

$$\text{Current Density} = \frac{\text{Current(A)}}{\text{Surface area of cathode(m2)}}$$

$$\text{Power Density} = \frac{\text{Voltage(V)} \times \text{Current(A)}}{\text{Surface area of cathode(m2)}}$$

(R. Kumar et al., 2020)

3.5. Remediation of heavy metals

To evaluate the remediation of heavy metals, which involves either the removal or reduction of heavy metals after the Microbial Fuel Cell (MFC) operation, Differential Pulse Voltammetry (DPV) of the cathodic samples was performed. DPV is an electrochemical technique used to analyze the concentration and redox state of metal ions in a solution. By analyzing the cathodic samples after the MFC operation, researchers can determine the effectiveness of the MFC in reducing or removing heavy metal ions from the system. This analysis provides valuable insights into the performance of the MFC and its potential application for the remediation of heavy metals in water or wastewater treatment processes.

3.5.1. Differential Pulse Voltammetry

The CH Instruments 660E Electrochemical Workstation was used to perform anodic stripping voltammetry and differential pulse voltammetry (DPV) for sample analysis. Three types of electrodes were utilized: the Calomel electrode as the reference electrode, the screen-printed carbon electrode as the working electrode, and the platinum electrode as the counter electrode. Before conducting the analysis, the standard reduction potential of all the heavy metals of interest was determined. This information is essential to indicate the potential window during DPV, as the peak of the current appears at its reduction potential in the Potential vs Current graph. The standard addition method was employed to construct the standard calibration curve. Stock solutions of 50mg/L $NaAsO_2$, 5000mg/L CH_3COOPb, $HgCl_2$, and $K_2Cr_2O_7$ were individually prepared in synthetic water with optimized COD. For background correction, 30µl of synthetic water was mixed with 9ml of 0.1M KCl (Potassium Chloride) in a small glass vessel. The electrodes were dipped and connected to a wire. It is important to ensure that the instrument is turned on before sample preparation in the electrolyte, and the electrodes must be washed with deionized water and wiped dry before use (Zinoubi et al., 2017 ; Rosolina et al., 2015).Once the setup was ready, the software for the instrument, Chi660e, was opened. To ensure proper connection in the cell, an open circuit potential measurement was performed first. Subsequently, potentiometric stripping analysis (PSA) was conducted for the electro-deposition, followed by DPV. The parameters for both PSA and DPV were provided in the attached Appendix IV. After the DPV, a Voltammogram was obtained in the graph of

Potential vs Current. For the standard calibration curve construction, 30µl of each stock heavy metal solution was mixed with the setup, and the same background correction process was repeated. After each DPV, 30µl of each heavy metal solution was added to establish the calibration curve for different concentrations. A Voltammogram was obtained for each concentration, and the current produced at the potential of the respective heavy metals was noted. A graph of Concentration vs Current was constructed for the calibration curve, which was used to calculate the unknown concentration of heavy metals after MFC operation. For the samples obtained after MFC operation, the same procedure was followed, except for the addition of heavy metal solutions after each DPV to assess the concentration of heavy metals in the cathodic samples.

CHAPTER IV

RESULTS & DISCUSSION

4.1. Environmental Parameters of the Samples

Various Environmental parameters were considered, including temperature, pH, Color, turbidity TDS (Total Dissolved Solids), TSS (Total Suspended Solids), COD (Chemical Oxygen Demand), and concentrations of organic pollutants and heavy metals.

4.1.1. Physical Parameters of the sample

Referring to Table 2, sample temperatures ranged from 10°C (minimum) to 26°C (maximum). During summer, pH levels increased, ranging from 6.2 to 7.5, falling within the WHO's (1999) recommended pH range of 6.5-8.5 for natural water. The river was black and turbid which changed to muddy turbid during summer with TSS levels exceeding the Ministry of Environment's (MOE 2010) guideline of 250mg/L. Notably, TSS exceeded the guideline value, but the trend varied among samples, increasing in Chovar during summer and decreasing in Kupondol and Balkhu.

Table 2 Values of physical characteristics of Bagmati River water samples

Sample location	Sample Code	Temperature (ºC)	pH	Color	Turbidity	TSS(mg/L)	TDS(mg/L)
Kupondol	BM-KD1	12	6.2	Black	Turbid	1420	3140
	BMII-KD1	26	7.3	Muddy	Turbid	800	700
Balkhu	BM-BK2	13	6.6	Black	Turbid	1360	40
	BMII-BK2	26	7.3	Muddy	Turbid	1000	400
Chovar	BM-CV3	10	7.2	Black	Turbid	720	60
	BMII-CV3	22	7.5	Muddy	Turbid	1960	420

Our research found that the pH levels were within the natural water pH range of 6.5 to 8.5, in line with previous studies (Baniya et al., 2019; Adhikari et al., 2019) and WHO guidelines (1999). However, unlike Baniya et al. (2019), we observed a decrease in TSS levels, possibly due to reduced industrial discharges and agricultural runoff. Comparing winter and summer, TSS decreased overall, except in Chovar, where it increased. This could be attributed to factors like vegetable market discharges in Balkhu, hospital runoff, and nearby agricultural practices affecting the river flowing through Nakkhu as water flowing from Balkhu and Nakkhu merged and flow along the Chovar. Aligning with the study of Adhikari et al., (2019), blackish turbid as well as muddy turbid appearance of river was reported that may be attributed to soluble conductive pollutants and insoluble suspended particles such as clay, silt, and mud respectively.

4.1.2. Chemical Parameters of the sample

The concentration of different chemical parameters including those of metal ions are presented in the Tables 3, 4 &5. COD, Ammoniacal Nitrogen, and Total Phosphorus though had decreased in summer however surpassed standard values: 250mg/L (MOE 2010),

0.2mg/L (WHO 2011), and 0.1mg/L (U.S. EPA 1986) respectively. Regarding heavy metals, lead exceeded MCL of 0.01mg/L (APHA, AWWA, WEF 2017), while no contamination occurred with As and Hg. Cr (VI) surpassed MCL of 0.05mg/L (WHO 2011) in winter, later decreasing in summer (Table 5).

Table 3 Analysis of chemical characteristics of the Bagmati River water

S.N.	Sample	Total reducing sugar(mg/L)	COD(mg/l)	Ammoniacal Nitrogen(mg/l)	Total Phosphorus(mg/l)
1.	BM-KD1	175.41 ± 5.01	1324 ± 12.16	9.19 ± 0.42	3.82 ± 0.15
	BMII-KD1	39.16 ± 0.95	421.32 ± 60.80	0.41 ± 0.03	1.07 ± 0.14
2.	BM-BK2	40.62 ± 11.37	666.38 ± 66.88	2.80 ± 0.01	3.31 ± 0.006
	BMII-BK2	35.88± 3.08	154.77 ± 85.12	0.51 ± 0.01	1.56 ± 0.13
3.	BM-CV3	51.66 ± 0.95	279.44 ± 54.72	9.30 ± 0.50	3.59 ± 0.003
	BMII-CV3	42.70 ± 0.95	571.79 ± 6.08	0.86 ± 0.02	0.57 ± 0.11

Table 4 Heavy Metals Concentration of the sampling sites

S.N.	Sample	Arsenic Concentration (mg/L)	Lead concentration (mg/L)	Mercury Concentration (mg/L)
1.	BM-KD1	< 0.005	< 0.01	< 0.005
	BMII-KD1	< 0.005	0.02	< 0.005
2.	BM-BK2	< 0.005	< 0.01	< 0.005
	BMII-BK2	< 0.005	0.02	< 0.005
3.	BM-CV3	< 0.005	0.01	< 0.005
	BMII-CV3	< 0.005	0.03	< 0.005

Table 5 Chromium Concentrations in sampling sites

S.N.	Sample	Chromium Concentration (mg/L)		
		Chromium(VI)	Total Chromium	Chromium(III)
1.	BM-KD1	0.25 ± 0.03	0.30 ± 0.04	0.05
	BMII-KD1	0.01 ± 0.003	0.04 ± 0.01	0.03
2.	BM-BK2	0.14 ± 0.02	0.39 ± 0.26	0.24
	BMII-BK2	0.03 ± 0.003	0.08 ± 0.01	0.04
3.	BM-CV3	0.090 ± 0.04	0.093 ± 0	0.002
	BMII-CV3	0.05 ± 0.003	0.14 ± 0.01	0.08

The COD value had decreased in comparison with the study of Baniya et al., (2019) this may be due to the reduction in pollution sources and also in our research, there is a risk of algal blooming since the total phosphorus exceeded the standard guideline, may be the organic compounds were up-taken by algae for their growth .In our research, COD decreased during summer for which the reason could be the effect of dilution of pollutants concentration caused by rainfall. Ammonia Concentration had increased during winter contrasting to Adhikari et al.'s 2019 research, this may be due to the entry of municipal waste and sewage as reported by Milner et al. (2015).

The ultimate target of water treatment is to make the resource available for the safe use of it; making it to a level of drinking water (WHO Guidelines for Drinking Water Quality, 4th edition, Arsenic: 0.01mg/L, Lead: 0.01mg/L, inorganic Mercury: 0.006mg/L Chromium: 0.05mg/L). In regard of the research by Baniya et al., (2019), pollution by As and Hg had decreased however lead pollution was found. The decrease in arsenicals discharge along with mercury might had led to the decrease in their concentration additionally with probability of natural microbial transformation to less soluble or less toxic forms thus reducing their availability in water. Rainfall, on the other hand could also dilute the concentration of these heavy metals. Lead pollution in water may had resulted from lead-based paints, plumbing, agricultural runoff, and other sources. Chovar had consistently high lead levels, possibly due to agricultural activities, garage discharges, urban development in Nakkhu, and manufacturing runoff from Balkhu-Kirtipur, as water from both Balkhu and Nakkhu converges in Chovar.

4.2. Biological Parameters of the Sample

4.2.1. Meta-genomic analysis of the sample

PCR analysis of the extracted DNA revealed the presence of bacterial DNA fragments of approximately 650 base pairs (Fig 6, A). The samples were dominated by the bacteria, however, some Archae was also found in BM-BK2 (Fig 6, B).

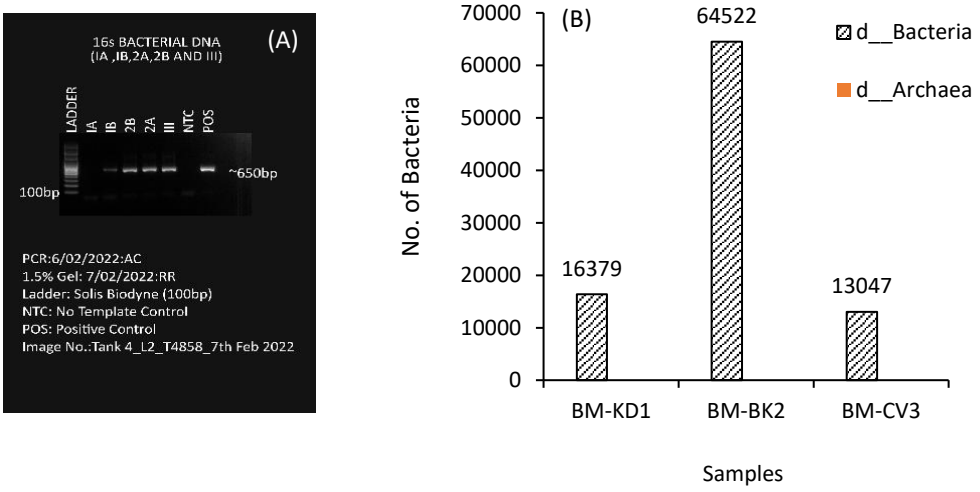

Figure 6 Results of Meta-genomic analysis of the Water samples, (A) Agarose Gel (1.5%) Electrophoresis of PCR product, (B) Distribution of microbial community in the water samples

4.2.1.1. Alpha Diversity of the samples

The samples showed presence of Bacteria and Archaea, with varying levels of diversity. BM-KD1 had 15 Phyla and 25 Class, and the dominant class was Verrucomicrobiae, followed by Gammaproteobacteria, Bacteroidia, and Alphaproteobacteria. The least dominant class was Lentisphaeria, (Figure 7). BM-BK2 had 30 Phyla and 59 Class, and it shared the three dominant bacterial classes with BM-KD1 (Verrucomicrobiae, Gammaproteobacteria, and Bacteroidia). However, in BM-BK2, the least dominant classes were Methylomirabilla and Berkelbacteria, as depicted in Figure 8. Similarly, BM-CV3 harbored Bacteria with 22 Phylum and 40 Class, and it also shared the same three dominant bacterial classes with BM-KD1 and BM-BK2. These classes were dominant in all three samples. Additionally, BM -CV3 had the least dominance of Phylum Proteobacteria, but the specific class was not mentioned, as shown in Figure 9.

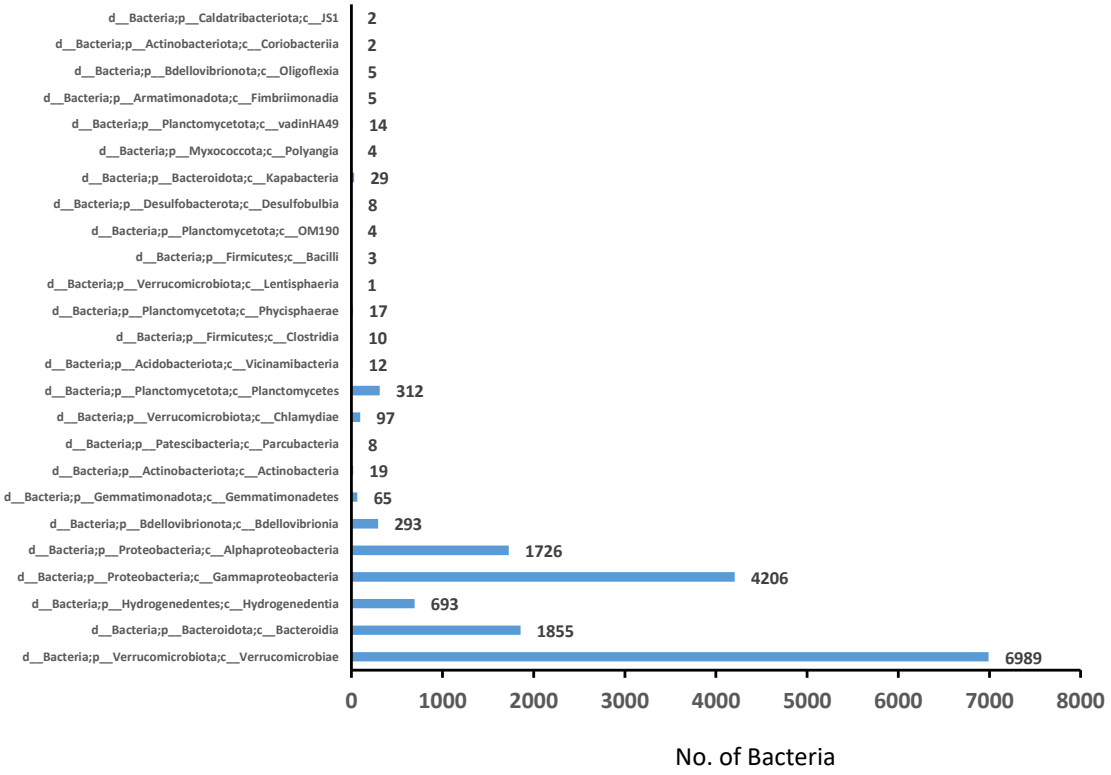

Figure 7 Graphical representation for the Alpha Diversity of BM-KD1

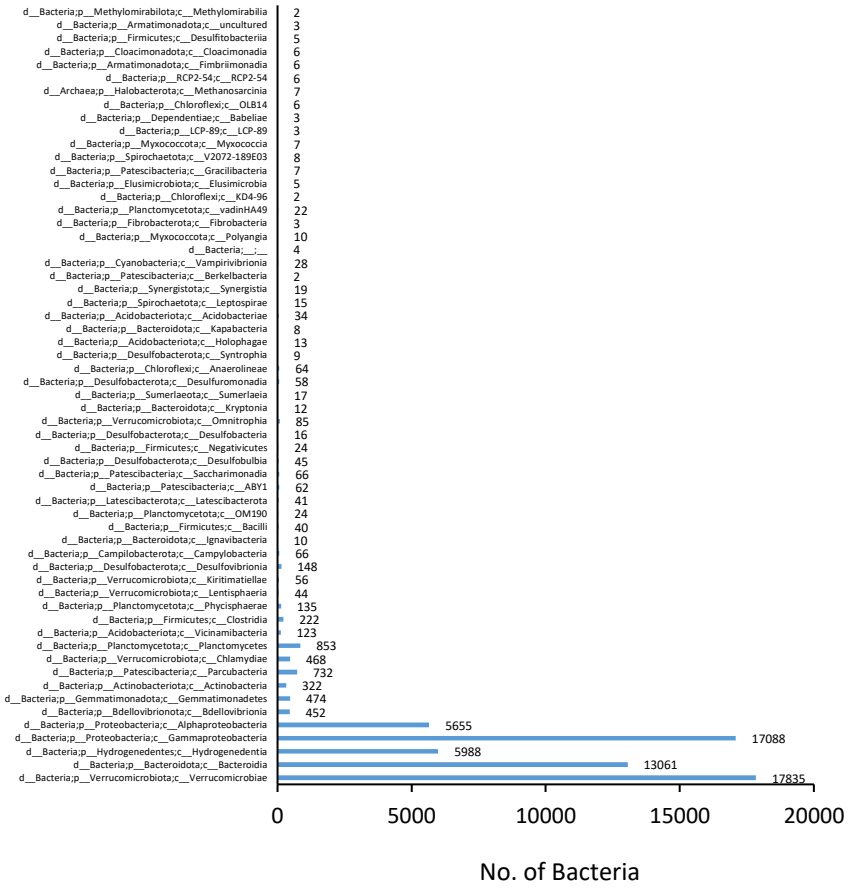

Figure 8 Graphical representation for the Alpha Diversity of BM-BK2

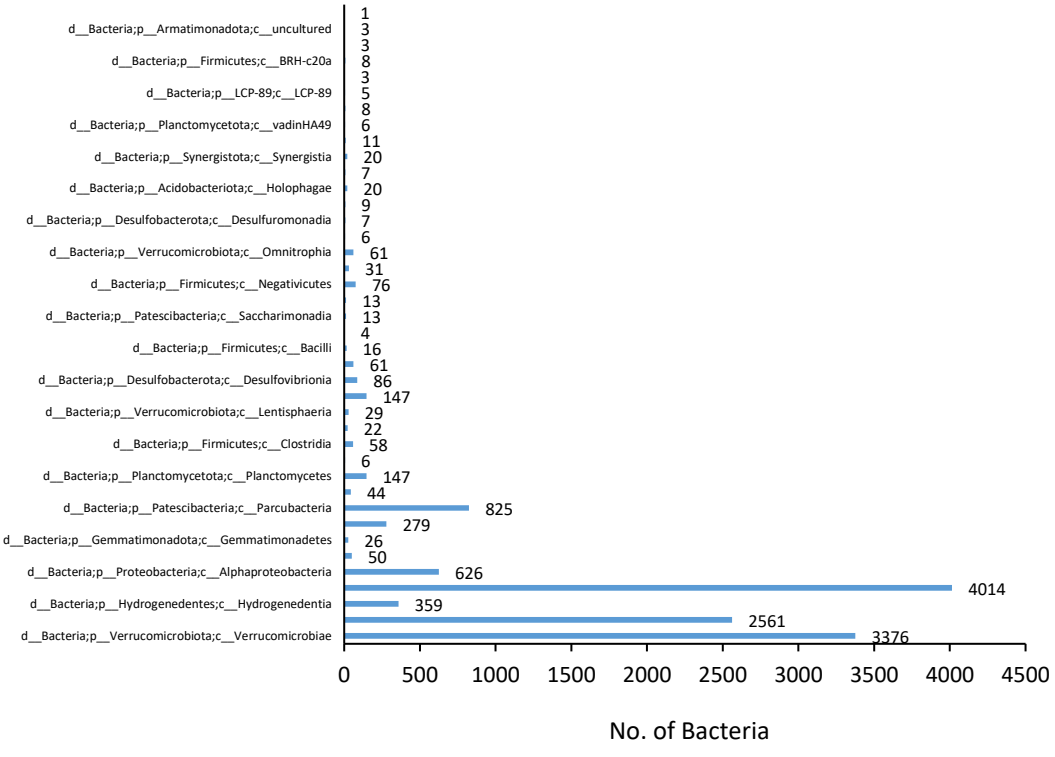

Figure 9 Graphical representation for the Alpha Diversity of BM-CV3

In Shrestha et al.'s (2019) research, the dominant bacterial phylum was Proteobacteria (59-80%), followed by Bacteroidetes (10-25%) and Firmicutes (6-15%) while Verrucomicrobiae was dominant class in our research, followed by Gammaproteobacteria, Bacteroidia, and Alphaproteobacteria with least dominant class being Lentisphaeria. The differences between Shrestha et al.'s (2019) research and the current study may be attributed to variances in the time and location of sample collection.

4.2.1.2. Beta Diversity of the Samples

Beta diversity quantifies the differences in composition between samples. Figure 10 illustrates the presence of graphically represented bacteria in all three samples (BM-KD1, BM-BK2, and BM-CV3), with variations in their numeric distribution. BM-BK2 exhibited the highest number of bacteria, followed by BM-KD1, while BM-CV3 had the lowest number. Figure 11 displays the distribution of bacteria and Archaea, revealing distinct patterns among the samples. Three bacterial classes (Class JS1, Coriobacteria, and Oligoflexia) were exclusively present in BM-KD1. BM-CV3 contained Phylum Proteobacteria (class not mentioned) and Phylum Firmicutes (Class BRH-C20a) exclusively. In contrast, BM-BK2 harbored 17 bacterial classes and one Archaea class (Methanosarcinia) that were unique to this sample. Additionally, there were common bacteria shared between at least two samples (BM-KD1 and BM-BK2, BM-BK2 and BM-CV3, and BM-KD1 and BM-CV3).

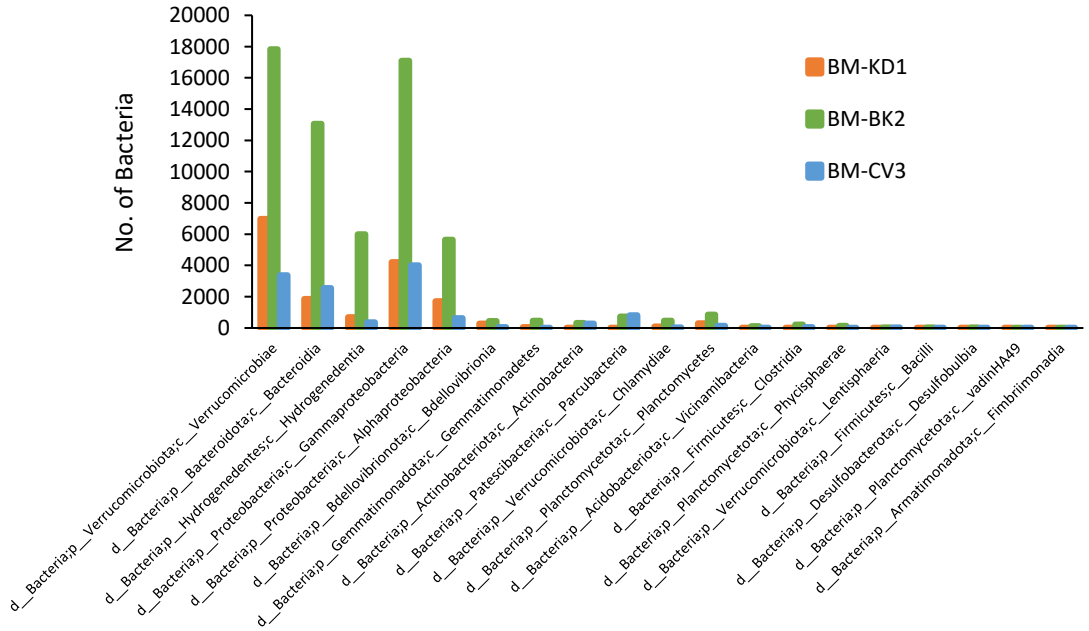

Figure 10 Graphical representation of bacteria common in all three samples for the Beta Diversity of water samples

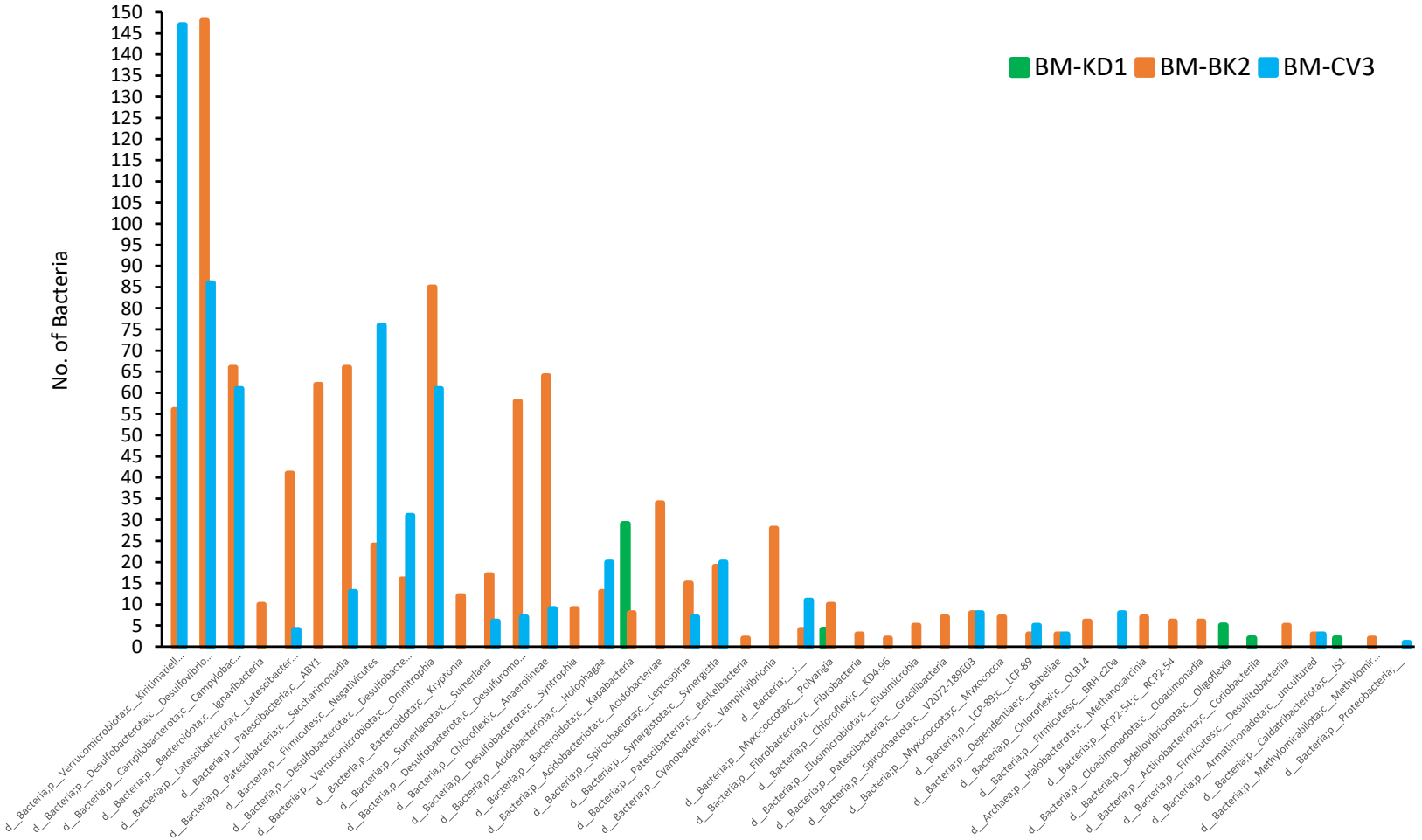

Figure 11 Graphical representation of bacteria in all three samples for the Beta Diversity of water samples

The presence of common bacteria in all three sampling sites of the Bagmati River can be attributed to factors like bacterial mobility, contamination sources, and specific ecological niches and interactions. Bacteria with mobility or the ability to be carried by water currents can disperse and colonize different areas. Contamination sources may introduce these bacteria into the river, leading to their consistent presence. Additionally, if certain bacteria have specific ecological niches and interactions in one part of the river, similar conditions may exist elsewhere, resulting in the same bacteria being found in multiple locations.

Bacterial diversification was also found between sampling sites which may be due to the physicochemical variation along with the variation in pollution level. In addition to this, confluences may create a unique environment favoring the growth of specific bacteria which thus can lead to microbial variations along the river's course.

4.2.1.3 Distribution of Electrogen between Samples

Electrogen is electrically active microbes, typically bacteria,that generate electricity in a microbial fuel cell (MFC) configuration. On metagenomics analysis, 4 of the electrogen belonging to the bacterial genus *Pseudomonas, Rhodobacter, Rhodoferax,* and *Shewanella* were found where *Shewanella* was present only in BM-BK2, Similarly, *Rhodoferax* was found in BM-CV3 and BM-BK2, and remaining two were found in all three samples as it can be seen in Figure 12. BM-BK2 comparatively was harboring the dominant number of bacteria.

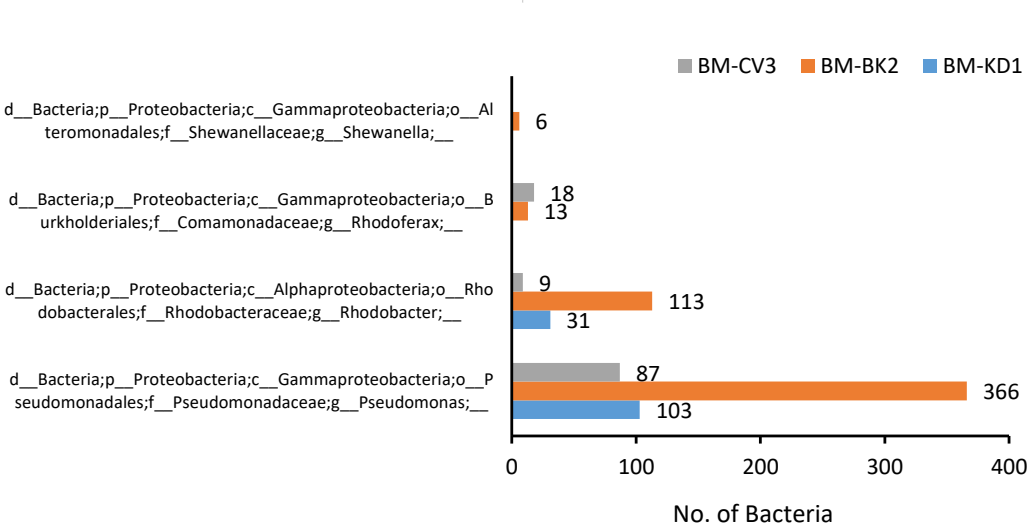

Figure 12 Graphical representation for the distribution of electrogen bacteria in all three samples

Our research disclosed the presence of four electrogenic bacteria that was also included in the study of Barbato et al., 2017; Jiang et al., 2015; Wang et al., 2016; Jayapriya and Ramamurthy, 2012, where microbial species *Geobacter* spp., *Shewanella* spp., *Rhodoferax ferrireducens, Aeromonas hydrophila, Pseudomonas aeruginosa, Clostridium butyricum, Shewanella oneidensis MR-1, Rhodobacter sphaeroide, and Enterococcus gallinarum* were

used for power generation in Microbial Fuel Cells (MFCs).Those electrogenic bacteria found in our research thus can also contribute to the electricity generation in MFC.

4.2.2. Isolation of Heavy Metals Resistant Bacteria

Heavy metals resistant bacteria isolated from BM-CV3 was tested further for its co-resistance where among selective six isolates (based on a colonial morphology-size and color) cultured in NA supplemented with 0.003M $NaAsO_2$, CH_3COOPb, 20mg/L of $HgCl_2$, and $K_2Cr_2O_7$, two of the isolates (3 and 5) were found susceptible and remaining four isolates were resistant, Figure 13 (C). These isolates were found resistant to the maximum heavy metal concentration of 0.005M $NaAsO_2$, CH_3COOPb, 40mg/L of $HgCl_2$, and K_2Cr2O_7, also to NA with 1mg/L $NaAsO_2$, 50mg/L CH_3COOPb, 50mg/L $HgCl_2$, and 50mg/L $K_2Cr_2O_7$ Figure 13 (D,E &F).

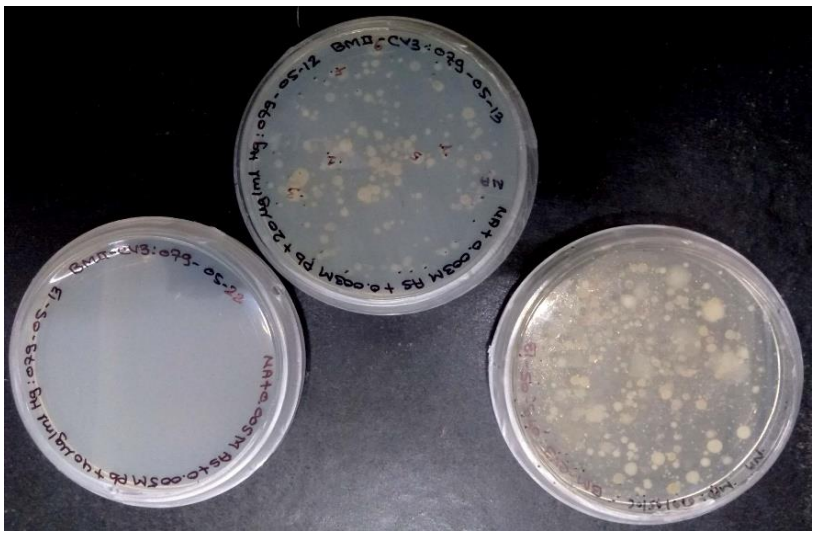

(A)

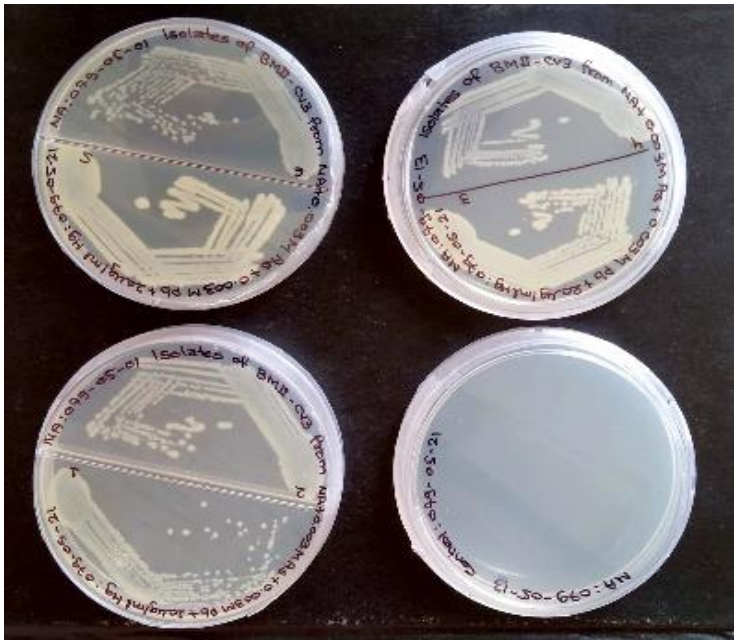

(B)

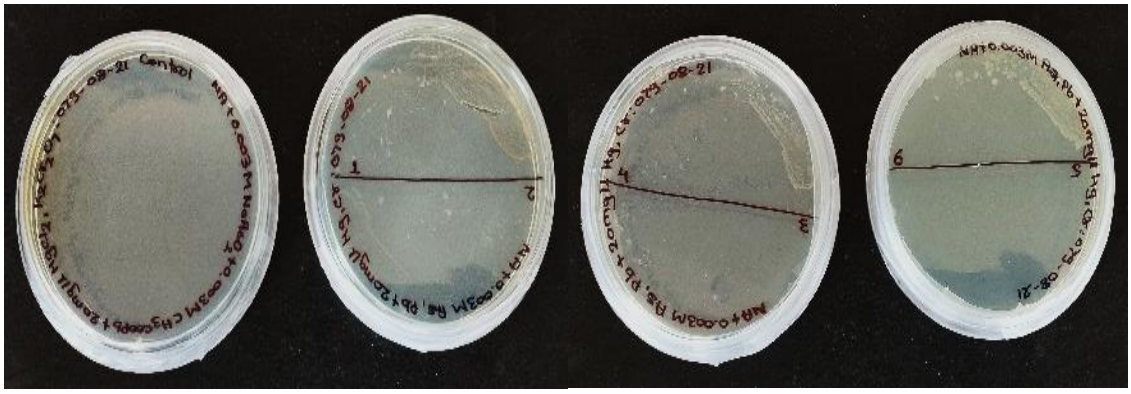

(C)

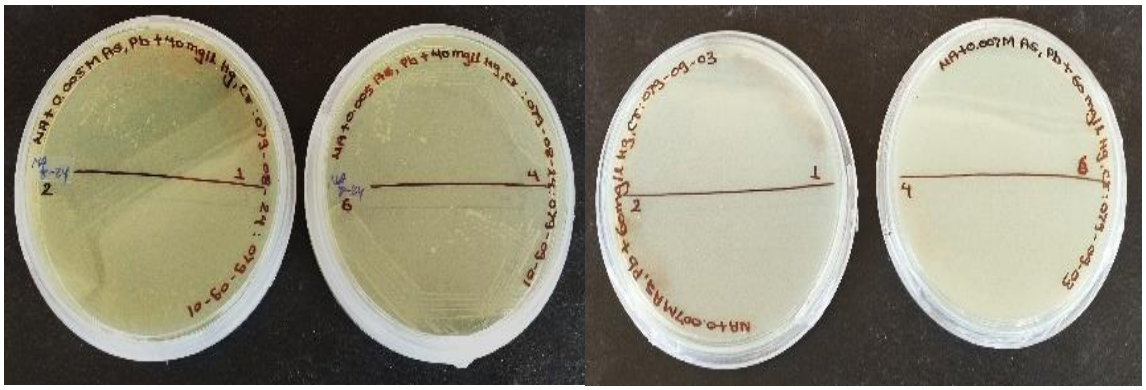

(D) (E)

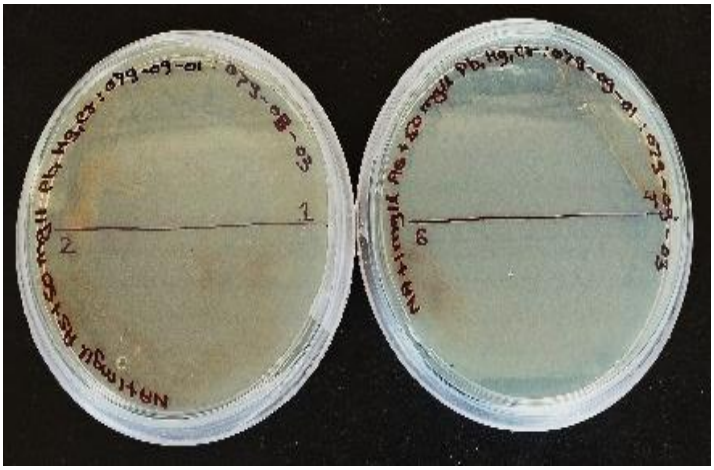

(F)

Figure 13 Isolation of Heavy metals resistant bacteria in NA supplemented with different concentrations of As, Pb, Hg, and Cr**, (A)**=isolation of bacteria from BMII-CV3 in NA supplemented with 0.003M $NaAsO_2$, CH_3COOPb, 20mg/L of $HgCl_2$, and NA with 0.005M $NaAsO_2$, CH_3COOPb, 20mg/L of $HgCl_2$ and also in NA only (Control) (**B)**= Selection of isolates based on color, size and their subculture in NA, (**C)** Testing Co-resistance of selected isolate to chromium by sub-culturing in NA supplemented with 0.003M $NaAsO_2$, CH_3COOPb, 20mg/L of $HgCl_2$, and $K_2Cr_2O_7$, **(D), (E), (F)** = Testing Maximum resistivity of isolates to the heavy metals in NA supplemented with 0.005M $NaAsO_2$, CH_3COOPb, 40mg/L of $HgCl_2$, and $K_2Cr_2O_7$, NA supplemented with 0.007M $NaAsO_2$, CH_3COOPb, 60mg/L of $HgCl_2$, and $K_2Cr_2O_7$ and NA supplemented with 0.003M $NaAsO_2$, CH_3COOPb, 40mg/L of $HgCl_2$, and $K_2Cr_2O_7$ respectively

4.2.3. Selection of best resistant isolate

Isolate 6 was resistant up to the heavy metals concentration of 0.005M $NaAsO_2$, CH_3COOPb, 40mg/L $HgCl_2$, $K2Cr_2O_7$, and 1mg/L $NaAsO_2$, CH_3COOPb, 50mg/L $HgCl_2$, $K_2Cr_2O_7$ as shown in Figure 14.Subsequently, under the spectrophotometric measurement, the robust growth of Isolate 6 marked it the best heavy metals resistant bacteria among four of the isolates (Table 6).

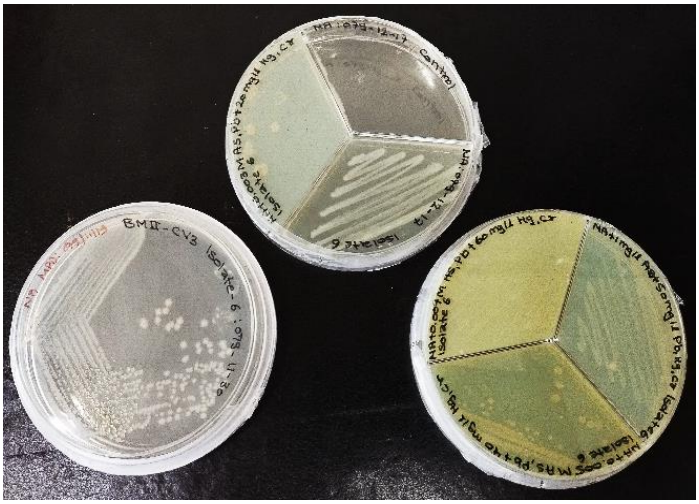

Figure 14 Pure culture of Isolate 6 and its resistivity Pattern to different concentrations of As, Pb, Hg, and Cr

Table 6 Spectrophotometric measurement of bacterial growth

Media	Isolates code	Absorbance(600nm)
NB+ 1mg/L $NaAsO_2$,	1	0.056
CH_3COOPb and 50mg/L of	2	0.026
$HgCl_2$, ($K_2Cr_2O_7$)	4	0.014
	6	0.057

4.2.4. Characterization of Heavy Metal Resistant Isolate

Based on the characteristics observed, Isolate 6 was cream-colored, round, 2mm-sized, flat, translucent, and a mucoid Gram-negative rod-shaped bacterium. It tested positive for catalase and oxidase. In the IMViC (Indole, Methyl Red, Voges Proskauer and Citrate) Test, it was motile, indole-positive, without H_2S(Hydrogen Sulphide) production, and tested positive for the MR(Methyl Red) and Citrate Utilization Tests, while testing negative for the VP(Voges-Proskauer) and urease tests. The TSIA(Triple Sugar Iron Agar) test indicated gas production along with the fermentation of glucose, lactose, and sucrose (A/AG); Acid/Acid Gas), which was further supported by the OF(Oxidative Fermentative) test confirming fermentative capabilities. The bacteria was suspected to be of the genus *Citrobacter.*

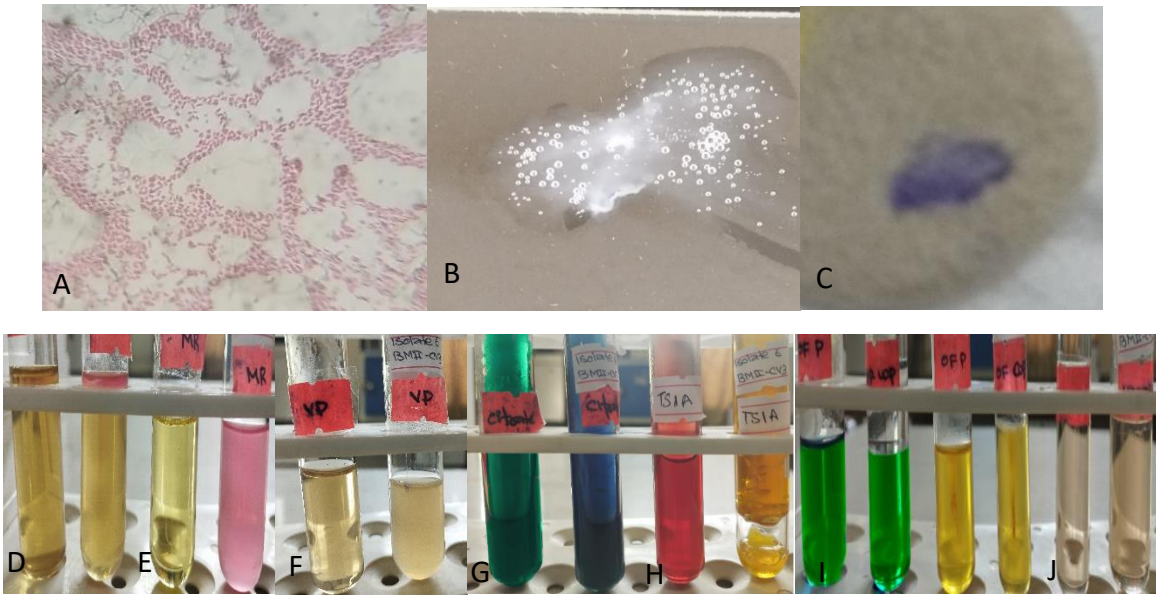

Figure 15 Identification of Bacteria isolated from BMII-CV3 by Gram staining and biochemical tests , A= Gram Staining, B= Catalase Test ,C= Oxidase Test, D= SIM test Left- Control, Right- Test, E= MR test Left- Control Right-Test, F= VP test Left- Control Right- Test, G= Citrate utilization Test Left-Control Right-Test, H= Triple Sugar Iron Agar(TSIA) test Left-Control Right-Test, I= OF test left 1st – Control without paraffin oil , 2nd- Control with paraffin oil, Right 1st- Test without Paraffin Oil 2nd- Test with paraffin oil, J=Urease test Left –Control Right-Test

Comparing our research with Rajbanshi (2009), bacteria with co-resistance to heavy metals were found, of which only one bacteria was preliminary identified to be of genus *Citrobacter* that was As, Pb, Hg resistant showing co-resistance to Cr(VI), while in Rajbanshi (2009), the *Citrobacter* spp. was found resistant to cadmium and the research didn't mention about co-resistance of *Citrobacter* with other heavy metals, may be it didn't show the co-resistance. This difference in metal resistant within the same genus may be because the degree of tolerance and specific mechanism employed can differ among the microbial species and even among the strains. Some microbes can be highly resistant to specific heavy metal while some may show wider resistance to multiple heavy metals. Subsequently, the concentration and availability of heavy metals can affect the resistance level of metals.

4.3. Microbial Fuel Cell Operation

4.3.1. OCV at different CODs

The operation of MFC for an average of 8 days showed that synthetic water with a COD value of 3500mg/L measured the high Open Circuit Voltage (OCV) of 379.5 ± 3.53 mV. It was then followed by synthetic water of COD 1500mg/L with the least OCV of 212.5 ± 2.12 mV with synthetic water of COD 800mg/L (Figure 16, A). There was an initial increase in OCV in control (Figure 16, B) however in the following days, it decreased indicating that the voltage output observed was not a result of chemical reactions within the medium but rather due to the microbial oxidation of organic matter occurring in the anode. The maximum COD removal of 74.73% was achieved with COD 3500mg/L and the least removal 55.05% was obtained with COD 800mg/L (Figure 17). While in Control, a

maximum of 50% COD removal was achieved with 3500mg/L but only 2.17% COD was removed when operated with COD 2500mg/L (Figure 17). Based on the maximum OCV and COD removal, the optimal COD for further MFC operation was synthetic water of 3500 mg/L.

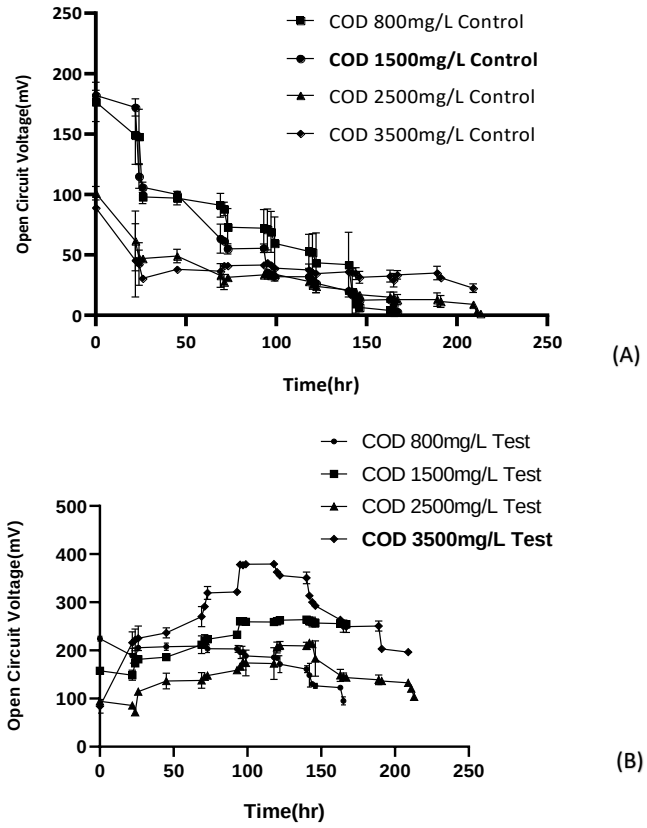

Figure 16 Graphical representation of OCV produced during the MFC Operation with Synthetic water of different COD, pH 7.0 ± 0.02, 1% bacterial consortium from BMII-CV3

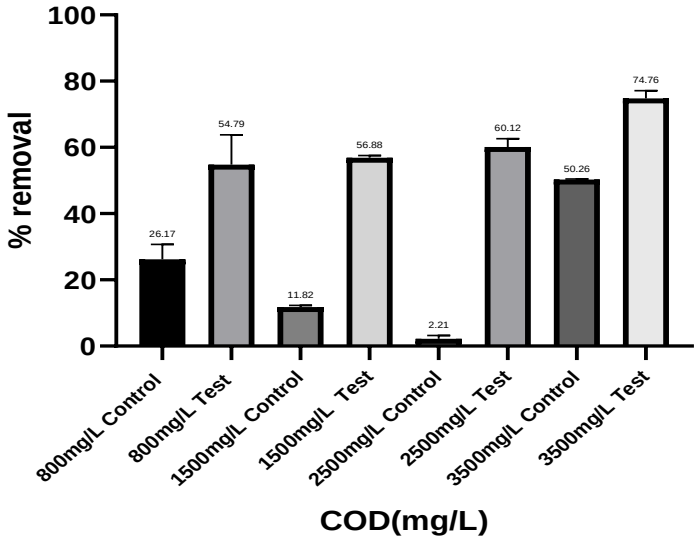

Figure 17 Comparative graphical representation of COD removal after MFC Operation with synthetic water of different COD, pH 7.0± 0.02, 1% bacterial consortium from BMII-CV3

In our study, we observed that as the COD value increased, the OCV initially increased. However, at a COD of 2500mg/L, the OCV decreased. This pattern aligns with findings by López Velarde Santos et al., 2017, who explained that the decrease in electric power at high COD values is due to anodic reactions in the MFC's anodic chamber, which depend on substrate characteristics and carbon availability. Additionally, electric power increased with increasing organic loads up to a certain concentration, but beyond a specific threshold, power declined, even though organic load removal continued to increase. This decline in power density at high COD concentrations can saturate the MFC, as observed in previous studies (Nam et al., 2010; Liu et al., 2011; Oliveira et al., 2013).

4.3.2. Optimization of electrode for MFC operation to remove heavy metals

On the microbial operation for an average of 8 days, the maximum OCV of 379.5 ± 3.53 mV was obtained with the electrode configuration: Graphite Rod anode and Platinum Cathode (Setup I), (Setup II) Graphite Felt anode and Platinum cathode (197.5± 10.60 mV) and the least of 82.5 ± 2.12 mV in Graphite felt anode and Graphite felt cathode (Setup III) (Figure 18, B). While in the control, the OCV initially increased and then decreased (Figure 18, A) indicating that the observed OCV was a result of microbial oxidation of organic matter, rather than a chemical reaction. The maximum COD removal of 74.73% was obtained from Setup I with Setup II being the least in COD removal (60.50%). In control, a maximum of 50.25% of COD removal (Figure 19) was achieved attributed to the chemical reaction. Thus, the optimal electrode configuration of Setup I was selected based on the high OCV and COD removal achieved.

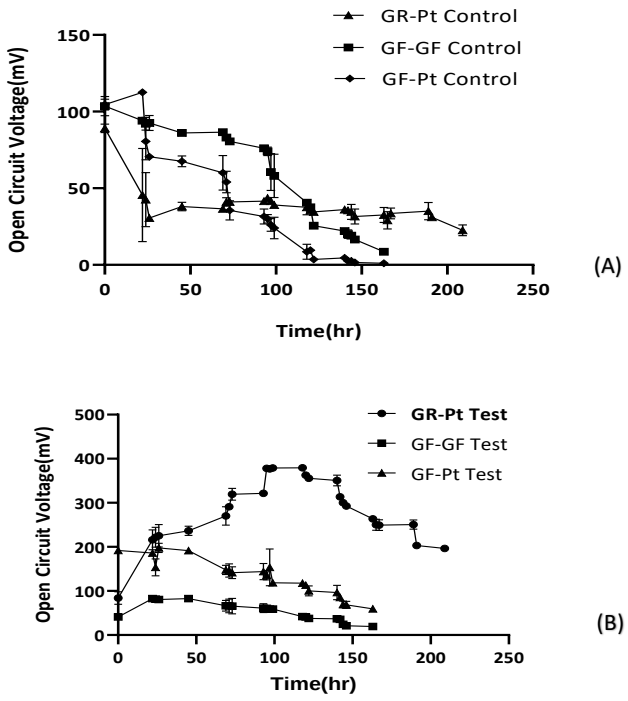

Figure 18 Graphical representation of OCV produced during the MFC Operation with Synthetic water of COD 3500mg/L, pH 7.0 ± 0.02,1% bacterial consortium from BMII-CV3 with different electrode composition

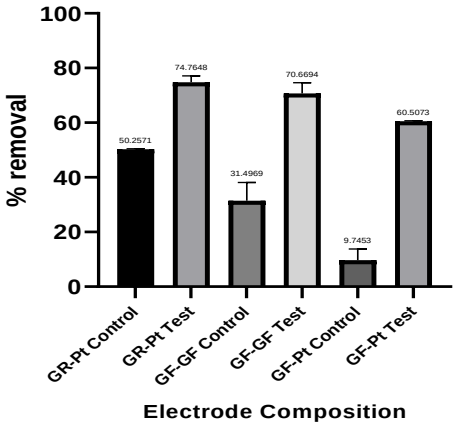

Figure 19 Comparative graphical representation of COD removal after MFC Operation with synthetic water of COD3500mg/L, pH 7.0± 0.02, 1% bacterial consortium from BMII-CV3

When using Graphite felt as both cathode and anode, the power density achieved was lower compared to the results reported by Wang et al. (2010) and Huang et al. (2015). This difference in performance can be attributed to variations in the catholyte, anolyte, and operational conditions employed in our study. Interestingly, our research indicated that Graphite Rods outperformed Graphite Felt, contrary to the expected advantage of the latter due to its high porosity and large surface area. One plausible explanation for this outcome is that electrochemical reactions were concentrated on the smaller electrode surface of the graphite rods, potentially facilitating more efficient electron exchange.

4.3.3. Optimization of Bio-anode for MFC Operation to remediate heavy metals

To optimize the microbial fuel cell (MFC) operation with real wastewater, considering the potential presence of dissolved heavy metals, a bio-anode optimization was conducted. The optimized configuration for COD and electrode was implied along with synthetic water and pH 7.0 and thus MFC operation for an average of 8 days showed the maximum OCV of 43.5 ± 3.53 mV by MFC operated with synthetic water supplemented with 1mg/L $NaAsO_2$, CH_3COOPb, and 50mg/L $HgCl_2$, $K_2Cr_2O_7$, along with a 1% bacterial consortium. It was then followed by MFC operated with heavy metals and 1%(bacterial consortium + resistant isolate) i.e. 42 ± 8.48 mV, the least was 41.5 ± 0.70 mV when MFC with heavy metals and 1% resistant isolate was used. In control the maximum OCV obtained was 20.5 ± 3.5 mV which then decreased, indicating the electric output was due to the microbial reaction but not the chemical reaction (Figure 20). Maximum COD removal was also achieved by MFC with heavy metals and 1% bacterial consortium i.e. 35.62% followed by 35.38% for MFC with heavy metals and 1% resistant isolate, with MFC operated along heavy metals and 1% (bacterial consortium and resistant isolate) being the least in removing COD (31.69%). The removal was < 20% in control (Figure 21), thus attributed to microbial oxidation. Therefore, the optimal configuration for MFC operation with real wastewater was determined to be the use of synthetic water supplemented with 1mg/L

$NaAsO_2$, CH_3COOPb, and 50mg/L $HgCl_2$, $K_2Cr_2O_7$, along with a 1% bacterial consortium. This configuration was selected based on the high voltage output and COD removal.

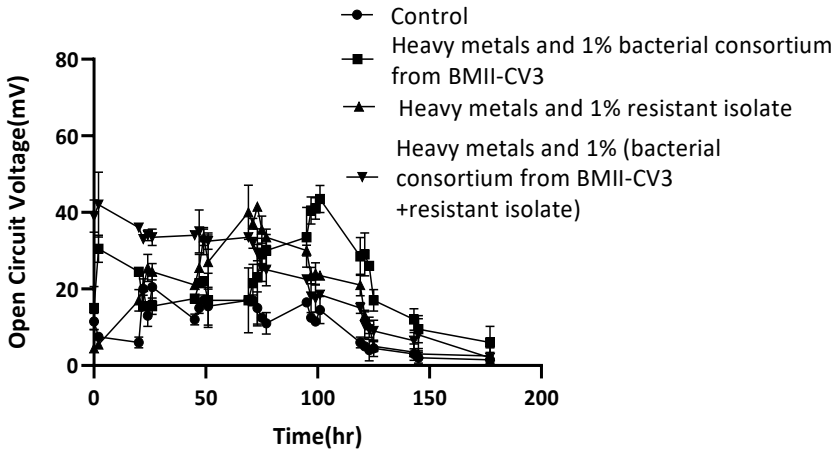

Figure 20 Graphical representation of OCV produced during the MFC Operation with Synthetic water of COD 3500mg/L, pH 7.0 ± 0.02

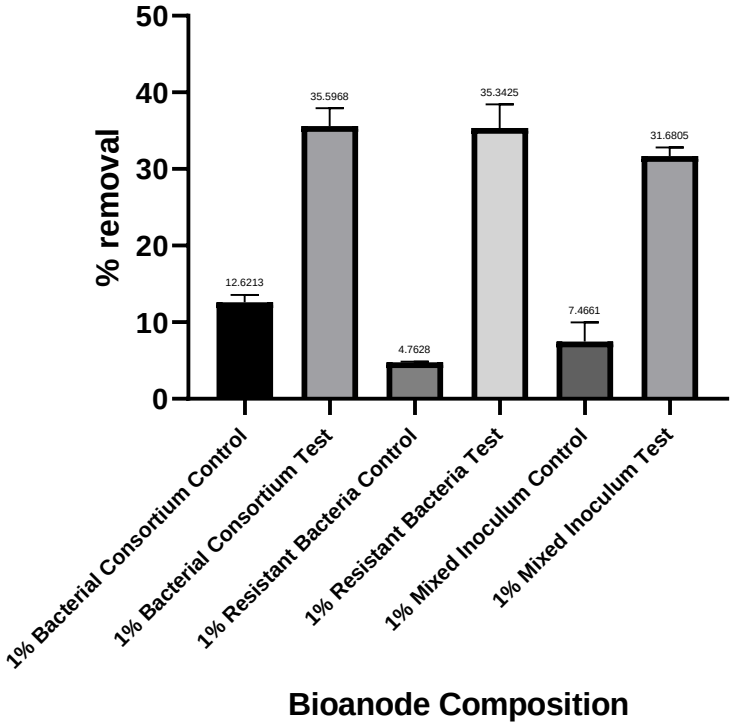

Figure 21 Comparative graphical representation of COD removal after MFC Operation with synthetic water of COD3500mg/L, pH 7.0± 0.02

In our study, unlike Genge & Khade (2019), a bacterial consortium outperformed the pure bacterial culture in terms of OCV generation. This is likely due to the complex synergistic relationships among the microbial species in the MFC. Mixed cultures have a broader metabolic capability, utilizing a wide range of organic compounds, and can establish a

natural redox potential gradient where some bacteria act as electron donors. Additionally, mixed cultures exhibit resilience to environmental changes, contributing to consistent MFC performance. Conversely, in Genge & Khade's (2019) study, the higher electricity generation from the pure culture may result from specialized electron transfer mechanisms developed by those specific bacteria.

4.4. MFC operation for Heavy Metals remediation

4.4.1. MFC operation using external 1.1kΩ resistor

The CCV of initial 0.005 V fluctuated with increase and decrease electric output over an average of 8 days, however before a subsequent decrease, a maximum CCV (Closed Circuit Voltage) recorded was 0.003 V for MFC operated with synthetic water of COD 3500mg/L, pH 7.0, Graphite rod anode and Platinum cathode along with 1 % bacterial consortium as shown in Figure 22, A. Similarly, for the voltage of 0.005 V, the current density recorded 0.05 ± 0.006 A/m^2 along with the power density of 0.0002 W/m^2 (Figure 22, B). These outputs were exceeded by MFC operated with Bagmati water enriched with 1% bacterial consortium followed by Bagmati water). Bagmati water enriched with bacterial consortium achieved a higher power density of 0.070 ± 0.002 W/m^2 at a current density of 0.8 ± 0.01 A/m^2 (Figure 23, C) and a CCV of 0.08 ± 0.001 V (Figure 23, A) while the MFC operated with Bagmati water achieved a power density of 0.0448 ± 0.009 W/m^2 at a current density of 0.6364 ± 0.06 A/m^2 (Figure 23, B) and a CCV of 0.07 V (Figure 23, A). Decreasing voltage resulted in a proportional decrease in both current density and power density. Similarly, the maximum COD removal was achieved by MFC Bagmati water enriched with the bacterial consortium (65.51%) followed by MFC operated with Bagmati water(64.38%), and the MFC Test operated with Synthetic water showed the COD removal of 63.45% with Control being comparatively less efficient in removal i.e. 51.68%. indicating microbial oxidation is more efficient (Table 7).

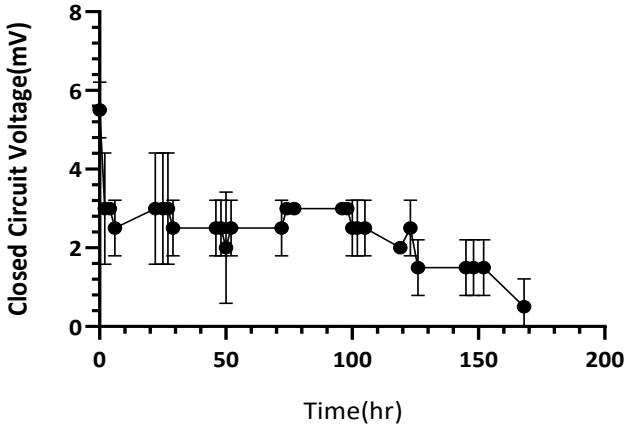

(A)

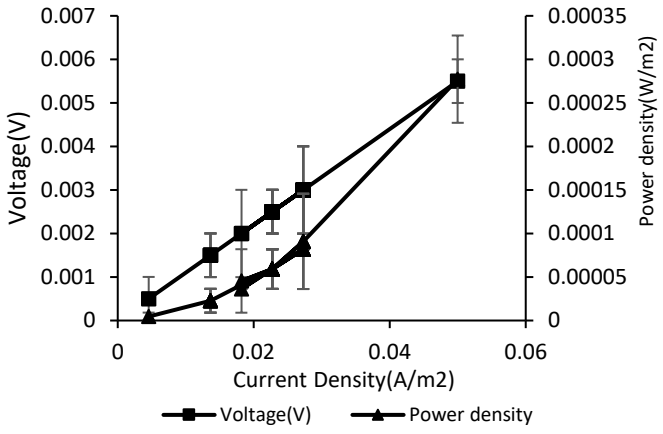

(B)

Figure 22 (A) Graphical representation of CCV produced during the MFC Test Operation with Synthetic water of COD 3500mg/L, pH 7.0 ± 0.02, 1% inoculum

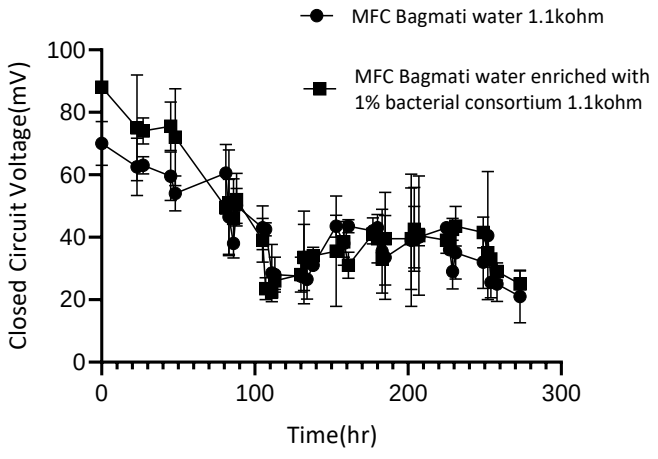

(A)

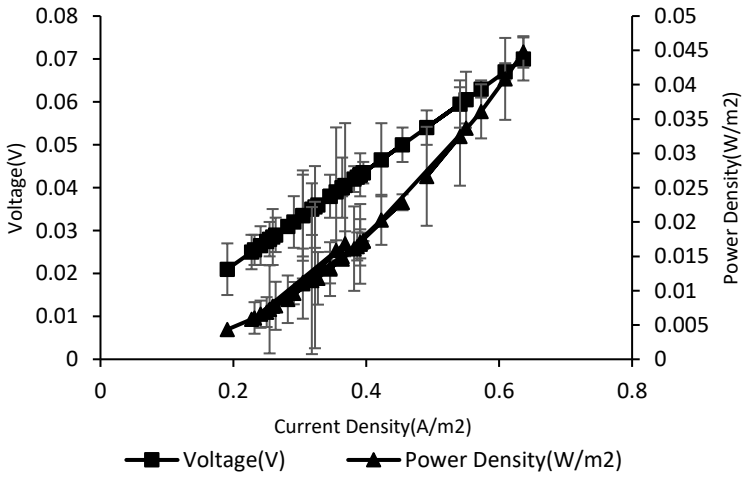

(B)

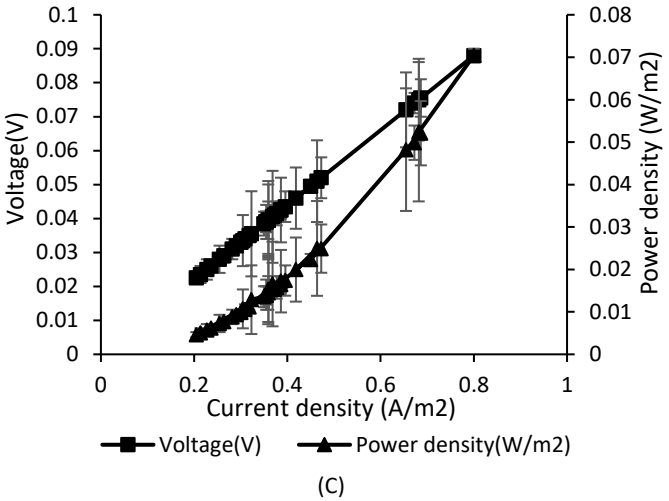

(C)

Figure 23 Electric Output after MFC Operation with Bagmati water using external resistance of 1.1KΩ, (A) Graphical representation of CCV produced during the MFC Operation with Bagmati water, pH 7.0 ± 0.02, (B), (C) Proportional Relationship between Voltage, Power density, and current density after MFC operated with same conditions mentioned above of MFC operated with Bagmati water and Bagmati water enriched with bacterial consortium respectively

Table 7 Comparative analysis for COD removal after MFC operation with pH 7.0 ± 0.02, 1% inoculum

S.N	Samples	Initial concentration(mg/L)	Final Concentration(mg/L)	% removal (mean % ± S.D.)
1.	MFC 3500mg/L Control	3371.73 ± 50.16	1629.068± 31.35	51.68 ± 0.21
2.	MFC 3500mg/L Test	3211.52± 30.40	1173.68 ± 18.24	63.45 ± 0.22
3.	MFC Bagmati water	313.84 ± 18.24	111.77 ± 48.64	64.77 ± 13.45
4.	MFC Bagmati water enriched with 1% bacterial consortium	249.35 ± 36.48	85.98 ± 36.48	64.06 ± 19.88

In comparing electric output from Microbial Fuel Cells (MFCs) using different types of water (synthetic, Bagmati, and Inoculum enriched Bagmati), several factors influence the observed results. When synthetic water was employed, despite having a higher Chemical Oxygen Demand (COD) than Bagmati water, the electric output was lower. This discrepancy can be attributed to the greater presence of electrolytes and nutrients in river water. River water also contains a complex mixture of organics, including those that are challenging to degrade. This provides a wider range of substrates for bacterial metabolism compared to the simpler and more easily degradable organic compounds present in synthetic wastewater.

Furthermore, even when the inoculum from the Bagmati River was introduced into the synthetic water setup, the adaptation of bacteria to the natural river environment led to a slightly higher electric output. Comparisons with other studies reveal additional insights. The electric output in our research using synthetic water was lower than in

studies by Wang et al. (2011) and Li et al. (2018). Operational configurations differences likely contribute to these variations. Similarly, contrasting with the findings of Das & Calay (2022), our research showed lower power density, current density, and voltage. This can be attributed to the fact that our synthetic water had a lower COD compared to the synthetic water mimicking dairy wastewater used in their study. When real wastewater was employed, our research yielded lower voltage, power density, and current density than Majumder et al. (2014). This difference can be attributed to variations in COD and the specific substrate used. In contrast, the study by Heinrichmeier et al. (2023), which utilized municipal wastewater, demonstrated higher current and power density compared to our research. This can be linked to the high conductivity of the wastewater, which reduces internal or ohmic resistance within the system. In summary, different MFC configurations and operating conditions lead to varying power densities and COD removal efficiencies, highlighting the importance of optimizing the MFC design for specific applications and wastewater characteristics.

4.4.2. Removal of Heavy metals after MFC operation for Synthetic as well as Bagmati water

The results of the analysis showed that the MFCs were effective in removing heavy metals, with arsenic being the most effectively removed at ~ 100%, followed by lead at ~ 99%, and chromium being the least effectively removed as shown in Figure 24. Although there were no significant differences observed among the three MFC operations, the inoculum enriched MFC (1% bacterial consortium) was found to be more efficient in removing heavy metals compared to the others.

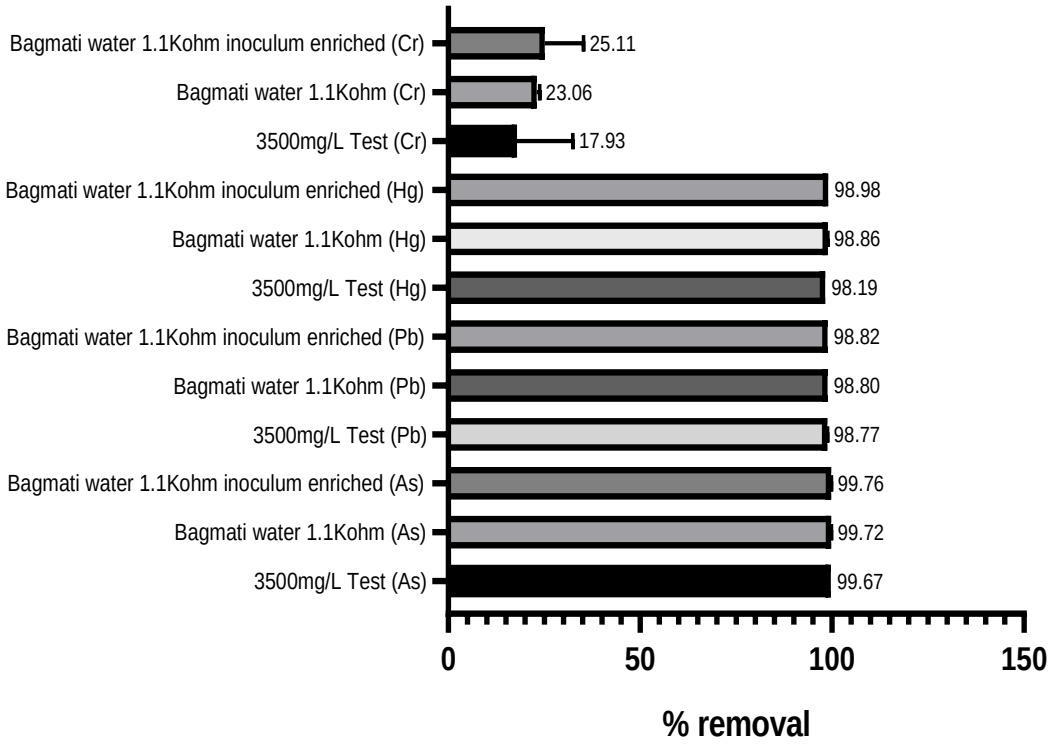

Figure 24 Analysis of heavy metals removal using Differential Pulse voltammetry (SCE Potential vs Current) of MFC operated with Synthetic water of COD 3500mg/L, Bagmati water, pH 7.0 ± 0.02, 1% inoculum

In the research conducted by X. Q. Wang et al., 2014 for the removal of Arsenite using an MFC, >95% of Arsenic (III) was removed, which was almost similar to our research that achieved an average removal of 99%. In the investigation by Z. Wang et al. (2011), a maximum of 99.54% Hg (II) removal was achieved for a concentration of 100 mg/L, using graphite felt and carbon paper as the anode and cathode, respectively. In our research, an average of 98% Hg (II) removal was achieved. Li et al. (2018) found that there was a 12.5% removal of Chromium (VI) at pH 7.0, but 100% removal at pH 2, 3, and 4 (initial concentration 80 mg/L). For the optimal MFC configuration, carbon felt and carbon cloth were used as the anode and cathode, respectively, with a pH of 2.0. In our research, at pH 7.0 ± 0.02, there was less removal of Cr (VI) similar to that in the study of Li et al., (2018). This may be because of the less ionic concentration of Cr (VI), on the contrary under acidic conditions, the reduction of Cr (VI) was thermodynamically favored due to the increase of standard potential along with hydrogen ion concentration. Song et al. (2016) achieved 15.5 ± 1.3% Cr (VI) removal with a configuration using graphite felt as both the anode and cathode. This operation was carried out with an external resistance of 1000Ω at 25°C. In the study conducted by Rajendran et al. (2021), a dual-chambered Microbial Fuel Cell (MFC) was operated using synthetic water with a pH of 3. The MFC had an anode electrode made of iodine-doped polythiophene-modified carbon cloth, while the cathode electrode was coated with platinum. *Shewanella putrefaciens* (MTCC no. 3525) was used as the microbial inoculum in the anode chamber. The catholyte in the MFC contained a 40 ppm lead solution. The researchers observed a remarkable 84.3% removal of Pb (II) during the operation of the MFC. This implies that the MFC configuration and the presence of *Shewanella putrefaciens* in the anode chamber contributed to the effective removal of lead ions from the solution. In our study, the MFC using synthetic water exhibited lower removal rates compared to the MFC using Bagmati river water. This difference can be attributed to the presence of nutrients in the river water, which supports the growth of metal-reducing microorganisms, ensuring a more active microbial community. Furthermore, the bacterial consortium in the Bagmati river water MFC was already adapted to the river's conditions, unlike the inoculum used in the synthetic water setup, which had to adjust to the altered environment. Also, in between Bagmati water and inoculum enriched Bagmati water, the latter showed slightly more removal which may be due to the increase in bacterial population which synergistically metabolize organic compounds generating more electrons.

CHAPTER V

SUMMARY

This research aimed to use Microbial Fuel Cell (MFC), an eco-friendly technique, for the removal of heavy metals from the Bagmati water source. The process relies on the cathodic reduction of heavy metals, where electrons released in the anodic chamber during microbial oxidation are accepted by the heavy metals in the cathode. This acceptance leads to the reduction of heavy metals into less toxic forms, effectively remediating them from the contaminated source. MFC offers the dual benefits of wastewater treatment and bio-electricity generation. Different physical, chemical, and biological parameters were carried out to understand the status of water quality. The optimization of configurations (Chemical Oxygen Demand (COD), electrodes, and bio-anode) in MFC was performed with synthetic water, and later the optimal configuration was implied on Bagmati water.

Chapter I of this study provided a general introduction to the research. It discussed the contamination of the Bagmati River with heavy metals such as Arsenic (As), Lead (Pb), Mercury (Hg), and Chromium (Cr), along with the sources of these heavy metals. The chapter also covered various approaches to remove these contaminants and highlighted the emergence of Microbial Fuel Cells (MFCs) as a potential method for their removal and remediation. Furthermore, Chapter I reviewed existing studies related to the use of MFC for treating heavy metal pollution and outlined the research scope it offered. MFC was shown to be an effective approach for wastewater treatment, offering the advantages of not causing secondary pollution, being cost-effective, eco-friendly, and not requiring additional energy input compared to other chemical and physical removal methods. The chapter also presented the hypotheses made for the research and outlined the objectives that needed to be achieved to support these hypotheses effectively.

Many researchers had also used MFC with some modifications in electrodes to achieve a good result for the heavy metals removal, as well as finding less expensive materials to be used as an electrode. Synthetic water has been used to study the electric output of the MFC alongside the potential of removing heavy metals. Their work excerpt has been included in Chapter II. In addition to previous work on MFC performed and the outcome achieved, different architectures and components of MFC have also been explicated. Based on the reviews done, different factors like anode and cathode material, cathode electron acceptor, temperature, pH, external resistance, and substrate type influenced the MFC performance.

Chapter III explained the materials and methods used for the research study, where sampling of three locations Kupondol, Balkhu, and Chovar was done twice i.e. in summer and in winter. This was to know the pollution level as the water flows by and the state of pollution for seasonal variance. Because the parameters of Bagmati water kept changing, synthetic water (Anode: synthetic water + bacteria, cathode: Synthetic water without

organic compounds + heavy metals) was prepared to introduce an optimal configuration for MFC operation. A batch operation of MFC was performed keeping the temperature and pH constant, the optimization was performed on COD value(800mg/L,1500mg/L,2500mg/L, and 3500mg/L), electrodes(Graphite rod, Graphite Felt, and Platinum) and bio-anode(1% bacterial consortium, 1% resistant bacteria, 1%(mix of bacterial consortium and resistant bacteria). The optimal configuration was selected based on the Open Circuit Voltage (OCV) and % COD removal. Microbial analysis of the Bagmati water was analyzed through Metagenomic sequencing and additionally, heavy metals resistant bacteria were also isolated and primarily identified to study the effectiveness of using heavy metal-resistant bacteria for the MFC optimization. Differential Pulse Anodic Stripping Voltammetry (DPASV) was used for the quantification of As (III), Pb (II), Hg (II), and Cr (VI) after MFC operation with optimal Configuration. After the obtainment of optimal configuration, the MFC was operated with Bagmati water.

The findings of the research were discussed in Chapter IV where the analysis of physical, and chemical parameters portrayed Bagmati River was not polluted with heavy metals since the targeted heavy metals As, Pb, Hg, and Cr were below the standard contamination level (mg/L) however, pollution from lead was found. On the closed-circuit operation(R_{ext} 1.1 KΩ)of MFC using Bagmati water supplemented with heavy metals, for initial concentration of 1mg/L As(III), 50mg/L of Pb(II), Hg(II) and Cr (VI), removal of almost 100% were achieved except for Cr(VI) which has the least removal. In conclusion, the research demonstrated the successful application of MFC for heavy metal remediation in water and highlighted its potential for sustainable wastewater treatment and bio-electricity generation.

CHAPTER VI

CONCLUSION

Microbial fuel cells (MFCs) can effectively remove heavy metals from wastewater with the generation of bio-electricity simultaneously. Based on the results obtained from COD, and TSS, the Bagmati River water of the sampling location was polluted since it exceeded the maximum discharge limit of 250mg/L and 50mg/L respectively as per the guideline of the Ministry of Environment (MoE 2010). Additionally, the water was polluted with lead however other heavy metals; As, Hg and Cr were below the maximum contaminant level (MCL). Metagenomics analysis revealed a diverse group of bacteria of which some electrogenic bacteria were also found in the sampled water that aided in the generation of electricity during the MFC operation. The maximum voltage of 0.08 ± 0.001 V, the current density of 0.8 ± 0.01 A/m^2, power density of 0.070 ± 0.002 W/m^2 were generated along with the removal of heavy metals, however, the power generation wasn't high enough to support any electrical appliances. Removal of approximately 100% As (III), Pb(II), and Hg(II) were achieved but there was < 50% removal of Cr(VI). Also, almost similar power generation and heavy metal removal were achieved even without the use of a Platinum electrode, so Graphite electrodes with modifications could be used to minimize the cost. Bagmati River water was successfully utilized as a substrate for MFC operation to have heavy metals removed from it. The efficiency of MFCs in removing multiple heavy metals simultaneously makes them a promising option for addressing water pollution in other contaminated water bodies. However, further research is needed to optimize MFC design, enhance efficiency, and evaluate long-term performance in large-scale applications. It is also important to assess the potential impacts of the remediation process on microbial communities and overall ecosystem dynamics to ensure ecological sustainability.

This study highlights the promising potential of microbial fuel cell technology for treating heavy metal contamination in water bodies like the Bagmati River. Continued exploration and development of this approach could lead to significant advancements in environmental remediation, providing a sustainable solution for restoring and preserving water quality in polluted rivers and other contaminated water sources.

CHAPTER VII

RECOMMENDATIONS

Based on the results obtained, it is recommended for:

1. Development of economically viable electrode materials with high porosity and conductivity along with new electrode modification techniques and the ability to achieve high current densities.
2. Acclimatization and stabilization of biofilms since the maturation of biofilms on the electrode plays a crucial role in achieving high MFC output.
3. Pilot-scale investigations, along with modeling and optimization outputs to establish the feasibility of MFCs for field-scale application in removing xenobiotic compounds

REFERENCES

Adhikari, M. P., Neupane, M. R., & Kafle, M. (2019). Physico-chemical Parameterization and Determination of Effect of Tributaries on Enhancement of Pollutants in Bagmati River. *Journal of Nepal Chemical Society*, *40*(December), 36–43. https://doi.org/10.3126/jncs.v40i0.27276

Aghababaie, M., Farhadian, M., Jeihanipour, A., and Biria, D. (2015). Effective factors on the performance of microbial fuel cells in wastewater treatment – a review. Environ. Technol. Rev. 4, 71–89. doi: 10.1080/09593330.2015.1077896

Al-Asheh, S., Bagheri, M., & Aidan, A. (2022). Removal of heavy metals from industrial wastewater using microbial fuel cell. Engineering in life sciences, 22(8), 535–549. https://doi.org/10.1002/elsc.202200009

Amira, S., Soesilo, T. E. B., & Moersidik, S. S. (2019). Environmental and Social Approach for Controlling Water Pollution in Krukut River, DKI Jakarta. *IOP Conference Series: Earth and Environmental Science*, *399*(1), 1–9. https://doi.org/10.1088/1755-1315/399/1/012092

Badr, N., & Al-Qahtani, K. M. (2013). Treatment of wastewater containing arsenic using rhazya stricta as a new adsorbent. Environmental Monitoring and Assessment, 185(12), 9669–9681. https://doi.org/10.1007/s10661-013-3220-5

Bagchi, S., & Behera, M. (2020). Assessment of Heavy Metal Removal in Different Bioelectrochemical Systems: A Review. *Journal of Hazardous, Toxic, and Radioactive Waste*, *24*(3). https://doi.org/10.1061/(asce)hz.2153-5515.0000500

Bakonyi P, Koók L, Kumar G, et al. Architectural engineering of bioelectrochemical systems from the perspective of polymeric membrane separators: a comprehensive update on recent progress and future prospects. J Memb Sci. 2018;564:508–522. doi: 10.1016/j.memsci.2018.07.051.

Baniya, B., Khadka, N., Ghimire, S. K., Baniya, H., Sharma, S., Dhital, Y. P., Bhatta, R., & Bhattarai, B. (2019). Water quality assessment along the segments of Bagmati River in Kathmandu valley, Nepal. Nepal Journal of Environmental Science, 7, 1–10. https://doi.org/10.3126/njes.v7i0.34314

Barbato, R. A., Foley, K. L., Toro-Zapata, J. A., Jones, R. M., & Reynolds, C. M. (2017). The power of soil microbes: Sustained power production in terrestrial microbial fuel cells under various temperature regimes. Applied Soil Ecology, 109, 14-22.

Bernhoft, R. A. (2012). Mercury toxicity and treatment: A review of the literature. Journal of Environmental and https://doi.org/10.1155/2012/460508 Public Health, 2012, 1–10.

Chakraborty, I., Sathe, S. M., Khuman, C. N., & Ghangrekar, M. M. (2020). Bioelectrochemically powered remediation of xenobiotic compounds and heavy metal toxicity using microbial fuel cell and microbial electrolysis cell. *Materials Science for Energy Technologies*, *3*, 104–115. https://doi.org/10.1016/j.mset.2019.09.011

Chaturvedi, V., & Verma, P. (2016). Microbial fuel cell: a green approach for the utilization of waste for the generation of bioelectricity. In *Bioresources and Bioprocessing* (Vol. 3, Issue 1). Springer. https://doi.org/10.1186/s40643-016-0116-6

Chen, Z., Lu, X., Yin, R., Luo, Y., Mai, H., Zhang, N., Xiong, J., Zhang, H., Tang, J., & Luo, D. (2018). Research on treatment of wastewater containing heavy metal by microbial fuel cell. *IOP Conference Series: Earth and Environmental Science*, *121*(3). https://doi.org/10.1088/1755-1315/121/3/032022

Colantonio, N. (2016). Heavy Metal Removal From Wastewater Using Microbial Electrolysis Cells. McMaster University.

Dahal, A., Khanal, M., & Ale, M. (2011). *BAGMATI RIVER FESTIVAL : CONSERVATION OF DEGRADING RIVER Achyut Dahal , Mausam Khanal , and Megh Ale*. *1990*.

Das, S., & Calay, R. K. (2022). Experimental Study of Power Generation and COD Removal Efficiency by Air Cathode Microbial Fuel Cell Using Shewanella baltica 20. Energies, 15(11). https://doi.org/10.3390/en15114152

Devi, N. R., Sasidharan, M., & Sundramoorthy, A. K. (2018). Gold Nanoparticles-Thiol-Functionalized Reduced Graphene Oxide Coated Electrochemical Sensor System for Selective Detection of Mercury Ion. *Journal of The Electrochemical Society*, *165*(8), B3046–B3053. https://doi.org/10.1149/2.0081808jes

Gao, C., Liu, L., & Yang, F. (2018). A novel bio-electrochemical system with sand/activated carbon separator, Al anode and bio-anode integrated micro 68 electrolysis/electro-flocculation cost effectively treated high load wastewater with energy recovery. Bioresource technology, 249, 24-34.

Gautam, K., Pant, V., Pradhan, S., Pyakurel, D., Bhandari, B., & Shrestha, A. (2020). Blood Lead Levels in Rag-Pickers of Kathmandu and its Association with Hematological and Biochemical Parameters. EJIFCC, 31(2), 125–133

Genge, A., & Khade, R. (2019). Isolation and Screening of Exoelectrogenic Bacteria from Waste Water. International Journal of Trend in Scientific Research and Development, Volume-3(Issue-3), https://doi.org/10.31142/ijtsrd23352

George, A. T., Ganesan, R., & Thangeeswari, T. (2016). Redox Deposition of Manganese Oxide Nanoparticles on Graphite Electrode by Immersion Technique for Electrochemical Super Capacitors. *Indian Journal of Science and Technology*, *9*(1), 1–7. https://doi.org/10.17485/ijst/2016/v9i1/85782

Giri, I., K.C., R., & Khadka, U. R. (2022). Water quality status in Bagmati River of Kathmandu Valley, Nepal. Ecological Significance of River Ecosystems, 481–502. https://doi.org/10.1016/b978-0-323-85045-2.00017-0

Hazrat, A., Ezzat, K., & Ilahi Ikram. (2019). Environmental Chemistry and Ecotoxicology of Hazardous Heavy Metals: Environmental Persistence, Toxicity, and Bioaccumulation. *Journal of Chemistry*, *2019*(Cd), 1–14. https://doi.org/10.1155/2019/6730305

Heidrich, E. S., Dolfing, J., Wade, M. J., Sloan, W. T., Quince, C., & Curtis, T. P. (2018). Temperature, inocula and substrate: Contrasting electroactive consortia, diversity and

performance in microbial fuel cells. *Bioelectrochemistry*, *119*, 43–50. https://doi.org/10.1016/j.bioelechem.2017.07.006

Heinrichmeier, J., Littfinski, T., Vasyukova, E., Steuernagel, L., & Wichern, M. (2023). On-site performance evaluation of a 1,000-litre microbial fuel cell system using submergible multi-electrode modules with air-cathodes for sustainable municipal wastewater treatment and electricity generation. *Water Science and Technology*, *87*(8), 1969-1981.

Huang, L., Liu, Y., Yu, L., Quan, X., & Chen, G. (2015). A new clean approach for production of cobalt dihydroxide from aqueous Co(II) using oxygen-reducing biocathode microbial fuel cells. *Journal of Cleaner Production*, *86*, 441–446. https://doi.org/10.1016/j.jclepro.2014.08.018

Isosaari, P., and Sillanpää, M. (2017). Use of sulfate-reducing and bioelectrochemical reactors for metal recovery from mine water. Separ. Purif. Rev. 46, 1–20. doi: 10.1080/15422119.2016.1156548

Jaishankar, M., Tseten, T., Anbalagan, N., Mathew, B. B., & Beeregowda, K. N. (2014). Toxicity, mechanism and health effects of some heavy metals. *Interdisciplinary Toxicology*, *7*(2), 60–72. https://doi.org/10.2478/intox-2014-0009

James, A. (2022). Ceramic-Microbial Fuel Cell (C-MFC) for waste water treatment: A mini review. *Environmental Research*, *210*, 112963. https://doi.org/10.1016/j.envres.2022.112963

Jayapriya, J., & Ramamurthy, V. (2012). Use of non-native phenazines to improve the performance of Pseudomonas aeruginosa MTCC 2474 catalysed fuel cells. Bioresource Technology, 124, 23-28.

Jiang, Y., Liang, P., Zhang, C., Bian, Y., Yang, X., Huang, X., & Girguis, P. R. (2015). Enhancing the response of microbial fuel cell based toxicity sensors to Cu (II) with the applying of flow-through electrodes potentials. Bioresource technology, 190, 367-372. and controlled anode

Jia, Q., Wei, L., Han, H., & Shen, J. (2014). Factors that influence the performance of two-chamber microbial fuel cell. International journal of hydrogen energy, 39(25), 13687-13693.

Kaushik, A., & Singh, A. (2020). Metal removal and recovery using bioelectrochemical technology: The major determinants and opportunities for synchronic wastewater treatment and energy production. *Journal of Environmental Management*, *270*(February), 110826. https://doi.org/10.1016/j.jenvman.2020.110826

Kumar, A., Kumar, A., Cabral-Pinto, M., Chaturvedi, A. K., Shabnam, A. A., Subrahmanyam, G., Mondal, R., Gupta, D. K., Malyan, S. K., Kumar, S. S., Khan, S. A., & Yadav, K. K. (2020). Lead toxicity: Health hazards, influence on food Chain, and sustainable remediation approaches. *International Journal of Environmental Research and Public Health*, *17*(7), 1–36. https://doi.org/10.3390/ijerph17072179

Kumar, R., Yadav, S., & Patil, S. A. (2020). Bioanode-Assisted Removal of Hg 2+ at the Cathode of Microbial Fuel Cells . *Journal of Hazardous, Toxic, and Radioactive Waste*, *24*(4), 1–6. https://doi.org/10.1061/(asce)hz.2153-5515.0000533

Kurbanoglu, S., Uslu, B., & Ozkan, S. A. (2017). Carbon-based nanostructures for electrochemical analysis of oral medicines. In *Nanostructures for Oral Medicine*. Elsevier Inc. https://doi.org/10.1016/B978-0-323-47720-8.00029-8

Leong JX, Daud WRW, Ghasemi M, et al. Ion exchange membranes as separators in microbial fuel cells for bioenergy conversion: a comprehensive review. Renew Sustain Energy Rev. 2013;28:575–587. doi: 10.1016/j.rser.2013.08.052.

Li, M., Zhou, S., Xu, Y., Liu, Z., Ma, F., Zhi, L., & Zhou, X. (2018). Simultaneous Cr(VI) reduction and bioelectricity generation in a dual chamber microbial fuel cell. *Chemical Engineering Journal*, *334*(November 2017), 1621–1629. https://doi.org/10.1016/j.cej.2017.11.144

Li, S., & Chen, G. (2018). Factors affecting the effectiveness of bioelectrochemical system applications: Data synthesis and meta-analysis. *Batteries*, *4*(3), 1–18. https://doi.org/10.3390/batteries4030034

Li, Y., Zhang, B., Cheng, M., Li, Y., Hao, L., & Guo, H. (2016). Spontaneous arsenic (III) oxidation with bioelectricity generation in single-chamber microbial fuel cells. *Journal of Hazardous Materials*, *306*, 8–12. https://doi.org/10.1016/j.jhazmat.2015.12.003

Liu Z., Liu J., Zhang S., Xing X.H. and Su Z. (2011). Microbial fuel cell based biosensor for in situ monitoring of anaerobic digestion process. Bioresour Technol. 102 (22), 10221-10229.

López Velarde Santos, M., Rodríguez Valadéz, F. J., Mora Solís, V., González Nava, C., Cornejo Martell, A. J., & Hensel, O. (2017). Performance of a microbial fuel cell operated with vinasses using different COD concentrations. *Revista internacional de contaminación ambiental*, *33*(3), 521-528.

Ma, J., Wu, S., Shekhar, N. V., Biswas, S., & Sahu, A. K. (2020). Determination of physicochemical parameters and levels of heavy metals in food waste water with environmental effects. Bioinorganic chemistry and applications, 2020.

Majumder, D., Maity, J. P., Tseng, M. J., Nimje, V. R., Chen, H. R., Chen, C. C., ... & Chen, C. Y. (2014). Electricity generation and wastewater treatment of oil refinery in microbial fuel cells using Pseudomonas putida. *International journal of molecular sciences*, *15*(9), 16772-16786.

Malar, S., Shivendra Vikram, S., JC Favas, P., & Perumal, V. (2014). Lead heavy metal toxicity induced changes on growth and antioxidative enzymes level in water hyacinths [eichhornia crassipes (Mart.)]. https://doi.org/10.1186/s40529-014-0054-6 Botanical Studies, 55(1)

Manandhar S., & Sharma S., (2013) Practical Approach to Microbiology, National Book center, Bhotahity, Kathmandu, 2nd ed.

Mathuriya AS (2014) Eco-affectionate face of microbial fuel cells. Crit Rev Environ Sci Technol 44(97–153):1080. doi:10.1080/ 10643389.2012.710445

Milner, H. Basnet, S. Gurung, R. Maharjan, T. Neupane, D. N. Shah, B. M. Shakya, R. Tachamo, R. D. Shah, and S. Vaidya, Bagmati River Expedition 2015: A baseline study along the length of the Bagmati River in Nepal to gather data on physical, chemical, and biological indicators of water quality and pollution; and document human- river interaction, Nepal River Conservation Trust and Biosphere Association, Kathmandu, Nepal, 2015.

Musselman, R. (2012). Sampling procedure for lake or stream surface water chemistry. United States Department of agriculture, Forest Service, Rocky Mountain Research Station.

Mustakeem, M. (2015). Electrode materials for microbial fuel cells : nanomaterial approach. Mater. Renew. Sustain. Energy 4, 1–11. doi: 10.1007/s40243-015-0063 8

Muthukalum, U. A. S. L., Gunathilake, C. A., & Kalpage, C. S. (2020). Removal of Heavy Metals from Industrial Wastewater Through Minerals. *Lecture Notes in Civil Engineering*, *44*(December), 615–632. https://doi.org/10.1007/978-981-13-9749-3_54

Nam J.Y., Kim H.W., Lim K.H. and Shin H.S. (2010). Effects of organic loading rates on the continuous electricity generation from fermented wastewater using a single chamber microbial fuel cell. Bioresour. Technol. 101 (1), 33-37. DOI: 10.1016/j.biortech.2009.03.062

Nicomel, N., Leus, K., Folens, K., Van Der Voort, P., & Du Laing, G. (2015). Technologies for arsenic removal from water: Current status and future perspectives. International Journal of Environmental Research and Public Health, 13(1), 62. https://doi.org/10.3390/ijerph13010062

Oliveira V.B., Simoes M., Melo L.F. and Pinto A.M.F.R. (2013). Overview on the developments of microbial fuel cells. Biochem. Eng. J. 73, 53-64. DOI: 10.1016/j.bej.2013.01.012

Pal, C. B., Pant, R. R., Rimal, B., & Mishra, A. D. (2021). Comparative Assessment 0f Water Quality in the Bagmati River Basin, Nepal. *ZOO-Journal*, *5*(December), 68–78. https://doi.org/10.3126/zooj.v5i0.34919

Pantha, K., Acharya, K., Mohapatra, S., Khanal, S., Amatya, N., Ospina-Betancourth, C., Butte, G., Shrestha, S. D., Rajbhandari, P., & Werner, D. (2021). Faecal pollution source tracking in the holy Bagmati River by portable 16S rRNA gene sequencing. *Npj Clean Water*, *4*(1), 1–11. https://doi.org/10.1038/s41545-021-00099-1

Pasternak G, Yang Y, Santos BB, et al. Regenerated silk fibroin membranes as separators for transparent microbial fuel cells. Bioelectrochemistry. 2019;126:146 155. doi: 10.1016/j.bioelechem.2018.12.004.

Pasupuleti SB, Srikanth S, Dominguez-Benetton X, et al. Dual gas diffusion cathode design for microbial fuel cell (MFC): optimizing the suitable mode of operation in terms of bioelectrochemical and bioelectro-kinetic evaluation. J Chem Technol Biotechnol. 2016;91:624–639. doi: 10.1002/jctb.4613.

Potter, M. C. (1908). Bacteria as agents in the oxidation of amorphous carbon. *Proceedings of the Royal Society of London. Series B, containing papers of a*

biological character, *80*(539), 239-259.

Potter, M. C. (1911). Electrical effects accompanying the decomposition of organic compounds. *Proceedings of the royal society of London. Series b, containing papers of a biological character*, *84*(571), 260-276.

Rajbanshi, A. (2009). Study on Heavy Metal Resistant Bacteria in Guheswori Sewage Treatment Plant. *Our Nature*, *6*(1), 52–57. https://doi.org/10.3126/on.v6i1.1655

Rajendran, R., Dhakshina Moorthy, G. P., Krishnan, H., & Anappara, S. (2021). A Study on Polythiophene Modified Carbon Cloth as Anode in Microbial Fuel Cell for Lead Removal. *Arabian Journal for Science and Engineering*, *46*(7), 6695–6701. https://doi.org/10.1007/s13369-021-05402-3

Rajkumar, M., Thiagarajan, S., & Chen, S. M. (2011). Electrochemical detection of arsenic in various water samples. *International Journal of Electrochemical Science*, *6*(8), 3164–3177. https://doi.org/10.1016/s1452-3981(23)18243-5

Rismani-Yazdi, H., Christy, A. D., Carver, S. M., Yu, Z., Dehority, B. A., & Tuovinen, O. H. (2011). Effect of external resistance on bacterial diversity and metabolism in cellulose-fed microbial fuel cells. *Bioresource Technology*, *102*(1), 278–283. https://doi.org/10.1016/j.biortech.2010.05.012

Rohrback, G. H., Scott, W. R., & Canfield, J. H. (1962, May). Biochemical fuel cells. In *Proceedings of the 16th Annual Power Sources Conference* (Vol. 18)

Rosolina, S. M., Chambers, J. Q., Lee, C. W., & Xue, Z. L. (2015). Direct determination of cadmium and lead in pharmaceutical ingredients using anodic stripping voltammetry in aqueous and DMSO/water solutions. *Analytica Chimica Acta*, *893*, 25–33. https://doi.org/10.1016/j.aca.2015.07.010

Sanders, T., Liu, Y., Buchner, V., & Tchounwou, P. B. (2009). Neurotoxic effects and biomarkers of lead exposure: a review. *Reviews on environmental health*, *24*(1), 15-46.

Sevda, S., Garlapati, V. K., & Sreekrishnan, T. R. (2023). Role of electrode and proton exchange membrane configurations on microbial fuel cell performance toward bioelectricity generation integrated wastewater treatment. *Journal of Environmental Science and Health - Part A Toxic/Hazardous Substances and Environmental Engineering*, *58*(1), 13–23. https://doi.org/10.1080/10934529.2023.2168998

Shrestha Ghaju, R., Tandukar, S., Sherchan, S. P., Bhandari, D., Tanaka, Y., Sherchand, J. B., & Haramoto, E. (2019). Prevalence of Arcobacter and other pathogenic bacteria in river water in Nepal.

Singh, D., Tiwari, A., and Gupta, R., 2012, Phytoremediation of lead from wastewater using aquatic plants, Journal of agricultural Technology, Vol. 8, no.1, 1-11.

Singh, V., Singh, N., Rai, S. N., Kumar, A., Singh, A. K., Singh, M. P., Sahoo, A., Shekhar, S., Vamanu, E., & Mishra, V. (2023). Heavy metal contamination in the aquatic ecosystem: Toxicity and its remediation using eco-friendly approaches. Toxics, 11(2), 147. https://doi.org/10.3390/toxics11020147

Smith & Cresser (Eds.) (2003). *Soil and Environmental Analysis*. https://doi.org/10.1201/9780203913024

Song, T. shun, Jin, Y., Bao, J., Kang, D., & Xie, J. (2016). Graphene/biofilm composites for enhancement of hexavalent chromium reduction and electricity production in a biocathode microbial fuel cell. *Journal of Hazardous Materials*, *317*, 73–80. https://doi.org/10.1016/j.jhazmat.2016.05.055

Stojanović, Z., Koudelkova, Z., Sedlackova, E., Hynek, D., Richtera, L., & Adam, V. (2018). Determination of chromium(vi) by anodic stripping voltammetry using a silver-plated glassy carbon electrode. *Analytical Methods*, *10*(24), 2917–2923. https://doi.org/10.1039/c8ay01047a

Strik, D. P., Picot, M., Buisman, C. J., & Barrière, F. (2013). pH and temperature determine performance of oxygen reducing biocathodes. Electroanalysis, 25(3), 652-655.

Tchounwou, P. B., Yedjou, C. G., Patlolla, A. K., & Sutton, D. J. (2012). Molecular, clinical and environmental toxicicology Volume 3: Environmental Toxicology. In *Molecular, Clinical and Environmental Toxicology* (Vol. 101). https://doi.org/10.1007/978-3-7643-8340-4

Thakur, J. K., Thakur, R. K., Ramanathan, A. L., Kumar, M., & Singh, S. K. (2010). Arsenic contamination of groundwater in Nepal—an overview. Water, 3(1), 1–20. https://doi.org/10.3390/w3010001

Thapa, D., Sharma, C., Kang, S., & Sillanpää, M. (2014). The risk of mercury exposure to the people consuming fish from Lake Phewa, Nepal. International Journal of Environmental Research and Public https://doi.org/10.3390/ijerph110706771 Health, 11(7), 6771–6779.

USEPA. (2018) Drinking water standards and health advisories. EPA 822-S-12-001.

Venton, B. J., & DiScenza, D. J. (2020). Voltammetry. Electrochemistry for Bioanalysis, 27-50.

Vishwanathan A. S. (2021). Microbial fuel cells: a comprehensive review for beginners. 3 Biotech, 11(5), 248. https://doi.org/10.1007/s13205-021-02802-y

Wang, J., Song, X., Wang, Y., Abayneh, B., Ding, Y., Yan, D., & Bai, J. (2016). Microbial community structure of different electrode materials in constructed wetland incorporating microbial fuel cell. Bioresource technology, 221, 697-702.

Wang, X. Q., Liu, C. P., Yuan, Y., & Li, F. bai. (2014). Arsenite oxidation and removal driven by a bio-electro-Fenton process under neutral pH conditions. *Journal of Hazardous Materials*, *275*, 200–209. https://doi.org/10.1016/j.jhazmat.2014.05.003

Wang, Z., Lim, B., & Choi, C. (2011). Removal of Hg2+ as an electron acceptor coupled with power generation using a microbial fuel cell. *Bioresource Technology*, *102*(10), 6304–6307. https://doi.org/10.1016/j.biortech.2011.02.027

Wang, Z., Lim, B. S., Lu, H., Fan, J., & Choi, C. S. (2010). Cathodic reduction of Cu 2+ and electric power generation using a microbial fuel cell. *Bulletin of the Korean Chemical Society*, *31*(7), 2025-2030.

Widjaja, T., Altway, A., & Soeprijanto, S. (2010). Performance of submerged membrane bioreactor combined with powdered activated carbon addition for the treatment of an industrial wastewater. IPTEK The Journal for Technology and Science, 21(1). https://doi.org/10.12962/j20882033.v21i1.24

Wiryawan, A., Retnowati, R., Burhan, P., & Syekhfani, S. (2018). METHOD OF ANALYSIS FOR DETERMINATION OF THE CHROMIUM (Cr) SPECIES IN WATER SAMPLES BY SPECTROPHOTOMETRY WITH DIPHENYLCARBAZIDE. *Journal of Environmental Engineering and Sustainable Technology*, *5*(1), 37–46. https://jeest.ub.ac.id/index.php/jeest/article/view/120

World Health Organization (2011) "Guidelines for Drinking-Water Quality 4th Ed, Geneva 27, Switzerland

World Health Organization (2017). Guidelines for drinking-water quality, 4th ed. Geneva, Switzerland

World Health Organization (1999), International Standard for Drinking Water, 3-6.

Wu, M. S., Xu, X., Zhao, Q., and Wang, Z. Y. (2017). Simultaneous removal of heavy metals and biodegradation of organic matter with sediment microbial fuel cells. RSC Adv. 7, 53433–53438. doi: 10.1039/C7RA11103G

Wu, S., Chandra Sekar, N., Tan, S. N., Xie, H., & Ng, S. H. (2016). Determination of chromium(III) by differential pulse stripping voltammetry at a chitosan-gold nanocomposite modified screen printed electrode. *Analytical Methods*, *8*(5), 962–967. https://doi.org/10.1039/c5ay03291a

Xue, A., Shen, Z.-Z., Zhao, B., & Zhao, H.-Z. (2013). Arsenite removal from aqueous solution by a microbial fuel cell–zerovalent iron hybrid process. Journal of Hazardous Materials, 261, 621–627. doi:10.1016/j.jhazmat.2013.07.072

Yang, Q., Liang, S., Liu, J., Jv, J., and Feng, Y. (2017). Analysis of Anodes of microbial fuel cells when. Catalysts 7:312. doi: 10.3390/catal7110312

Yaqoob, A. A., Ibrahim, M. N. M., Umar, K., Parveen, T., Ahmad, A., Lokhat, D., & Setapar, S. H. M. (2021). A glimpse into the microbial fuel cells for wastewater treatment with energy generation. *Desalination and Water Treatment*, *214*, 379–389. https://doi.org/10.5004/dwt.2021.26737

Zinoubi, K., Majdoub, H., Barhoumi, H., Boufi, S., & Jaffrezic-Renault, N. (2017). Determination of trace heavy metal ions by anodic stripping voltammetry using nanofibrillated cellulose modified electrode. *Journal of Electroanalytical Chemistry*, *799*(May), 70–77. https://doi.org/10.1016/j.jelechem.2017.05.039

APPENDICES

APPENDIX I

Lists of materials, apparatus, instruments, chemicals, and media

- **Materials**

1. Gloves
2. Nafion 177
3. Forceps
4. Copper tape, Tape
5. Scissors
6. Glass spreader
7. Platinum sheet
8. Graphite rod
9. Graphite felt

- **Chemicals**

1. Glucose
2. Potassium Hydrogen Pthalate
3. Potassium Dichromate
4. Mercury Sulphate
5. Concentrated Sulphuric acid
6. Silver Sulphate
7. Ammonia Nitrogen
8. Boric acid
9. Sodium Hydroxide
10. Sodium tetraborate
11. Potassium dihydrogen phosphate
12. Ammonium Molybdate antimony potassium tartarate
13. Ascorbic acid
14. Sodium bisulfate
15. Sodium Arsenite
16. Lead acetate
17. Mercuric Chloride
18. Potassium dichromate
19. Methanol
20. Ethanol
21. Acetone

- **Apparatus**

1. Sample bottle
2. Conical Flask
3. Test Tubes
4. Beakers
5. Plexiglass MFC set
6. Culture tubes
7. Reagent bottle
8. Petri-dish
9. Measuring Cylinder
10. RB(Round Bottom) flask
11. Condenser
12. Cuvette

- **Instruments**

1. pH meter
2. Laboratory thermometer
3. Hot air Oven
4. Centrifuge
5. Micropipette, tips
6. Electrochemical workstation(CHI 660E)

- **Reagents**

1. DNS reagent
2. Nessler's reagent
3. Crystal Violet
4. Gram's iodine
5. Decolorizer
6. Saffranin

APPENDIX II

Reagents preparation for the analysis of Chemical Parameters of the Sample

A. Preparation of DNS Reagent

For the final volume of 100ml, 30gm of Sodium Potassium Tartrate was mixed in 50ml deionized water (Solution I). To 20ml deionized water, 1.6gm Sodium Hydroxide and 1gm DNS were added and mixed (Solution II). Solution I and II were then mixed and the volume was maintained to 100ml with deionized water.

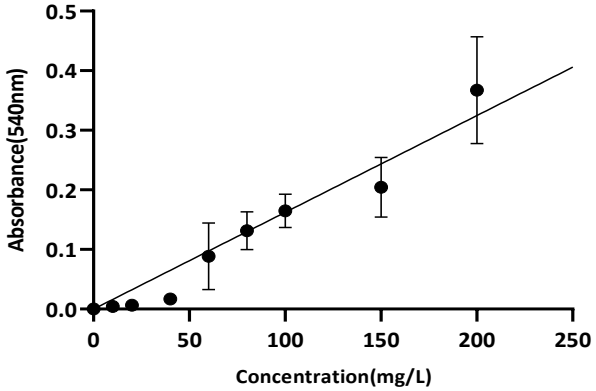

Figure 25 Standard Calibration Curve of Glucose for the determination of Total Reducing Sugar (Abs: 540nm, UV Spectrophotometer (UV-1800)) Y = 0.001624*X + 0.000, R^2 = 0.9622, Significant at 95% Confidence Interval, P value (two-tailed) < 0.0001

B. Potassium Phthalate Stock Solution (1000mg/L)

In a 100ml volumetric flask, 0.085gm Potassium phthalate was dissolved and volume was maintained.

C. Preparation of Digestion Solution

For the preparation of 100ml digestion solution, to 50ml of deionized water, 1.02gm $K_2Cr_2O_7$ was dissolved in 16.7ml 20% H_2SO_4, and 3.33gm Mercuric Sulphate was added and mixed. Then the volume was maintained at 100ml.

D. Preparation of Catalyst Solution

For a final volume of 100ml, 0.9mg of Silver Sulphate ($AgSO_4$) was mixed with 100ml of Conc. H_2SO_4.

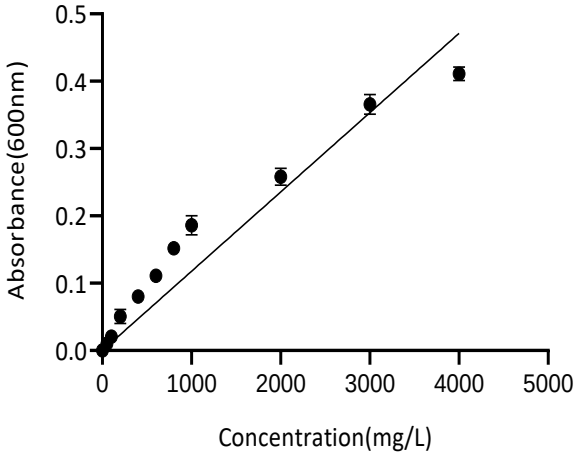

Figure 26 Standard Calibration Curve of Potassium Phthalate for the determination of COD (Abs: 600nm, UV Spectrophotometer (UV-1800)) Y = 0.0001178*X + 0.000, R^2 = 0.9581, Significant at 95% Confidence Interval, P value (two-tailed) < 0.0001

Components	COD 1500 (mg/L)	COD 2500 (mg/L)
Glucose	882.90	1472.00
Glutamate acid	396.80	661.10
CH_3COONH_4	320.70	534.60
$NaHCO_3$	343.80	343.80
NH_4Cl	130.90	218.20
KH_2PO4	52.26	52.26
K_2HPO4	37.59	37.59
$MgSO_4.7H_2O$	20.35	20.35
$MnSO_4.H_2O$	13.57	13.57
$FeCl_3.6H_2O$	6.78	6.78
$CaCl_2.2H_2O$	37.59	37.59
NaCl	48.05	48.05

(Widjaja et al., 2010)

Figure 27 Preparation of Synthetic water of different concentrations

E. Preparation of Ammonia-Nitrogen Stock Solution (10mg/L)

The First Stock of 1000mg/L was prepared by mixing 0.38gm ammonium chloride in 70ml deionized water and then volume was maintained to 100ml. For stock of 10mg/L, 1ml of 1000mg/L was diluted to 100ml (1: 100 dilution).

F. Preparation of Boric Acid Solution

To 70ml of deionized water in a reagent bottle, 2gm boric acid was mixed, and then a final volume of 100ml was maintained.

G. Preparation of Sodium Hydroxide Solution, 0.1mol/L

For 100ml, 0.4gm Sodium Hydroxide (NaOH) was mixed with 70ml of deionized water, and the final volume was maintained.

H. Preparation of Sodium Tetra-borate Solution,0.025mol/L

For 100ml, 0.5gm of anhydrous sodium tetra-borate was dissolved in 70ml deionized water and then the volume was maintained.

I. Preparation of Borate Buffer, pH 9.5

For 100ml, 8.8ml of 0.1mol/L NaOH was mixed with 50ml of 0.025mol/L Sodium tetra-borate, and then the final volume of 100 ml was maintained.

J. Nessler's reagent Composition

Ingredients	**Amount**
Mercuric Chloride	10gm
Potassium Iodide	7gm
Sodium hydroxide	16gm
Deionized Water	100ml
Final pH 9 (at 25°C)	**13.2 ± 0.05**

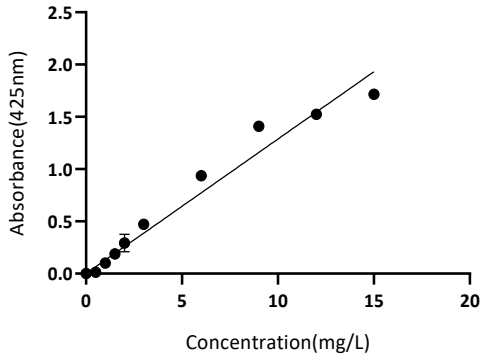

Figure 28 Standard Calibration Curve of Ammonium Chloride for the determination of Ammoniacal Nitrogen (Abs: 425nm, Y = 0.1287*X + 0.000, R^2 = 0.9656, Significant at 95% Confidence Interval, P value (two-tailed) < 0.0001

K. Preparation of H_2SO_4 , 0.5mol/L

For 100ml, 2.7ml H_2SO_4 was mixed with 97.2ml deionized water.

L. Preparation of Ammonium Molybdate-Antimony Potassium Tartrate Solution

For 100ml, 0.8gm ammonium Molybdate was added, and to that 0.02gm antimony potassium tartrate was dissolved in 70ml of deionized water and the final volume was maintained.

M. Preparation of Ascorbic Acid Solution

For the final volume of 100ml, 6gm ascorbic acid was dissolved in 70ml water and 0.2ml acetone was added and volume was maintained.

N. Preparation of Sodium Bisulfate

To 70ml of 0.5mol/L H_2SO_4, 5.2gm Sodium Bisulfate was dissolved and mixed, then the volume was maintained to 100ml with 0.5mol/L H_2SO_4.

O. Preparation of Phosphorus Stock Solution (100mg/L P)

For 100ml, 0.043gm Pre-dried (105°C for 1 hr) KH_2PO_4 was dissolved in 70ml of deionized water and maintained to the final volume. [1ml=0.1mg P]

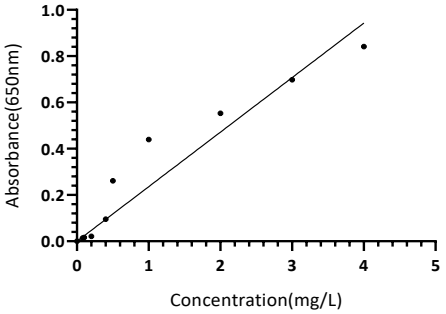

Figure 29 Standard Calibration Curve of $KH_2PO_4$for the determination of Phosphorus (Abs: 650nm, Y = 0.2357*X + 0.000, R^2 = 0.9271, Significant at 95% Confidence Interval, P value (two-tailed) < 0.0001

P. Preparation of Stock $K_2Cr_2O_7$(20mg/L)

For 100ml, 2mg $K_2Cr_2O_7$ was dissolved in 70ml of deionized water, and volume was maintained.

Q. Preparation of 0.05% DPC in Acetone

To 70ml of Acetone, 0.05gm DPC was dissolved and volume was maintained to 100ml.

R. Preparation of Concentrated H_2SO_4 (1:3)

To 66.67 ml deionized water, 33.33 ml Conc. H_2SO_4 was mixed, for a total volume of 100ml.

S. Preparation of 1M Phosphoric Acid

To 90.2 ml of deionized water, 9.8 ml of phosphoric acid was mixed for a total Volume of 100 ml.

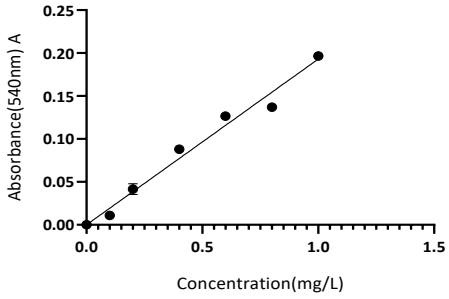

Figure 30 Standard Calibration Curve of $K_2Cr_2O_7$ for the determination of Chromium (Total, Hexavalent) (Abs: 540nm, Y = 0.1930*X + 0.000, R^2 = 0.9802, Significant at 95% Confidence Interval, P value (two-tailed) < 0.0001

APPENDIX III

Bacterial DNA extraction for metagenomics analysis

The bacterial DNA was extracted directly from the Bagmati water, so before extraction, pre-processing of the three samples was done.

A. Pre-Processing of the sample

1. In a Falcon tube, a 30ml sample was taken and centrifuged at 1000rpm for 2 minutes, to remove unnecessary debris.
2. The supernatant was transferred to a new falcon tube and was again centrifuged at 3500rpm for 40 minutes.
3. For viral concentration, supernatant could be used and for bacteria, the pellet was processed further.
4. The pellet was re-suspended in 300µl TE buffer and centrifuged at 5000rpm for 10 minutes.
5. The supernatant was discarded and the pellet was suspended in 300µl CTAB buffer.

B. Extraction of Bacterial Genomic DNA

1. The pellet suspension was centrifuged at 1200rpm for 1 minute, and the supernatant was discarded.
2. The pellet was re-suspended in 567µl TE buffer by repeated pipetting. Then 30µl of 10% SDS and 3µl of 20mg/ml Proteinase K were added to the pellet, mixed thoroughly, and incubated for 1 hour at 37^{o}C. (The solution should become viscous since the detergent lyses the cells)
3. After incubation, 100µl of 5M NaCl was added and mixed thoroughly.
   This step is important since CTAB-nucleic acid precipitate will form if salt concentration decrease below 0.5M at room temperature, and in this step, the nucleic acids are retained in the solution while removing any debris, denatured protein, and polysaccharides-CTAB.
4. To the mixture,80 µl CTAB/NaCl solution was added and thoroughly mixed, then was incubated for 10 minutes at 65^{o}C
5. Then an equal volume (0.7ml -0.8ml) of Chloroform: Isoamyl alcohol (24:1) was added, thoroughly mixed, and centrifuged for 5 minutes at 13000rpm.
   In this step, CTAB-Protein/Polysaccharides complexes will be removed and a white interface should be visible after centrifugation.
6. The upper aqueous layer was collected in a fresh Eppendorf tube, leaving the interface behind. Then an equal volume of Phenol: Chloroform: Isoamyl alcohol (25:24:1) was added and vertex to mix.
7. The mixture was then centrifuged for 5 minutes at 13000rpm, and the supernatant was collected in a fresh epi-tube.
8. To the tube, 0.6ml chilled isopropanol was added to precipitate the nucleic acid. The tube was shaken back and forth until a stringy white DNA precipitate becomes

visible and was allowed to stand for 5 minutes. It was then centrifuged at 13000rpm for 8 minutes.

9. Then, the supernatant was discarded and the pellet was washed with 70% ethanol while centrifuging for 5 minutes at 13000rpm. The supernatant was pipetted out and it was again shortly centrifuged to take off any ethanol left.
10. After the ethanol wash, the pellet was allowed to air dry, and then it was re-suspended in 40 µl TE buffer.
11. Then for the quantitation, Nano-drop was performed and the gel electrophoresis was carried out with 0.8% Agarose in TAE for 45 minutes at 90 volts after completion, the gel was visualized under UV-trans-illuminator or Gel Doc.

C. Preparation of Agarose Gel (0.8%)

1. In 40ml of TAE, 0.32gm Agarose was dissolved and boiled till the mixture homogenized and became clear.
2. When the gel cooled to a palm-tolerable temperature, 2 µl EtBr was mixed and the conical flask was swirled and carefully it was poured into the electrophoretic cassette and let to set. (The comb should be kept before the pouring of gel)

D. Loading of sample in the gel

1. After the gel was set, it was carefully transferred to an electrophoretic tank with TAE buffer.
2. In a 1 µl loading dye, a 5 µl sample was mixed with repeated pipetting and then carefully loaded into the gel.

Preparation of extraction buffers and chemicals

a. TE buffer Solution (pH 8.0): At first, Tris-Cl of 1M was prepared by mixing 15.76gm for the total volume of 100ml, and 14.612 gm EDTA was mixed for the same volume separately. For TE buffer of pH 8.0,

Reagent	Volume	Final Concentration
1M Tris-Cl pH 8.0	1ml	10mM
0.5M EDTA pH 8.0	0.2ml	1mM
Deionized water	98.8ml	-

The buffer solution was then autoclaved.

b. 10% SDS: For 100ml, 1gm SDS was dissolved in sterile deionized water since SDS shouldn't be autoclaved.

c. 5M NaCl: In 70ml of deionized water, 81.22gm NaCl was dissolved and the final volume of 100ml was maintained and autoclaved.

d. CTAB-NaCl (10% CTAB and 0.7M NaCl): For 100ml, 10gm CTAB was dissolved in 70ml deionized water and then 4.08gm NaCl was added and the volume was maintained and autoclaved.

e. Chloroform: Isoamyl Alcohol (24:1): It was freshly prepared. For 100ml, 96ml Chloroform and 4ml Isoamyl alcohol was mixed.

f. **Phenol: Chloroform: Isoamyl alcohol(25:24:1):** For 100ml, 50ml Phenol, 48ml chloroform, and 2ml Isoamyl alcohol was mixed and it was also freshly prepared.
g. **50X TAE:** To prepare the 50X TAE (Tris-Acetate-EDTA) buffer, the Tris-base (MW = 121.14 g/mol) was weighed out to 242 grams and dissolved in approximately 700 milliliters of deionized water. Caution was taken, and safety guidelines were followed during the handling of chemicals. Next, 57.1 milliliters of 100% glacial acid (or acetic acid) and 100 milliliters of 0.5 M EDTA (pH 8.0) were carefully added to the Tris-base solution. Precise measurements were crucial to achieving an accurate buffer composition. After combining the ingredients, the solution was adjusted to a final volume of 1 liter using deionized water. The pH of this buffer was not adjusted and remained around 8.5, which was suitable for various applications. Finally, the prepared 50X TAE stock solution was stored at room temperature to maintain its stability over time.

PCR reaction mixtures and Conditions

	Volume
Microbial DNA (5ng/µl)	2.5 µl
Amplicon PCR Forward Primer 1 µM	5 µl
Amplicon PCR Reverse Primer 1 µM	5 µl
2X KAPA HiFi HotStart ReadyMix	12.5 µl
Total	**25 µl**

16S Amplicon PCR Forward Primer = 5'
TCGTCGGCAGCGTCAGATGTGTATAAGAGACAGCCTACGGGNGGCWGCAG

16S Amplicon PCR Reverse Primer = 5'
GTCTCGTGGGCTCGGAGATGTGTATAAGAGACAGGACTACHVGGGTATCTAATCC

Steps	**Temperature(°C)**	**Time**	**No. of Cycle**
Initial Denaturation	95	3 minutes	1
Denaturation	95	30seconds	
Annealing	55	30seconds	25
Extension	72	30seconds	
Final Extension	72	5 minutes	1
Hold	4		

Isolation of Heavy Metal Resistant Bacteria by Spread Plate Technique

a. For the isolation, 0.1ml of the samples were suspended in the NA media supplemented with 0.003M Sodium Arsenite ($NaAsO_2$), Lead acetate (CH_3COOPb), and 20mg/L of Mercuric Chloride ($HgCl_2$), Potassium dichromate ($K_2Cr_2O_7$), and spread homogeneously with the spreader, till the sample dried out.

APPENDIX IV

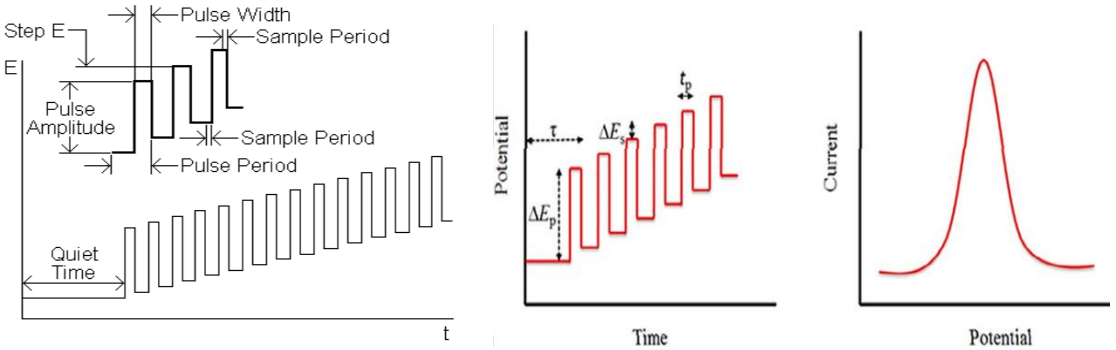

Figure 31 Principle of Differential Pulse Voltammetry

Parameters for Potentiometric Stripping Analysis

Deposition E (V): -1.5
Deposition Time (Sec): 600
Final E (V): 0.25
Stripping Current (A): 0.02
Sample Interval (Sec): 0.01
Quiet Time (Sec): 10

Parameters for Differential Pulse Voltammetry

Initial E (V): -1.5
Final E (V): 1.64
Incr E (V): 0.004
Amplitude (V): 0.025
Pulse Width (Sec): 0.05
Sampling Width (Sec): 0.02
Pulse Period (Sec): 0.5
Quiet Time (Sec): 10
Sensitivity (A/V): 1 e-006 (1 e-005, 1 e-004, 1 e-003, when there was overflow)

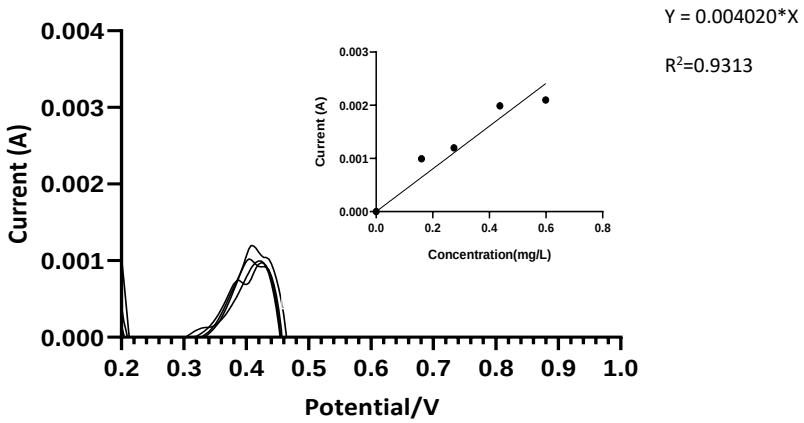

Figure 32 Standard Calibration Curve of Arsenic, P value= 0.0078

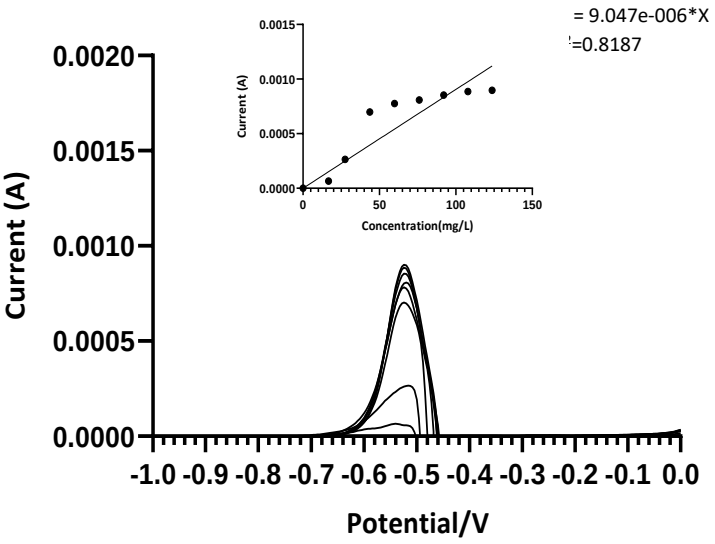

Figure 33 Standard Calibration Curve of Lead, P value 0.0008

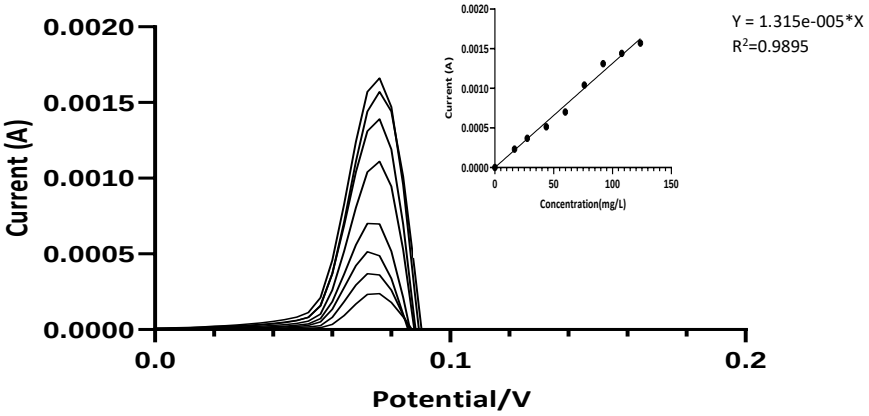

Figure 34 Standard Calibration curve of Mercury, P value <0.0001

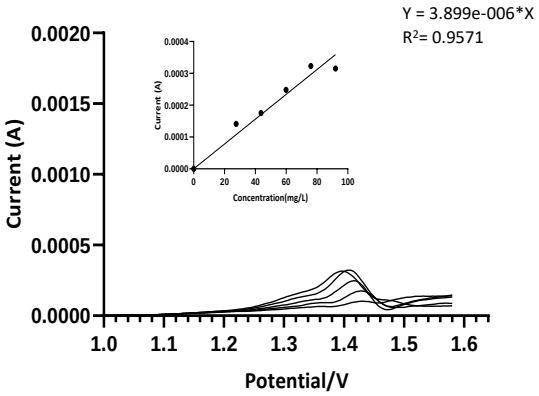

Figure 35 Standard calibration curve of Chromium, P value= 0.0007

X

APPENDIX V

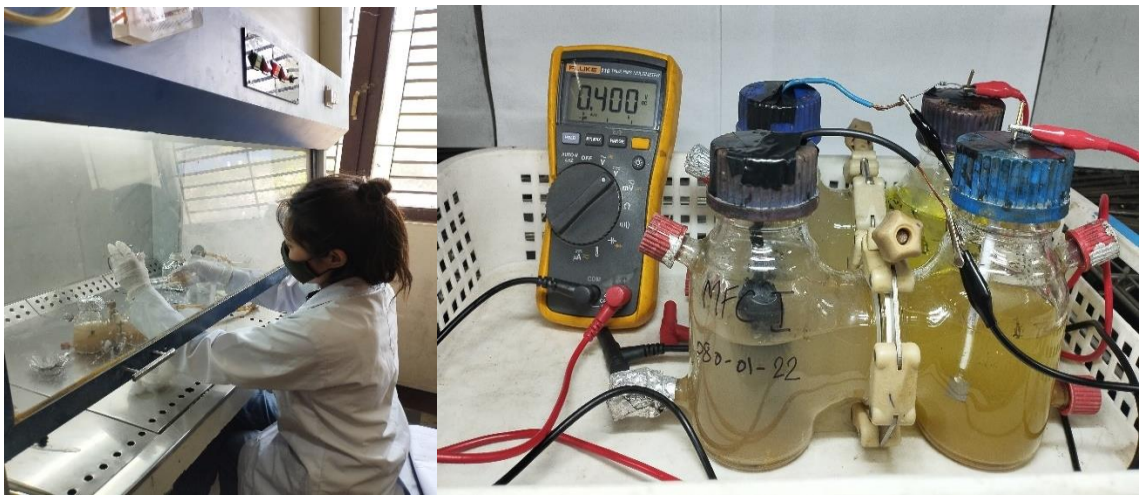

Figure 36 MFC Operation (Bagmati water and synthetic water with Graphite Rod Anode and Platinum Cathode electrode

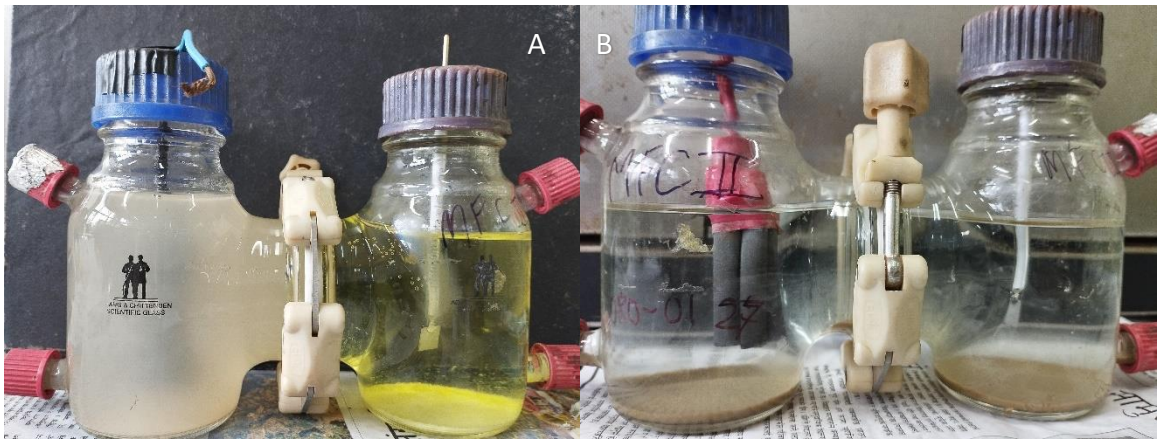

Figure 37 Anolyte and Catholyte after MFC Operation of 8 days (A: Synthetic water, B: Bagmati water)

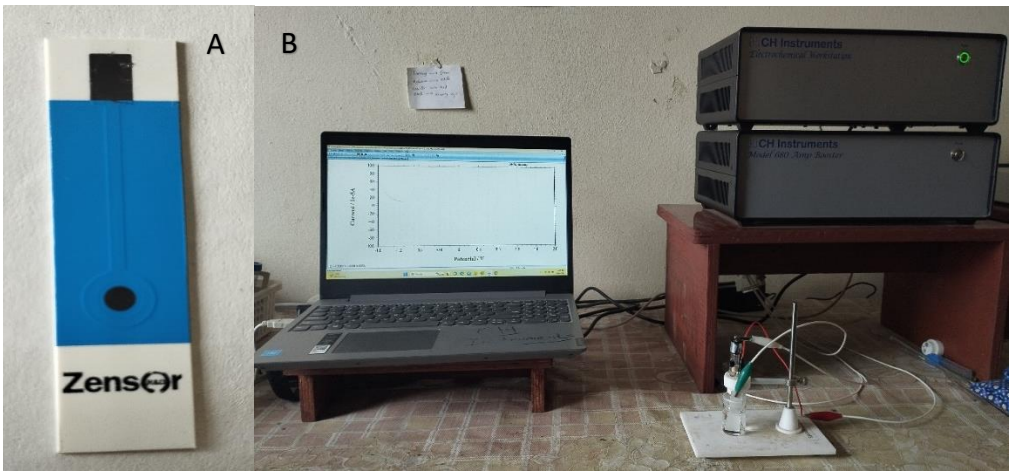

Figure 38 Differential Pulse Voltammetry Set up (A: Screen Printed Carbon Electrode, B: CHI 660E Electrochemical Workstation)